# Homoclinic Bifurcation from Heteroclinic Cycles with Periodic Orbits and Tracefiring of Pulses

a

Dissertation

submitted to the faculty of the Graduate School

of the University of Minnesota

by

Jens Diederich Michael Rademacher

in partial fulfillment of the requirements

for the degree of

Doctor of Philosophy

Adviser Arnd Scheel

May 2004

Acknowledgement

I would like to express my sincere gratitude to Arnd Scheel, without whom this thesis would not have been written. His knowledge, patient advise, time and friendship have been invaluable. I am grateful for the precious help and support of Björn Sandstede. For their feedback in many discussions I thank Bernold Fiedler, Jörg Härterich, Stefan Liebscher, Harald Engel, Grigory Bordiougov and all the other helpful minds. I am indebted to Bernold Fiedler for the hospitality in his research group and support for a long time. I thank Vivien Kirk for sharing at the time preliminary results.

This work has been supported in part by NSF grant DMS-0203301, DFG Priority Research Program SFB 555, and the Minnesota Supercomputing Institute at the University of Minnesota.

*to Sonia and my parents*

**Abstract**

Heteroclinic networks can form a skeleton for the nearby dynamics in terms of other heteroclinic, homoclinic or periodic solutions. In many cases such solutions occur as spatial profiles of fronts, pulses or wave-trains of certain spatially one-dimensional partial differential equations in a comoving frame. The present thesis was motivated by the numerical discovery of a self-organized periodic replication process of travelling pulses, termed 'tracefiring', in the three-component Oregonator model of the light-sensitive Belousov-Zhabotinskij reaction.

In the first part of this thesis we consider ordinary differential equations in three or higher dimensions and analyze homoclinic orbits bifurcating from certain heteroclinic cycles between an equilibrium and a periodic orbit. Such heteroclinic cycles differ significantly from heteroclinic cycles between equilibria, in particular the periodicity induces a lack of hyperbolicity. We establish existence and uniqueness of countably infinite families of curves of 1–homoclinic orbits *accumulating* at certain codimension–1 or –2 heteroclinic cycles of this type. The main result shows the *bifurcation* of finitely many curves of 1–homoclinic orbits from such codimension–2 heteroclinic cycles depending on global topological properties of the heteroclinic sets. In addition, a leading order expansion of the associated curves in parameter space is derived.

These heteroclinic cycles occur in spatial dynamics of spatially one-dimensional reaction diffusion systems. Codimension–1 corresponds to fronts connecting stable states and codimension–2 certain stable and unstable ones. The second part of this thesis provides an analysis of the structure of relevant essential spectra, and boundary as well as absolute spectra in the sense of Sandstede and Scheel (Physica D 145, 233–277, 2000). Our analysis includes vanishing diffusion rates as well as the case of asymptotically periodic fronts and parts of their absolute spectra.

In the third part, the theoretical results are used to partially explain the aforementioned tracefiring, which also occurs in other models. Codimension–1 heteroclinic cycles can be viewed as a general framework for the constituents of tracefiring. For the Oregonator model, a codimension–2 heteroclinic cycle and the spectral theory can explain the onset of tracefiring. This is corroborated by numerical computation of relevant spectra and solutions.

# Contents

# List of Figures

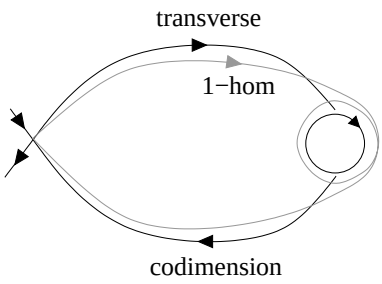


Figure 1: Schematic picture of a typical heteroclinic cycle between an equilibrium and periodic orbit, and a nearby 1–homoclinic orbit.

# 1 Introduction

Heteroclinic connections in ordinary and partial differential equations can serve as models or explanations for interfaces and switching between two states. They frequently occur in the spatial dynamics of spatially one-dimensional partial differential equations and systems with symmetries, cf. [9, 37]. Heteroclinic networks, where heteroclinic connections are building blocks, allow to model more complicated switching behavior between several states. An important basic case is a heteroclinic cycle, where connections in the network allow to return to a previous state. A natural question is whether the building blocks of the heteroclinic network form a skeleton for the nearby dynamics in phase space for close-by parameters. When all nodes in the network are hyperbolic fixed points, several questions of this type have been addressed and answered for generic or symmetric flows and diffeomorphisms [11, 36, 39, 50]. For instance, from a nondegenerate homoclinic orbit to a hyperbolic equilibrium a locally unique family of periodic orbits bifurcates, which in this sense accompany the homoclinic orbit, cf. [2, 5]. The presence of a Shil'nikov-type homoclinic orbit has rather extreme consequences for the nearby dynamics, which admit very complicated behaviors, cf. [63].

The first and main part of this thesis is contained in chapter 2, where bifurcation studies of heteroclinic networks are extended to certain heteroclinic cycles which involve periodic orbits. Such networks have been considered previously for *diffeomorphisms* in terms of nonwandering sets and topology of bifurcation sets, cf. [19], and near homoclinic orbits to an equilibrium at a Hopf bifurcation, cf. [18, 32]. Numerically and analyti-

cally, heteroclinic cycles with periodic orbits have recently been found in several cases, cf. [9, 29, 35, 41, 64, 65]. An important difference to heteroclinic cycles between equilibria is that the phase shift of a periodic orbit introduces a center direction which counts towards stable as well as unstable dimensions. As a consequence, heteroclinic cycles between two periodic orbits may be structurally stable, which is not possible for heteroclinic cycles between equilibria.

The main results in this chapter concern homoclinic bifurcation from heteroclinic cycles between an equilibrium $p_0$ and a periodic orbit $\gamma$ as depicted in figure 1. These results are valid for vector fields in any ambient dimension under generic and Melnikov-type conditions. The result concerning bifurcation of homoclinic orbits assumes an additional global topological condition. We define the codimension of such heteroclinic cycles as one plus the dimension of $p_0$'s unstable manifold minus the dimension of $\gamma$'s center-unstable manifold. The cases where this codimension is 1 or 2 after possibly changing the direction of time are considered. A homoclinic orbit to the equilibrium near such a cycle is called 1–homoclinic orbit, if it leaves and enters a neighborhood of the equilibrium only once. The four main results can be described as follows.

*Theorem 2.2:* Fix a pair of solutions which converge to a hyperbolic periodic orbit in forward and backward time respectively with the same asymptotic phase. All solutions in a neighborhood of these can be parametrized by a countably infinite family of smooth curves which wind around the periodic orbit $j$–times for any sufficiently large $j$. These solutions are exponentially close in $j$ to the given pair of solutions.

*Theorem 2.3:* Arbitrarily close to such a typical codimension–1 or –2 heteroclinic cycle, there exists a countably infinite family of smooth curves of 1–homoclinic orbits to the equilibrium. There is $j_0$ such that 1–homoclinic orbits from the $j$–th connected curve wind around the periodic orbit $(j + j_0)$–times.

*Theorem 2.5:* From a typical codimension–2 cycle with finite winding number $m \geq 1$, i.e. 'rich' transverse heteroclinic set (see hypothesis 5), $m$ smooth curves of 1–homoclinic orbits to the equilibrium bifurcate.

*Theorem 2.6:* In the codimension–2 case and under hypothesis 5, depending on the leading Floquet-exponents and the winding number $m \geq 1$, the parameter curve of 1–homoclinic orbits spirals or converges monotonically to the parameter value for the heteroclinic cycle to leading order.

The main technique to prove theorems 2.2 and 2.3 is an extension of Lin's method, cf. [39], which uses exponential di- and trichotomies for the variation about heteroclinic connections towards equilibrium and periodic orbit respectively. Major difficulties in this approach are the lack of hyperbolicity due to the phase shift of the periodic orbit, and the periodic distance of forward versus backward approach to the periodic orbit. The first corresponds to presence of essential spectrum in the case of spatial dynamics and is essentially overcome using exponentially weighted spaces. The second difficulty generally excludes a connected curve of 1–homoclinic orbits which stays close to the heteroclinic cycle due to a phase coherence condition with respect to the periodic orbit.
The winding number of the heteroclinic cycle that appears in theorem 2.5 describes how often the transverse heteroclinic set winds around the periodic orbit and equilibrium. For instance, it is 1 if the periodic orbit stems from a nearby Hopf-bifurcation of the equilibrium. While the bifurcation of 1–homoclinic orbits may not be surprising, the influence of the global topology suggests that bifurcation from such heteroclinic cycles may be rather complicated.
Theorem 2.6 in fact states that the parameter curve geometry has one frequency which is a fraction of the winding number, and another frequency given by the imaginary parts of leading stable Floquet exponents. If both frequencies are nontrivial, resonances conceivably prevent a spiraling curve, which is not possible for analogous heteroclinic cycles between equilibria. In addition, intersections with non-leading strong stable fibers may be structurally stable which alludes to the possibility of a countably infinite number of structurally stable bifurcations akin to orbit flip bifurcations. These bifurcations occur at homoclinic orbits with a non-leading rate of convergence, cf. e.g. [50]. However, we do not pursue a further analysis of this observation.

Chapter 3 bridges these results to an application in reaction diffusion equations. In addi-

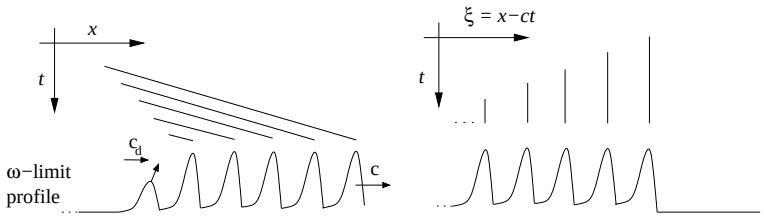


Figure 2: Schematic space-time plot of tracefiring, in the original frame and comoving with the primary pulse with speed $c > 0$.

tion, we report and augment results on the structure of essential, absolute and boundary spectra for travelling waves in spatially one-dimensional reaction diffusion equations. Our approach is guided by the work of Sandstede and Scheel, cf. e.g. [25, 51]. More precisely, we consider spectra of travelling waves which connect stationary, spatially uniform or periodic solutions, and pulses with long periodic plateaus. In the latter case, the associated spatially homoclinic orbit is close to a heteroclinic cycle with a periodic orbit. These results clarify the generic structure of essential spectra for such solutions and the relation of Neumann and Dirichlet boundary conditions. In addition, spectra and solutions are shown to typically converge locally in the limit for vanishing diffusion using singular perturbation theory. Thus, on the one hand, we can conveniently rely on analytic semigroups assuming small diffusion, but analyze solutions for vanishing diffusion, i.e. in fewer dimensions. On the other hand, weak diffusion can be typically, accurately modeled by zero diffusion.
The main new result on the structure of spectra establishes the presence absolute spectrum in certain regular critical isola of the essential spectrum of a periodic solution (theorem 3.3). Moreover, we consider relations between spectra of travelling waves – an infinite dimensional problem – and properties of the associated solutions in the travelling wave ordinary differential equation (ODE) – a finite dimensional problem. In particular, we are interested in Morse indices and codimensions of heteroclinic connections given the essential spectrum of the associated solutions for the partial differential equation (PDE).

In chapter 4 the results of chapters 2 and 3 are used to partially explain the phenomenon of 'tracefiring', in particular for the three-component Oregonator model of the light-sensitive Belousov-Zhabotinskij reaction. In fact, the work presented in chapters 2 and 3 originated from analyzing tracefiring.

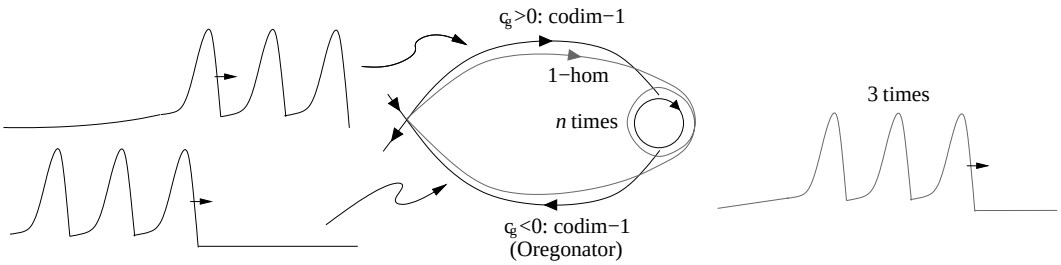


Figure 3: Schematic picture of the heteroclinic cycle occurring in spatial dynamics of tracefiring.

In tracefiring, a primary pulse loses stability and starts to replicate itself: secondary pulses periodically grow out the wake of the preceding travelling pulse-chain whose length is thereby incremented periodically. This self-organized process has two characteristic speeds: the speed of the primary pulse and the replication speed, see figures 2 and 16. The term 'tracefiring' is introduced in the present work, with emphasis on the Oregonator model. It has been observed numerically in several other models [8, 17, 66, 67], and named e.g. 'secondary trailing waves' in [67]. The patterns involved are also reminiscent of intermittency patterns for coupled cell dynamics found e.g. in [9].

In a comoving frame with the primary pulse's constant speed, stationary building blocks of tracefiring together constitute a heteroclinic cycle in the spatial direction ('spatial dynamics'), cf. figure 3. Now $n$–pulses correspond to 1–homoclinic orbits close to the heteroclinic cycle.

We explain the existence of these building blocks by the bifurcation theory of chapter 2 from a codimension 1 heteroclinic cycle between the background state and the stationary periodic wave train. The results of chapter 3 imply that a spatially heteroclinic cycle between a stable steady state and stable wave train is codimension–1, and the wave train's group velocity determines which of the connections is codimension–1, cf. figure 3.

For the Oregonator, the loss of stability of the primary pulse is mediated by pronounced oscillations in its wake. We explain the instability by numerical computations of the relevant spectra and solutions, the spectral theory of chapter 3 as well as the results of chapter 2 concerning homoclinic bifurcation from codimension–2 heteroclinic cycles, cf. figure 4.

The results of chapter 2 establish a correspondence of codimension–2 heteroclinic cy-

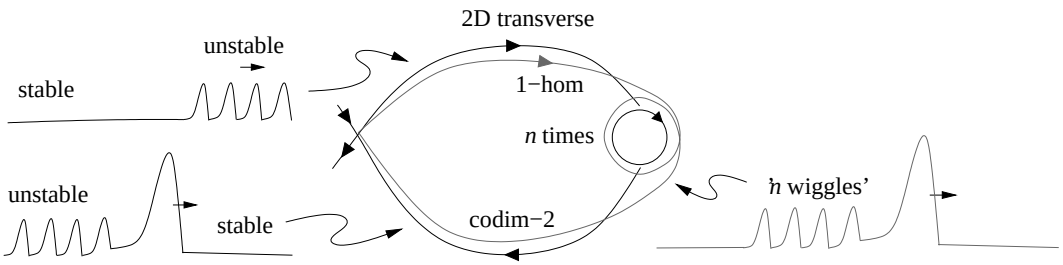


Figure 4: Schematic picture of the heteroclinic cycle mediating the instability in the Oregonator.

cles between an equilibrium and periodic orbit with winding number 1 and analogous codimension–2 heteroclinic cycles between two equilibria called 'T-points' (for 'terminal points'), cf. [28]. The latter have been used to partially explain trace- and the related backfiring, cf. [6], in cases where a second steady state interacts with the pulse. This has been found in several models, and T-points have been viewed as organizing centers [38, 65, 66]. The results of chapter 2 imply that for both types of heteroclinic cycles, suitable conditions cause the bifurcation of a locally unique curve of 1–homoclinic orbits of the parameter curves. In addition, the geometry of the parameter curve is related to the absolute spectrum of the periodic orbit or second equilibrium $p_1$.

In the case of two equilibria, neglecting technical details, if only one curve of the essential spectrum of $p_1$ is unstable and the absolute spectrum of $p_1$ contains the origin, then the path spirals to leading order, otherwise it is monotone. Leading order spiraling of the parameter curve actually allows to conclude an absolute instability for the partial differential equation from the finite dimensional travelling wave ODE, cf. [42, 49, 52]. In an absolute instability perturbations are not convected away, but grow pointwise, cf. [53]. As mentioned above, homoclinic bifurcations from heteroclinic cycles with a periodic orbit are generally different. Firstly the global topology causes the bifurcation of several curves of 1–homoclinic orbits in a typical setting if the winding number is larger than one. Secondly, due to possible resonances of eigenvalues and the period of the periodic orbit, the parameter curves may be monotone to leading order despite an absolute instability involving the origin.

# 2 Homoclinic bifurcation from heteroclinic cycles with periodic orbits

The aim of this chapter is to find curves of homoclinic orbits near heteroclinic cycles between an equilibrium and a periodic orbit of codimension 1 oder 2, as described in the introduction. For the main results of this chapter listed in the introduction, the notion of codimension of these heteroclinic cycles plays a crucial role. A natural definition of the codimension of a heteroclinic *connection* is the number of dimensions the connection lacks for transversality: the ambient dimension plus the dimension of the intersection minus the sum of stable and unstable dimension of target and source respectively. In case this number is non-positive, the intersection is transverse.

The codimension of a heteroclinic cycle between two objects is then naturally the vector of the two codimensions. However, a numeral suffices for the cases we consider, namely the sum of only the positive codimensions of the connections. We will see later that this coincides with the definition given in the introduction. Notice that this number does not distinguish codimension $(1,1)$ and $(2,m)$, where $m \leq 0$. Counting dimensions, a cycle between two equilibria has $m = 0$, while $m = -1$ for a cycle between an equilibrium and a periodic orbit, because the center direction counts towards stable and unstable dimensions. Hence, the sum of the codimensions of the connections is 2 for the case of two equilibria and 1 for the case of one equilibrium and one periodic orbit. Therefore, codimension $(1,1)$ does not occur for heteroclinic cycles between an equilibrium and a periodic orbit. In this thesis, we only consider heteroclinic cycles between an equilibrium and a periodic orbit with codimensions $(1,0)$ or $(2,-1)$.

**Definition 1** *A heteroclinic cycle between an equilibrium and a periodic orbit is called codimension–$d$ for $d = 1,2$, if one heteroclinic connection is transverse and the other codimension–$d$.*

Unless stated otherwise, in the following a codimension–$d$ heteroclinic cycle for $d = 1,2$ is between an equilibrium and a periodic orbit. Notice that in the codimension–1 case one heteroclinic connection is codimension 0, i.e. it is typically one-dimensional and transverse. Similarly, for codimension 2 one heteroclinic connection is codimension $(-1)$,

i.e. it is typically two-dimensional and transverse. We will discuss this more formally below.

Before presenting the detailed statements and proofs of the results described in the introduction, we extend that discussion to emphasize the relation to previous results.

Firstly, we consider theorem 2.3 as formulated in the introduction. We call a heteroclinic orbit converging towards the periodic orbit 'front' and the heteroclinic orbit diverging from the periodic orbit 'back' of a potential 1–homoclinic orbit, cf. figure 2. In the case of codimension–1 heteroclinic cycles theorem 2.3 states that all 1–homoclinics close to front and back have almost matching phases with respect to the phase of the periodic orbit. This phase coherence is satisfied periodically and enumerates the countably infinite family of curves of 1–homoclinic orbits which accumulate at the heteroclinic cycle. Since homoclinic orbits are also codimension–1, one might already expect that 1–homoclinic orbits do not bifurcate from a codimension–1 heteroclinic cycle.

The problem of coherent phases does not appear for heteroclinic cycles between equilibria, and poses major challenges for the analysis presented here. These appear already on the level of theorem 2.2, which parametrizes all solutions close the heteroclinic cycles by fixed points of a certain solution operator derived from the variation of constants formula.

The main point concerning theorem 2.5 is that codimension–2 heteroclinic cycles have a winding number, which describes how often the transverse heteroclinic set winds around the periodic orbit and equilibrium. For instance this is 1 near a Hopf bifurcation, and 2 if the two-dimensional transverse heteroclinic set is a Möbius strip near the periodic orbit. If the winding number $m$ satisfies $1 \leq m \leq \infty$, then theorem 2.5 proves the bifurcation of $m$ curves of 1–homoclinic orbits from the codimension–2 heteroclinic cycle.

Since the length of these 1–homoclinic orbits diverges, we can interpret this bifurcation as a 'blue sky catastrophe' for homoclinic orbits. This notion has been introduced for periodic orbits as a codimension–1 bifurcation where both period and length diverge to infinity, cf. e.g. [62]. We expect that the periodic orbits which accompany these homoclinic orbits undergo a 'classical' blue sky catastrophe.

For a codimension–2 heteroclinic cycle with winding number *zero*, the phase coherence problem generally prevents a homoclinic bifurcation from the cycle, but the countably

infinite family of 1–homoclinics may consist of relatively long curve segments.

In chapters 3 and 4, we will see that codimension–1 cycles can be expected in spatial dynamics of certain reaction-diffusion equations. With a parameter in the reaction kinetics, we expect to be able to observe codimension–2 cycles, because the speed of the travelling wave provides an additional parameter. Indeed, codimension–1 and –2 heteroclinic cycles between equilibria and periodic orbits have been found numerically in several applications:

- Spatial dynamics in [65]: connected curves of homoclinic orbits bifurcating from codimension 1 and 2 in nine ambient dimensions for calcium flow models.
- In a center manifold of a laser model, codimension 2 in four ambient dimensions [64].
- In ODEs with symmetry: coupled cells [9], and in a singular limit [41].
- In celestial mechanics [35].

We point out analytic work concerning similar bifurcations for periodically forced systems in [72] and Hamiltonian systems near resonance in [29], as well as heteroclinic bifurcation near Shil'nikov-Hopf bifurcations in [12, 18, 32]. Generic *diffeomorphisms* with codimension–1 heteroclinic cycles, corresponding to codimension–2 for flows, have been analyzed e.g. in [19], and abstract results concerning existence of generically unfolding families of homoclinic orbits, as well as ergodic properties near the cycle were obtained. Very recently, the splitting of the codimension–2 heteroclinic connection in codimension–2 heteroclinic cycles with winding number 1 has been shown in [48]. This also follows from the results in this chapter.

The results in the present work appear to be the first ones concerning homoclinic bifurcation from heteroclinic cycles with periodic orbits in flows. They are independent of the ambient dimension and amenable to identifying any $n$–homoclinic or periodic orbit near the heteroclinic cycle. We expect the method applies to more general codimensions and networks, and possibly to infinite dimensions. The periodic orbits are not assumed small or near a Hopf bifurcation, nor is the system assumed to be nearly Hamiltonian. Our setup is based on hyperbolicity and transversality. The backbone of the method are

recurrent dynamics and uniform estimates near the periodic orbit, as well as exponential trichotomies. The latter are projections like exponential dichotomies, which in addition account for the center direction induced by the phase shift of the periodic orbit.

## 2.1 Setting

**Notation** *In the following, we use $d$ to denote the codimension of the heteroclinic cycles between an equilibrium and periodic orbit we will consider in this chapters. Unless stated otherwise, $d = 1$ or $d = 2$ are both valid.*

We consider the following ODE in $\mathbb{R}^n$ with $n \geq 2 + d$, $\mu \in \mathbb{R}^d$, and $\dot{} = \frac{\mathrm{d}}{\mathrm{d}\xi}$, $f$ of class $C^{k+1}$ in $u$ and $\mu$ for $k \geq 1$.

$$\dot{u} \quad = \quad f(u;\mu) \tag{2.1}$$

We assume that for $\mu = 0$ equation (2.1) has an equilibrium $p_0$ and a periodic solution $\gamma$ of minimal period $T_\gamma > 0$. Consider the first variation[1] about $\gamma$, $\dot{v} = \partial_u f(\gamma(\xi);0)v$, with associated evolution operator $\Phi_\gamma(\xi,\zeta) : \mathbb{R}^n \to \mathbb{R}^n$, $\xi, \zeta \in \mathbb{R}$. By periodicity there is a Floquet representation $\Phi_\gamma(\xi, 0) = A_{\mathrm{per}}(\xi)\mathrm{e}^{R\xi}$, where $A_{\mathrm{per}}(\xi + T_\gamma) = A_{\mathrm{per}}(\xi)$, $A_{\mathrm{per}}(0) = \mathrm{Id}$ and $R$ has a kernel, cf. [14]. We assume hyperbolicity, i.e. the zero eigenvalue of $R$ is algebraically and geometrically simple and there are constants $\kappa_0 > 0$ and $\kappa > 0$ such that for $\mathrm{dist}(A, B) := \inf\{|a - b|, a \in A, b \in B\}$ it holds that

$$\mathrm{dist}(\mathrm{spec}(\partial_u f(p_0;0)), \mathrm{i}\mathbb{R}) > \kappa_0 \ \text{ and } \ \mathrm{dist}(\mathrm{spec}(R) \setminus \{0\}, \mathrm{i}\mathbb{R}) > \kappa. \tag{2.2}$$

For simplicity, we do not distinguish leading stable and unstable rates.

**Definition 2 (Morse indices)** *The Morse index $i_{p_0}$ of the equilibrium $p_0$ is the dimension of the unstable manifold $\mathcal{W}^{\mathrm{u}}(p_0)$. The Morse index $i_\gamma$ of the periodic orbit $\gamma$ is the dimension of the center-unstable manifold $\mathcal{W}^{\mathrm{cu}}(\gamma)$.*

Any solution $u$ to (2.1) that converges to $\gamma$ in forward time has an asymptotic phase $\alpha \in [0, T_\gamma)$: $u(\xi) - \gamma(\xi + \alpha) \to 0$ as $\xi \to \infty$, cf. [14]. The collection of all points in the

[1] The letter $v$ will be used to denote different objects in this chapter.

stable manifold with the same asymptotic phase $\alpha$ is the strong stable fiber $\mathcal{W}^{\rm ss}_\alpha(\gamma)$ and the stable manifold satisfies $\mathcal{W}^{\rm cs}(\gamma) = \cup_{\alpha\in[0,T_\gamma)}$, see e.g. Theorem 2.2, Chapter 13 in [14]. Using a suitable Euler multiplier and coordinate change near $\gamma$ for $f$, $\gamma$ is the locally unique hyperbolic periodic orbit of $f(\cdot;\mu)$ with hyperbolicity rate $\kappa$ and Morse index $i(\gamma)$ for all $\mu \in \Lambda \subset \mathbb{R}^d$, where $\Lambda$ is a neighborhood of zero, cf. e.g. [48].

We assume there are heteroclinic orbits $q_1(\xi)$, $q_2(\xi)$ with asymptotic phase 0, which connect $p_0$ to $\gamma$ and $\gamma$ to $p_0$ respectively. This heteroclinic cycle needs at least three ambient dimensions, because the periodic orbit needs nontrivial stable and unstable manifolds. Recall that the codimension of a heteroclinic connection was defined as the sum of unstable and stable dimension minus the sum of ambient dimension and dimension of the intersection. We assume throughout that the connection is maximally transverse and so the intersection is one-dimensional. Suppose $i_{p_0} = i_\gamma + d - 1$, which is the definition of codimension used in chapter 1. Since the stable dimension of $\gamma$ is $n - i_\gamma + 1$ the following computation shows that the cycle is codimension–$d$ in the sense of definition 1:

$$\begin{aligned} n+1-(\dim(\mathcal{W}^{\rm u}(p_0)+\dim(\mathcal{W}^{\rm sc}(\gamma)) &= n+1-(i_\gamma+d-1+n-i_\gamma+1) = 1-d \\ n+1-(\dim(\mathcal{W}^{\rm s}(p_0)+\dim(\mathcal{W}^{\rm sc}(\gamma)) &= n+1-(n-(i_\gamma+d-1)+i_\gamma-n-1) = d \end{aligned}$$

As mentioned in the discussion of codimension, the connection from $p_0$ to $\gamma$ is typically $d$–dimensionally transverse and the connection from $\gamma$ to $p_0$ is typically lacks $d$ dimensions for transversality. Due to the center direction we have $i_\gamma \geq 2$, and since $i_{p_0} = i_\gamma + 1$ for $d = 2$, it follows that $i_{p_0} \geq 3$ and so $\dim(\mathcal{W}^{\rm s}(p_0)) \geq 1$ implies $n \geq 4$.

**Remark 1** *A codimension–d heteroclinic cycle between an equilibrium and a periodic orbit requires* $3 + d$ *ambient dimensions.*

For later reference we summarize the assumptions.

**Hypothesis 1** *At* $\mu = 0$ *the flow of equation (2.1) possesses a hyperbolic equilibrium* $p_0$ *and a hyperbolic periodic orbit* $\gamma$ *with rates of hyperbolicity* $\kappa_0$ *and* $\kappa$ *as in (2.2). There are heteroclinic orbits* $q_1(\xi)$, $q_2(\xi)$, *which connect* $p_0$ *to* $\gamma$ *and* $\gamma$ *to* $p_0$ *respectively and both have asymptotic phase* 0 *with respect to* $\gamma$. *The heteroclinic cycle consisting of* $p_0$, $\gamma$, $q_1$ *and* $q_2$ *is codimension–d.*

Under the hyperbolicity assumption, theorem 4.3 in chapter 13 of [14] implies that there is a constant $K_0 > 0$ such that ($\alpha = 0$ under hypothesis 1)

$$\begin{aligned} |q_1(\xi) - \gamma(\xi + \alpha)| &\leq K_0 \mathrm{e}^{-\kappa\xi} \text{ for } \xi \geq 0 \\ |q_2(\xi) - \gamma(\xi)| &\leq K_0 \mathrm{e}^{\kappa\xi} \text{ for } \xi \leq 0 \\ |q_1(\xi) - p_0| &\leq K_0 \mathrm{e}^{\kappa_0\xi} \text{ for } \xi \leq 0 \\ |q_2(\xi) - p_0| &\leq K_0 \mathrm{e}^{-\kappa_0\xi} \text{ for } \xi \geq 0. \end{aligned} \tag{2.3}$$

Note that there is some freedom in choosing $\kappa_0$ and $\kappa$. Let $\nu_0 \neq 0$ be an eigenvalue of $R$ so that for any other eigenvalue $\nu \neq 0$ of $R$ it holds that $|\Re(\nu_0)| \leq |\Re(\nu)|$. Then for any $\epsilon > 0$ we can choose $\kappa = |\Re(\nu_0)| + \epsilon$, and if $\nu_0$ is algebraically simple, then we can choose $\kappa = |\Re(\nu_0)|$, cf. e.g. theorem 4.3 in chapter 13 of [14].

Since any orbit converging to $\gamma$ has an asymptotic phase in $[0, T_\gamma)$, $\alpha = 0$ may be achieved by considering $q_1(\cdot - \alpha)$ instead of $q_1$. The assumption on the zero asymptotic phase of $q_2$ when approaching $\gamma$ in backward time may be achieved independently by a suitable choice of $\gamma(0)$ or $q_2(0)$.

The role of $\alpha$ will become clear in section 2.4, where heteroclinic orbits in $\mathcal{W}_1 := \mathcal{W}^{\mathrm{u}}(p_0) \cap \mathcal{W}^{\mathrm{cu}}(\gamma)$ are varied.

Notice $\gamma(T_\gamma/2) = \gamma(-T_\gamma/2)$, so the heteroclinics to $\gamma$ and their asymptotic phases in (2.3) give rise to an unbounded sequence $T_j := jT_\gamma/2$ so that

$$|q_1(T_j) - q_2(-T_j)| \leq C\mathrm{e}^{-\kappa T_j}. \tag{2.4}$$

This expresses the asymptotically periodic distance along the heteroclinics towards $\gamma$, cf. figure 5, and $2j$ counts how often $q_1(\xi)$ and $q_2(\xi)$ wind around $\gamma$ for $\xi \in [0, T_j]$.

**Notation** *We use the following convention about constants that depend on $f(\cdot; 0)$, but not on $\mu$ or $L$ in estimates: $C$ denotes constants, which in between steps of a computation may absorb multiplicative factors or take a maximum value of finitely many constants. This is implicitly done to serve readability by focussing on the essential asymptotic analysis. The main ingredients of these constants are denoted $K_j$ for integers $j$. Constants $C_j$ with some subscript $j$ are fixed constants.*

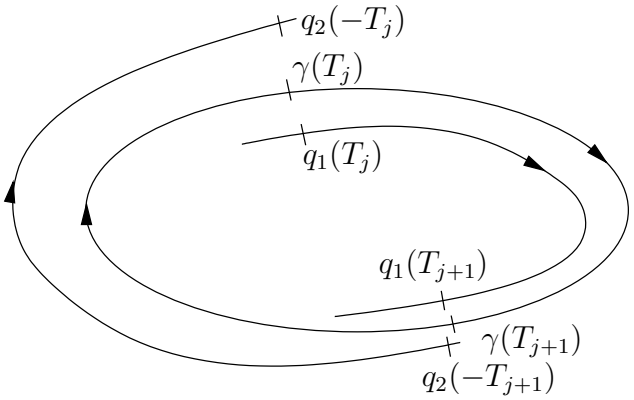


Figure 5: Schematic picture of the asymptotically $(T_\gamma/2)$–periodic of $q_1(T_j)$ and $q_2(-T_j)$.

The variation $w_j = u - q_j$ about the heteroclinics $q_j$, $j = 1, 2$ (see figure 6) satisfies

$$\begin{aligned} \dot{w}_j &= f(q_j(\cdot) + w_j; \mu) - f(q_j(\cdot); 0) = A_j(\cdot) w_j + g_j(w_j, \cdot; \mu) \\ A_j(\xi) &:= \partial_u f(q_j(\xi); 0) \\ g_j(w_j, \xi; \mu) &:= f(q_j(\xi) + w_j; \mu) - f(q_j(\xi); 0) - A_j(\xi) w_j. \end{aligned} \tag{2.5}$$

From the definitions of $g_j$ and the independence of $\gamma$ on $\mu$, we can conclude that there is a constant $K_1$ so that for all $\xi$ and $w_1$, $w_2$ in a neighborhood of zero

$$\begin{aligned} |g_j(w_j, \xi; \mu)| &\leq K_1(|w_j|^2 + |\mu|(|w_j| + |q_j(\xi) - \gamma(\xi)|) \\ |\partial_{w_j} g_j(w_j, \xi; \mu)| &\leq K_1(|w_2| + |\mu|). \end{aligned} \tag{2.6}$$

Let $\Phi_j$ be the solution operators (evolutions) to

$$\dot{v} = A_1(\cdot) v \tag{2.7}$$

$$\dot{v} = A_2(\cdot) v. \tag{2.8}$$

## 2.2 Exponential trichotomies

**Notation** *In the following, slashes '/' separate alternative, valid choices.*

**Definition 3** *Let $\phi(\xi, \zeta)$ be the evolution operator of a linear non-autonomous ODE $\dot{u} = A(\xi)u$. We say this ODE has an **exponential trichotomy** on $I = \mathbb{R}$, $I = \mathbb{R}^+$ or $I = \mathbb{R}^-$, if there exist families of complementary projections $P^{\mathrm{s}}(\xi)$, $P^{\mathrm{c}}(\xi)$ and $P^{\mathrm{u}}(\xi)$, i.e. $P^{\mathrm{s}} + P^{\mathrm{c}} + P^{\mathrm{u}} \equiv \mathrm{Id}$ and $P^{\mathrm{s}}(P^{\mathrm{c}} + P^{\mathrm{u}}) \equiv 0$, $P^{\mathrm{c}}(P^{\mathrm{s}} + P^{\mathrm{u}}) \equiv 0$, $P^{\mathrm{u}}(P^{\mathrm{s}} + P^{\mathrm{c}}) \equiv 0$. In addition,*

*these are continuous for $\xi \in I$, and there exist constants $K_2 > 0$, $-\kappa^s < 0 < \kappa^u$, such that for $\xi, \zeta \in I$, $u \in \mathbb{R}^n$*

$$
\begin{aligned}
|\phi(\xi,\zeta)P^{\mathrm{s}}(\zeta)u| &\leq K_2 \mathrm{e}^{-\kappa^s(\xi-\zeta)}|u|, \quad \xi \geq \zeta \\
|\phi(\xi,\zeta)P^{\mathrm{u}}(\zeta)u| &\leq K_2 \mathrm{e}^{\kappa^u(\xi-\zeta)}|u|, \quad \xi \leq \zeta \\
|\phi(\xi,\zeta)P^{\mathrm{c}}(\zeta)u| &\leq K_2|u|, \quad \forall \xi,\zeta \\
\phi(\xi,\zeta)P^{\mathrm{s/c/u}}(\zeta) &= P^{\mathrm{s/c/u}}(\xi)\phi(\xi,\zeta),\ \xi \geq \zeta \text{ or } \xi \leq \zeta \text{ as above.}
\end{aligned}
\tag{2.9}
$$

*We call $P^{\mathrm{s}}$ the stable, $P^{\mathrm{c}}$ the center, and $P^{\mathrm{u}}$ the unstable projection, and their images $E^{\mathrm{s/c/u}}(\xi) := \mathrm{Rg}(P^{\mathrm{s/c/u}}(\xi))$ stable, center and unstable spaces. The $\xi$-independent dimension $\dim(\ker((P^{\mathrm{u}}+P^{\mathrm{c}})(\xi)))$ is referred to as the Morse index of the exponential trichotomy. If $P^{\mathrm{c}} \equiv 0$ the exponential trichotomy is called an* ***exponential dichotomy****.*

The estimate for the center direction is cast for our applications, where the center space is always one-dimensional. For more general purposes the center estimate $K_2$ is replaced by $\tilde{K}_2 e^{\tilde{\eta}|\xi|}$, $0 < \tilde{\eta} \leq \kappa^{\mathrm{u}}, \kappa^{\mathrm{s}}$, see e.g. [60]. While the crucial estimates and statements we will derive also hold for this definition, the above formulation suffices and is more convenient. Since the trichotomy projections are complementary, we obtain $P^{\mathrm{sc}} := P^{\mathrm{s}} + P^{\mathrm{c}}$ and $P^{\mathrm{u}}$ as complementary families of projections as well as $P^{\mathrm{cu}} := P^{\mathrm{s}} + P^{\mathrm{c}}$ and $P^{\mathrm{s}}$. We define center-stable and center-unstable families of spaces $E^{\mathrm{sc}}(\xi) := \mathrm{Rg}(P^{\mathrm{sc}}(\xi))$, and $E^{\mathrm{cu}}(\xi) := \mathrm{Rg}(P^{\mathrm{cu}}(\xi))$.

**Remark 2** *The main example of a trichotomy on $\mathbb{R}$ for our purposes occurs in $\dot{v} = \partial_u f(\gamma(\xi);0)v$, with $\kappa^{\mathrm{s/u}} \geq \kappa$. By the hyperbolicity assumption, the center space is one-dimensional and the trichotomy estimates follow from the spectral assumptions on $R$ from the aforementioned Floquet representation of the evolution $\Phi_\gamma(\xi,0) = A_{\mathrm{per}}(\xi)\mathrm{e}^{R\xi}$. Let $P_\gamma^{\mathrm{s/c/u}}(\xi)$ be the stable/center/unstable projections for this trichotomy. We further conclude that the images of the stable and unstable projections are the stable and unstable eigenspaces $E_R^{\mathrm{s/u}}$ of $R$ transported with $A_{\mathrm{per}}(\xi)$, because $E_\gamma^{\mathrm{s/u}}(\xi) = A_{\mathrm{per}}(\xi)E_R^{\mathrm{s/u}}$. Since $\dot{\gamma}$ is a periodic solution and $\ker(R)$ one-dimensional $E_\gamma^{\mathrm{c}}(\xi) = \mathrm{span}\{\dot{\gamma}(\xi)\}$.*

**Lemma 1 (and notation)** *Under hypothesis 1, equation (2.7) possesses an exponential dichotomy on $\mathbb{R}^-$ and equation (2.8) on $\mathbb{R}^+$ with stable and unstable rates at least $\kappa_0$.*

*We denote the stable and unstable projections of these by* $P^{\mathrm{s}}_{-1}(\xi)$, $P^{\mathrm{u}}_{-1}(\xi)$, $\xi \leq 0$, *for (2.7) and* $P^{\mathrm{s}}_{+2}(\xi)$, $P^{\mathrm{u}}_{+2}(\xi)$, $\xi \geq 0$, *for (2.8).*

*Furthermore, (2.7) possesses an exponential trichotomy on* $\mathbb{R}^+$ *and (2.8) on* $\mathbb{R}^-$, *with* $\kappa^{\mathrm{s/u}} \geq \kappa$. *We denote the stable/center/unstable projections for (2.7) by* $P^{\mathrm{s/c/u}}_{+1}(\xi)$, $\xi \geq 0$, *and for (2.8) by* $P^{\mathrm{s/c/u}}_{-2}(\xi)$, $\xi \leq 0$. *The projections' images* $E^{\mathrm{s/c/u}}(\xi)$ *inherit the sub-indices of the projections and*

$$E^{\mathrm{c}}_{+1}(\xi) = \mathrm{Rg}(P^{\mathrm{c}}_{+1}(\xi)) = \mathrm{span}\{\dot{q}_1(\xi)\},\ \xi \geq 0$$
$$E^{\mathrm{c}}_{-2}(\xi) = \mathrm{Rg}(P^{\mathrm{c}}_{-2}(\xi)) = \mathrm{span}\{\dot{q}_2(\xi)\},\ \xi \leq 0$$

**Proof.** Generally, if $A_j(\xi)$, $j = 1, 2$, is asymptotically constant and hyperbolic then $\dot{u} = A_j(\xi)u$ has exponential dichotomies on $\mathbb{R}^+$ and $\mathbb{R}^-$, cf. e.g. [16]. This implies the claim about exponential dichotomies, because by assumption $\lim_{\xi\to\infty} A_2(\xi) = \lim_{\xi\to-\infty} A_1(\xi) = \partial_u f(p_0; 0)$ is hyperbolic with rate $\kappa_0$, cf. (2.2).

However, the other asymptotic state $\partial_u f(\gamma(\xi); 0)$ is periodic with precisely one vanishing Floquet exponent in the direction of $\gamma'$. In this case, we use that trichotomies on $\mathbb{R}$ or $\mathbb{R}^\pm$ are equivalent to two dichotomies of properly, exponentially shifted flows (cf. [60] Lemma 45.4 and choose the non-unique stable/unstable spaces correctly). For the existence of these dichotomies we can apply Proposition 2.2 of [44], because the shifted matrices $A_j(\xi) \pm \eta\mathrm{Id}$ for $j = 1, 2$ and $\kappa > \eta > 0$ are asymptotically periodic with non-vanishing Floquet exponents for $\xi \to -(-1)^j\infty$.

The expressions for the center-spaces follow, because these are one-dimensional, $\dot{q}_j(\xi)$, $j = 1, 2$ solve the respective variational equations and satisfy the center estimate. □

The next lemma establishes projections that couple those of (2.7) and (2.8) near $\gamma$. We say that a collection of projections is complementary, if the image of any one projection lies in the kernel of the others, and the sum of the projections is the identity.

**Lemma 2** *Assume hypothesis 1 and consider the projections* $P^{\mathrm{s/u/c}}_{+1}(L)$, $P^{\mathrm{s/u/c}}_{-2}(-L)$ *from the exponential trichotomies of (2.7) on* $\mathbb{R}^+$ *and (2.8) on* $\mathbb{R}^-$. *There exists strictly positive constants* $\epsilon_0 < T_\gamma/2$, $K_3$, $L_0$ *such that the following holds. For* $L \geq L_0$, *with* $|L - T_j| \leq \epsilon_0$ *for some* $j$, *there exist complementary projections* $P^{\mathrm{s/u/c}}_L$, *continuous in* $L$, *whose images*

*satisfy* $\mathrm{Rg}(P_L^{\mathrm{s}}) = E^{\mathrm{s}}{}_{-2}(-L)$, $\mathrm{Rg}(P_L^{\mathrm{u}}) = E^{\mathrm{u}}_{+1}(L)$, $\mathrm{Rg}(P_L^{\mathrm{c}}) = E^{\mathrm{c}}{}_{-2}(-L) = \mathrm{span}\{\dot{q}_2(-L)\}$, *and* $|P_L^{\mathrm{s/u/c}}| \leq K_3$. *In particular*

$$P_L^{\mathrm{s}} + P_L^{\mathrm{c}} + P_L^{\mathrm{u}} = \mathrm{Id}. \tag{2.10}$$

**Proof.** To obtain the desired uniformly bounded projections, we can apply lemma 7 from [69] to $P^{\mathrm{sc}}_{-2}(\xi)$ and $P^{\mathrm{u}}_{+1}(\xi)$, which converge to the complementary projections $P^{\mathrm{sc}}_{\gamma}(\xi)$ for $\xi \to -\infty$ and $P^{\mathrm{u}}_{\gamma}(\xi)$ for $\xi \to \infty$ respectively. The proof in [69] does not use the fact that the matrices involved are asymptotically constant and applies with minor modifications here as long as $L$ is sufficiently close to the sequence $T_j$, i.e. there is $j$ such that $|L - T_j| \leq \epsilon_0$ for some $\epsilon_0 > 0$. We obtain a pair of complementary projections $P_-^{\mathrm{s/u}}(L)$, as smooth in $L$ as the original projections, and which satisfy

$$\begin{aligned} \mathrm{Rg}(P_-^{\mathrm{s}}(L)) &= E^{\mathrm{sc}}_{-2}(-L) \\ \mathrm{Rg}(P_-^{\mathrm{u}}(L)) &= E^{\mathrm{u}}_{+1}(L). \end{aligned}$$

Using these and the center projection $P^{\mathrm{c}}{}_{-2}(-L)$ for the variation about $q_2$, we define

$$\begin{aligned} P_L^{\mathrm{sc}} &:= P_-^{\mathrm{s}}(L) \\ P_L^{\mathrm{c}} &:= P^{\mathrm{c}}{}_{-2}(-L) P_L^{\mathrm{sc}} \\ P_L^{\mathrm{s}} &:= P_L^{\mathrm{sc}} - P_L^{\mathrm{c}} \\ P_L^{\mathrm{u}} &:= P_-^{\mathrm{u}}(L) \end{aligned}$$

We first verify the ranges. By definition $\mathrm{Rg}(P_L^{\mathrm{u}}) = E^{\mathrm{u}}_{+1}(L)$, while $\mathrm{Rg}P_L^{\mathrm{c}} = \mathrm{span}\{\dot{q}_2(-L)\}$ and $\mathrm{Rg}P_L^{\mathrm{s}} = E^{\mathrm{s}}{}_{-2}(-L)$ follow from

$$\begin{aligned} \mathrm{Rg}(P_L^{\mathrm{sc}}) &= E^{\mathrm{sc}}_{-2}(-L) = E^{\mathrm{s}}{}_{-2}(-L) \oplus \mathrm{span}\{\dot{q}_2(-L)\} \\ \mathrm{Rg}(P^{\mathrm{c}}{}_{-2}(L)) &= \mathrm{span}\{\dot{q}_2(-L)\}. \end{aligned}$$

We conclude from the complementarity that $P_L^{\mathrm{s}} + P_L^{\mathrm{c}} + P_L^{\mathrm{u}} = \mathrm{Id}$.
As to the kernels, the definitions give $\ker(P_L^{\mathrm{u}}) = \mathrm{Rg}(P_L^{\mathrm{sc}})$, $\mathrm{Rg}(P_L^{\mathrm{u}}) = \ker(P_L^{\mathrm{sc}}) \subset \ker(P_L^{\mathrm{c}})$, and the above implies $\mathrm{Rg}(P_L^{\mathrm{s}}) \subset \ker P_L^{\mathrm{c}}$, and $\mathrm{Rg}(P^{\mathrm{c}}{}_{-2}(L) \subset \mathrm{Rg}(P_L^{\mathrm{sc}})$ so

$$\begin{aligned} \ker(P_L^{\mathrm{c}}) &= \mathrm{Rg}(P_L^{\mathrm{u}}) + \mathrm{Rg}(P_L^{\mathrm{s}}) \\ \ker(P_L^{\mathrm{s}}) &= \ker(P_L^{\mathrm{sc}} - P_L^{\mathrm{c}}) = \mathrm{Rg}(P_L^{\mathrm{c}}) + \mathrm{Rg}(P_L^{\mathrm{u}}). \end{aligned}$$

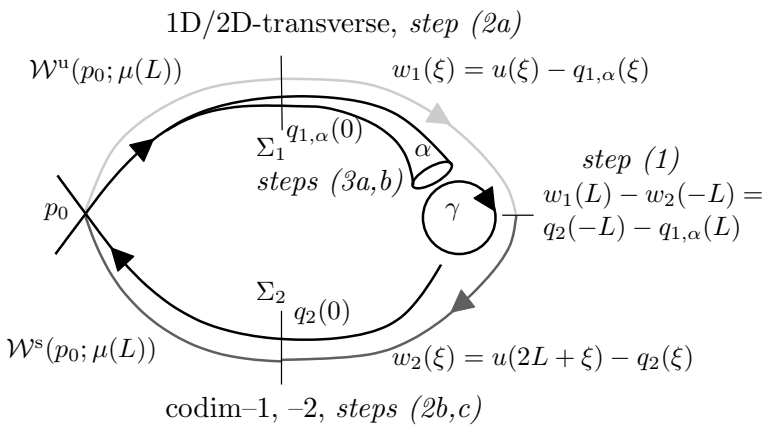


Figure 6: Schematic picture of adapted Lin's method to find 1–homoclinic orbits near the heteroclinic cycle with a periodic orbit. Numbers indicate the steps describe in the text. For the codimension–2 case $\alpha$ parametrizes distinct heteroclinic orbits.

□

**Remark 3** *Let $L \geq L_0$, $|L - T_j| \leq \epsilon_0$ for some $j$. Notice that $E^{\mathrm{c}}_{+1}(L)$ is not necessarily contained in a specific kernel of the projections $P^{\mathrm{s/c/u}}_L$. But $\dot{q}_1(L)$ is exponentially close to $\dot{\gamma}(L)$, while $q_2(-L)$ is exponentially close to $\dot{\gamma}(-L)$. So in terms of suitable unit basis vectors $E^{\mathrm{c}}_{-2}(-L)$ and $\mathrm{Rg}(P^{\mathrm{c}}_L)$ are exponentially close to $\mathrm{span}\{\dot{\gamma}(-L)\}$ and $\mathrm{Rg}(P^{\mathrm{c}}_\gamma)$ respectively. Using the sequence $T_j$ introduced above, the spaces $E^{\mathrm{c}}_{+1}(T_j)$ and $E^{\mathrm{c}}_{-2}(-T_j)$ are exponentially close to $\mathrm{span}\{\dot{\gamma}(T_j)\}$ in this sense. In particular, $P^{\mathrm{c}}_L P^{\mathrm{u}}_{-2}(-L) = O(\mathrm{e}^{-\kappa L})$, and $P^{\mathrm{c}}_L P^{\mathrm{s/u}}_{+1}(L) = O(\mathrm{e}^{-\kappa L})$, $P^{\mathrm{s/u}}_{+1}(L) P^{\mathrm{c}}_L = O(\mathrm{e}^{-\kappa L})$, see e.g. [44, 50].*

## 2.3 1–homoclinic orbits near heteroclinic cycles with periodic orbits

Using to the variations (2.5) about the heteroclinics, we next set up a fixed point formulation akin to Lin's method [39] to find 1–homoclinic orbits near the heteroclinic cycle in parameter and phase space.

The method to prove theorem 2.5 consists of three major steps, see figure 6: Firstly, in section 2.3.1, for codimension 1 and 2 we parametrize all small 'glued' variational solutions. These consist of two parts, one near a heteroclinic from $p_0$ to $\gamma$ and one near the heteroclinic from $\gamma$ to $p_0$, which are 'glued together' near $\gamma$. Secondly, in section 2.3.2,

for codimension 1 and 2 we show that parameters can be chosen such that some of these solutions lie in the stable/unstable manifold of the equilibrium $p_0$. This gives the desired 1–homoclinic orbits. Thirdly, in section 2.4 and for the codimension–2 case, we patch these 1–homoclinic orbits together and obtain a connected curve that actually bifurcates from the heteroclinic cycle. More precisely, the process consist of six steps, cf. figure 6:

(1) Parametrize all solutions passing near $\gamma$ and $q_1$, $q_2$ (this proves theorem 2.2), i.e. 'glue' variations $w_1(L)$, $w_2(-L)$ and $q_{1,\alpha}(L)$, $q_2(-L)$ together to obtain continuous solutions to (2.1).

(2a) Match the glued solutions with $\mathcal{W}^{\mathrm{u}}(p_0)$ near the transverse intersection $\mathcal{W}_1 = \mathcal{W}^{\mathrm{u}}(p_0) \cap \mathcal{W}^{\mathrm{cu}}(\gamma)$.

(2b) Match the transverse part by Ljapunov-Schmidt reduction near the intersection of $\mathcal{W}^{\mathrm{s}}(p_0)$ and $\mathcal{W}^{\mathrm{cu}}(\gamma)$.

(2c) Match the remaining part by Melnikov's method (this proves theorem 2.3) to obtain a family of curves of 1–homoclinic orbits.

(3a) Patch part of the curves of 1–homoclinics together by varying the underlying heteroclinic for $d = 2$.

(3b) Patch all 1–homoclinics together using the global topological hypothesis 5 to obtain a smooth connected curve of 1–homoclinic orbits and parameters that bifurcate from the heteroclinic cycle

**Remark 4** *For the codimension–2 case, let $\Gamma$ denote a curve of heteroclinic points transverse to the flow. For the codimension–1 case set $\Gamma := \{q_1(0)\}$. In figure 6, the parameter $L$ geometrically means the semi travel time between some small transverse sections $\Sigma_1$ and $\Sigma_2$ near $\Gamma$ and $q_2(0)$ respectively: any solution $u$ passing near the heteroclinic cycle has unique 'hit' times $\xi_1$, $\xi_2$ at which $u(\xi_1) \in \Sigma_1$ and $u(\xi_2) \in \Sigma_2$. The uniquely defined semi-travel-time from $\Sigma_1$ to $\Sigma_2$ is then $L = (\xi_2 - \xi_1)/2$. However, in the approach below, we need more flexibility and do not interpret $L$ as this strict semi travel time. Instead, we first view $L$ as an abstract parameter, and a posteriori it turns out $L$ is close to the above*

*semi travel time. In particular, for homoclinic solutions it turns out that $L$ is the semi travel time up to an exponentially small adjustment, see remark 7.*

Steps 1-2c involve successive elimination of variables by the following slightly non-standard, but well known, implicit function theorem. In lack of a reference, we prove it here in a unified form to be conveniently used for all the steps.

**Theorem 2.1** *Let $X$, $Y$ and $Z$ be open neighborhoods of zero, and $I$ an open set, all in some ambient Banach spaces. For convenience, we denote all norms by $|\cdot|$. Let $Q : Z \times I \to \mathcal{L}(Y, X)$, $R : Y \times Z \times I \to X$ and $S : I \to X$ be $C^k$, $k \geq 1$, in all variables. Assume that for $z \in Z$, $L \in I$ the linear map $Q(z, L)$ invertible and there exists positive constants $C_1$, $C_2$ such that $||Q^{-1}(z, L)|| \leq C_1$ and*

$$|R(y, z, L)| \leq C_2((|z| + |y|)|y| + |z|). \tag{2.11}$$

*Let $C_* := C_1C_2$, $r_y := \frac{4C_*+1}{4C_*(2C_*+1)}$, $r_z := \frac{1}{4C_*(2C_*+1)}$. Then any solution to*

$$Q(z, L)y + R(y, z, L) = S(L) \tag{2.12}$$

*for $y \in Y_* := \{y \in Y \,|\, |y| < r_y\}$, $z \in Z_* := \{z \in Z \,|\, |z| < r_z\}$ and $L \in I$ satisfies*

$$|y| \leq 2(C_*|z| + C_1|S(L)|). \tag{2.13}$$

*If in addition $C_1|S(L)| \leq \frac{1}{8C_*}$ for $L \in I$ and*

$$|\partial_y R(y, z, L)| \leq C_2(|z| + |y|), \tag{2.14}$$

*then there exists a $C^k$ function $y^* : Z_* \times I \to Y_*$ such that $y^*(z, L)$ uniquely solves (2.12) for $y \in Y_*$.*

**Proof.** By assumption on $Q$, we can rewrite the equation to be solved as

$$y = r(y, z, L) := -Q(z, L)^{-1}(R(y, z, L) + S(L)) \tag{2.15}$$

with a $C^k$ function $r : Y \times Z \times I \to Y$, and for $y \in Y_*$ and $z \in Z_*$ we have by assumption $C_*(|z| + |y|) \leq \frac{1}{2}$. Since $||Q^{-1}(z, L)|| \leq C_1$ it follows from (2.11) that (2.15) implies

$$\begin{aligned} |y| &\leq \tfrac{1}{2}|y| + C_*|z| + C_1|S(L)| \\ \Rightarrow |y| &\leq 2(C_*|z| + C_1|S(L)|). \end{aligned} \tag{2.16}$$

Assumption (2.14) yields $r(\cdot, z, L)$ a uniform contraction of $Y_*$ for $z \in Z_*$, $L \in I$, because

$$|r(y_1, z, L) - r(y_2, z, L)| \leq \sup_{y \in Y_*} |Q(z, L)^{-1}(\partial_y R(y, z, L))||y_1 - y_2| \leq \frac{1}{2}|y_1 - y_2|.$$

Finally, $C_1|S(L)| \leq \frac{1}{8C_*}$ for $L \in I$ implies $r(\cdot, z, L)$ maps $Y_*$ into itself for all $z \in Z_*$ and $L \in I$, because it follows from (2.16) and $|z| \leq r_z$ that

$$|r(y, z, L)| \leq \frac{1}{2}|y| + C_*|z| + C_1|S(L)|) < \frac{1}{2}r_y + \frac{1}{4(2C_* + 1)} + \frac{1}{8C_*} = r_y$$

Hence, the uniform contraction principle, e.g. [13] theorem 2.2, provides the locally unique fixed point $y^* \in Y_*$, which is $C^k$ in $z \in Z_*$ and $L \in I$. □

### 2.3.1 Glued solutions

In this step, we only use the local structure near the periodic orbit. The global heteroclinic structure plays no role, and for any pair of solutions, one converging forward and one backward to a hyperbolic periodic orbit, we parametrize all orbits passing the periodic orbit near this solution pair using the approximate semi travel time $L$.

For $L > 0$, we consider solutions $w_1(\xi_+)$, $\xi_+ \in [0, L]$, and $w_2(\xi_-)$, $\xi_- \in [-L, 0]$, to (2.5), and for $L \geq L_0$ we use the projections from lemma 1 to denote $w_{+1}^{\mathrm{s/c/u}}(\xi_+) := P_{+1}^{\mathrm{s/c/u}}(\xi_+)w_1(\xi_+)$, $w_{-2}^{\mathrm{s/c/u}}(\xi_-) := P_{-2}^{\mathrm{s/c/u}}(\xi_-)w_2(\xi_-)$, as well as

$$W\begin{pmatrix}\xi_+\\ \xi_-\end{pmatrix} := \begin{pmatrix} w_1(\xi_+) \\ w_2(\xi_-) \end{pmatrix} = \begin{pmatrix} w_{+1}^{\mathrm{s}}(\xi_+) + w_{+1}^{\mathrm{u}}(\xi_+) + w_{+1}^{\mathrm{c}}(\xi_+) \\ w_{-2}^{\mathrm{s}}(\xi_-) + w_{-2}^{\mathrm{u}}(\xi_-) + w_{-2}^{\mathrm{c}}(\xi_-) \end{pmatrix} \tag{2.17}$$

In the following, we write vectors as columns or rows interchangeably. The glued solutions will be concatenations of $w_1(\xi_+) + q_1(\xi_+)$ and $w_2(\xi_-) + q_2(\xi_-)$ on $[0, 2L]$ by means of

$$u(\xi) = \begin{cases} q_1(\xi) + w_1(\xi)\,,\ \xi \in [0, L] \\ q_2(\xi - 2L) + w_2(\xi - 2L)\,,\ \xi \in [L, 2L] \end{cases} \tag{2.18}$$

Hence, the variational parts have to satisfy the boundary condition $w_1(L) + q_1(L) = w_2(-L) + q_2(-L)$ or equivalently the 'gluing condition'

$$b_L := q_2(-L) - q_1(L) = w_1(L) - w_2(-L). \tag{2.19}$$

We call variational solutions $w_1$, $w_2$ *glued*, if they satisfy (2.19). For the contraction argument to find glued solutions, we will need $b_L$ to be small. Since $b_L$ is asymptotically

periodic, we cannot expect to be able to track glued solutions for all $L$ by our method without further assumptions.

**Lemma 3** *Assume hypothesis 1. There exists a sequence of disjoint open intervals $I_j$ for a $j_0 \geq 0$ with length $|I_j| \leq \mathrm{e}^{-\kappa \sup I_j} \leq \epsilon_0$ such that if $L \in I_j$ for some $j \geq 0$, then*

$$|b_L| \leq K_4 \mathrm{e}^{-\kappa \sup I_j}$$

**Proof.** As noted in (2.4), for the period $T_\gamma$ of $\gamma$ we have that $\gamma(T_\gamma/2) - \gamma(-T_\gamma/2) = 0$. Hypothesis 1 implies that for $\xi \geq 0$ we have

$$\begin{aligned} |q_1(\xi) - \gamma(\xi)| &\leq K_0 \mathrm{e}^{-\kappa\xi} \\ |q_2(-\xi) - \gamma(-\xi)| &\leq K_0 \mathrm{e}^{-\kappa\xi}. \end{aligned}$$

Hence, for $T_j := jT_\gamma/2$ it holds that $|b(T_j)| = |q_1(T_j) - q_2(-T_j)| \leq C\mathrm{e}^{-\kappa T_j}$. Define $I_j := (T_j - \mathrm{e}^{-\kappa(T_j+1)}/2, T_j + \mathrm{e}^{-\kappa(T_j+1)}/2)$, so the lengths satisfy $|I_j| \leq \exp(-\kappa \sup I_j)$. For $\bar{K}_4 := \sup_{\xi\in\mathbb{R}^+} |q_1'(\xi)| + \sup_{\xi\in\mathbb{R}^-} |q_2'(\xi)|$ and all $L \in I_j$ we have

$$|q_1(L) - q_1(T_j)| + |q_2(-L) - q_2(T_j)| \leq \sup_{\xi\in I_j} |q_1'(\xi)|\, |L - T_j| \leq \bar{K}_4 |I_j|.$$

Thus, if $L \in I_j$ for some $j \geq 0$ then it holds that

$$\begin{aligned} |b_L| &= |q_1(L) - q_2(-L)| \leq |q_1(L) - q_1(T_j)| + |q_1(T_j) - q_2(T_j)| + |q_2(T_j) - q_2(L)| \\ &\leq \bar{K}_4 |I_j| + 2K_0 \mathrm{e}^{-\kappa T_j} \leq (\bar{K}_4 + 2K_0 \mathrm{e}^{\kappa T_\gamma/2}) \mathrm{e}^{-\kappa \sup I_j} \leq C\mathrm{e}^{-\kappa \sup I_j}. \end{aligned}$$

□

There is $j_0 \geq 0$ so that for $j \geq j_0$ the intervals $I_j$ are all disjoint, because $|I_j| \to 0$.

**Notation** *$I_b := \cup_{j\geq j_0} I_j \subset \mathbb{R}^+$ is the set of almost phase coherent parameters $L$.*

The periodic orbit's phase shift introduces lack of hyperbolicity, which causes some difficulties to obtain uniform estimates in $L$ below. However, analogues of these can be achieved in exponentially weighted norms. It turns out that a good choice of space for the fixed point formulation of glued solutions is the product $\mathcal{X}^\eta_{\tilde{L}}$ of exponentially weighted spaces $C_{\eta,\tilde{L}} = C^0([0,\tilde{L}],\mathbb{R}^n)$ and $C_{-\eta,\tilde{L}} = C^0([-\tilde{L},0],\mathbb{R}^n)$ with norms

$$\begin{aligned} ||w_1||_{\eta,\tilde{L}} &:= \sup_{0\leq\xi\leq\tilde{L}} |\mathrm{e}^{\eta\xi} w_1(\xi)| \\ ||w_2||_{-\eta,\tilde{L}} &:= \sup_{-\tilde{L}\leq\xi\leq 0} |\mathrm{e}^{-\eta\xi} w_2(\xi)|. \end{aligned}$$

With $W = \binom{w_1}{w_2}$ we define

$$\begin{aligned} \mathcal{X}_{\tilde{L}}^{\eta} &:= C_{\eta,\tilde{L}} \times C_{-\eta,\tilde{L}} \\ ||W||_{\tilde{L}}^{\eta} &:= ||w_1||_{\eta,\tilde{L}} + ||w_2||_{-\eta,\tilde{L}} \end{aligned} \tag{2.20}$$

We will consider spaces for fixed $\tilde{L}$ and variational solutions with $L \leq \tilde{L}$ to be able to conclude smoothness in $L$ in a fixed space.

**Notation** *Throughout this chapter, we fix an arbitrary $\eta$ so that $0 < \eta < \kappa$, and only consider the spaces $\mathcal{X}_L^{\eta}$ as well as $\mathcal{X}_L^0$. For convenience we set $\mathcal{X}_L := \mathcal{X}_L^{\eta}$ and $||\cdot||_L := ||\cdot||_L^{\eta}$. In addition, we omit dependence of constants on $\eta$.*

The norms on $\mathcal{X}_L^0$ and $\mathcal{X}_L$ are equivalent for $L < \infty$, but one of the constants relating the norms diverges continuously as $L \to \infty$. Hence, for $L < \infty$ the spaces coincide as sets and smoothness in one space implies it in the other. For any $0 < L_1 \leq L_2$ we have

$$\sup_{0\leq\zeta\leq L_1} |w(\xi)| \leq ||w||_{\eta,L_1} \leq ||w||_{\eta,L_2} \ , \quad \sup_{-L_1\leq\zeta\leq 0} |w(\xi)| \leq ||w||_{-\eta,L_1} \leq ||w||_{-\eta,L_2}, \tag{2.21}$$

hence $||W||_{L_1}^0 \leq ||W||_{L_1}$ and for $W \in \mathcal{X}_{L_1} \cap \mathcal{X}_{L_2}$ we have $||W||_{L_1} \leq ||W||_{L_2}$. Analogously, we obtain $||W||_L \leq \mathrm{e}^{\eta L}||W||_L^0$ for any $L$.

**Notation** *We denote by $B_\rho(y)$ be the open ball of radius $\rho$ centered at $y$ in a metric space given by the context. For the spaces introduced above, we denote $B_\rho(W;L) := B_\rho(W) \subset \mathcal{X}_L$, and $B_\rho^0(W;L) := B_\rho(W) \subset \mathcal{X}_L^0$.*

So for $L_1 \leq L_2$ and $W \in \mathcal{X}_{L_2}$ it holds that as sets $B_\rho(W;L_1) \supset B_\rho(W;L_2)$, and for any $L > 0$ we have $B_\rho^0(W;L) \supset B_\rho(W;L) \supset B_{\rho\exp(-\eta L)}^0(W;L)$.
To obtain smoothness in $L$, we will fix the space, i.e. an $\tilde{L} \in I_b$. By the estimate $||W||_L \leq ||W||_{\tilde{L}}$ for any $L < \tilde{L}$ uniform estimates in $\tilde{L}$ that only depend on $\tilde{L} - L$ are possible. Given $\tilde{L} \in I_b$, let $\tilde{I}$ be the interval in $I_b$ containing $\tilde{L}$, and denote $I_b(\tilde{L}) := \tilde{I} \cap (0, \tilde{L})$. See figure 7 for these definitions. For $L_0$ from lemma 2, denote $I_b^0 := I_b \cap (L_0, \infty)$, $I_b^0(\tilde{L}) := I_b(\tilde{L}) \cap I_b^0$. The set $I_b^0$ can be thought of as the set of phase coherent approximate semi-travel times $L$ between sections $\Sigma_1$ and $\Sigma_2$. In the course of this chapter more restrictions on $L$ will be imposed and the lower bound will be $L_0$ increased.

To prepare the precise statement of theorem 2.2, we establish some more notation. Let

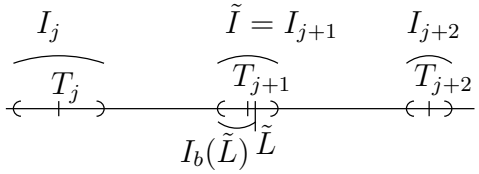


Figure 7: Image of the definitions for sets of approximate semi travel times.

$\Lambda^\delta_{\tilde{L}} := B_{\delta \exp(-\eta \tilde{L})}(0) \cap \Lambda \subset \mathbb{R}^d$. The parts of the initial conditions that decay towards $\gamma$ in light of the trichotomy estimates (2.9) will be taken as parameters and denoted

$$W_0 \;:=\; \begin{pmatrix} \tilde{w}_1 \\ \tilde{w}_2 \end{pmatrix} := \begin{pmatrix} w^{\mathrm{s}}_{+1}(0) \\ w^{\mathrm{u}}_{-2}(0) \end{pmatrix}$$

To compensate not using transverse sections $\Sigma_j$ for the initial conditions of the variations, see remark 4, we need to consider shifted variations: given a solution $u$ to (2.1) define

$$\begin{aligned} w_1(\xi;\sigma) &:= u(\xi+\sigma) - q_1(\xi) \\ w_2(\xi;\sigma,L) &:= u(2L+\sigma+\xi) - q_2(\xi) \\ W(\sigma,L) &:= (w_1(\cdot;\sigma), w_2(\cdot;\sigma,L)) \\ W_0(\sigma,L) &:= (P^{\mathrm{s}}_{+1}(0) w_1(0;\sigma), P^{\mathrm{u}}_{-2}(0) w_2(0;\sigma,L)) \end{aligned} \tag{2.22}$$

The solution operator $\mathcal{G}$ referred to in the following theorem will be defined below.

**Theorem 2.2** *Assume hypothesis 1. There exist positive constants $\epsilon, L_1, \delta, C > 0$ such that the following holds for all $\tilde{L} \in I^0_b \cap (L_1, \infty)$, $L \in I^0_b(\tilde{L}) \cap (L_1, \infty)$ and $\mu \in \Lambda^\delta_{\tilde{L}}$, $W_0 \in B_\delta(0) \subset E^{\mathrm{s}}_{+1}(0) \times E^{\mathrm{u}}_{-2}(0)$. There exists $W^1(W_0, \mu, L) \in \mathcal{X}^0_{\tilde{L}}$, which is $C^k$ in $(W_0, \mu, L)$ and a fixed point of $\mathcal{G}$. Any fixed point of $\mathcal{G}$ for $|\mu| < \delta$, $|W_0| < \delta$ and $L \geq L_1$ satisfies*

$$||W^1(W_0,\mu,L)||_{\tilde{L}} \;\leq\; C(|\mu| + |W_0| + \mathrm{e}^{(\eta-\kappa)\tilde{L}}). \tag{2.23}$$

*Let $u$ be a solution to (2.1) for $\mu \in \Lambda$ and assume there are $\sigma \in \mathbb{R}$ and $L \geq L_1$ such that $\mu \in \Lambda^\delta_L$ and for the variations $||W(\sigma,L)||^0_L < \epsilon$. There exists $\ell_L \in I^0_b \cap (L_1, \infty)$ and a unique $\sigma_L = \sigma + O(|w^{\mathrm{c}}_{+1}(L;\sigma)|)$ which is $C^k$ in $L$, so that $W(\sigma_L, \ell_L) = W^1(W_0(\sigma_L, \ell_L), \mu, \ell_L)$.*

Notice that for fixed $\mu$, the parameters $W_0$ and $L$ give $n$ dimensions. Since the ambient space has this dimension, a one-dimensional set of solutions given by the theorem is necessarily related by time shifts. We define $I^1_b := I^0_b \cap (L_1, \infty)$ and $I^1_b(\tilde{L}) := I^0_b(\tilde{L}) \cap I^1_b$.

**Remark 5** *It follows from (2.23) that for $\mu, W_0 \to 0$ and $L \to \infty$ fixed points of $\mathcal{G}$ converge to the set of heteroclinic points $\{q_1(\xi)|\xi \geq 0\} \cup \{q_2(\xi)|\xi \leq 0\}$. While solutions to (2.1) with approximate semi travel time $L \notin B_\epsilon(I_b^1)$ are beyond the reach of theorem 2.2, such solutions cannot lie arbitrarily close to $q_1$ and $q_2$ simultaneously.*
*For an approach to the uniqueness of small glued solutions using an unambiguous semi travel time $L$ we refer to remark 4. Notice that, the ambiguity in defining the approximate semi0travel time is resolved in theorem 2.2 by the unique small time shift $\sigma_L$, and parameters $W_0, L, \mu$ in ranges given in the theorem identify glued solutions with small variation uniquely up to this time shift.*

Counting parameters and boundary/initial conditions for $q_1$ and $q_2$ there are $2n+2$ degrees of freedom. We aim to satisfy (2.19) using $n$ initial conditions, leaving the rest for the matching steps 2a-2c.
For the existence proof, we will set up the solution operator assuming $P_L^{\mathrm{c}} w_1(L) = 0$, which means $w_{+1}^{\mathrm{c}}(L) = 0$ by closeness of $\mathrm{Rg}(P^{\mathrm{c}})$ and $\mathrm{span}\{\dot{q}_1(L)\}$, see remark 3. The second statement of the theorem means that *all* solutions which are simultaneously close to $q_1$ and $q_2$ in phase and parameter space can be parametrized by $W^1$ up to a small shift in time. In slight abuse of language we interpret this as a uniqueness statement of nearby solutions in terms of $W^1$. To prove this uniqueness, we will solve $w_{+1}^{\mathrm{c}}(L;\sigma,L) := P_{+1}^{\mathrm{c}}(L)(u(L+\sigma) - q_1(L)) = 0$, in terms of $\sigma$, if $w_1(L;\sigma_0,L)$ is small for a given solution $u$. For the codimension–2 case, we will later show that a topological assumption on $\mathcal{W}_1$ allows to choose heteroclinics in $\mathcal{W}_1$ so that $w_{+1}^{\mathrm{c}}(L;\sigma_0,L) = 0$ for any homoclinic $u$ which is uniformly close the heteroclinic cycle.
The formulation of (2.19) as a contraction fixed point problem should be set up so we can expect small solutions. To achieve this, boundary conditions at $L$ for $w_{+1}^{\mathrm{u}}(L)$ and $w_{-2}^{\mathrm{s}}(-L)$ are promising by the trichotomy estimates (2.9). Similarly, initial conditions $W_0 = (w_{+1}^{\mathrm{s}}(0), w_{-2}^{\mathrm{u}}(0))$ will render $w_{+1}^{\mathrm{s}}(L)$, $w_{-2}^{\mathrm{u}}(-L)$ small. The following ad hoc derivation of a solution operator for glued solutions will be justified in lemma 4. We shall use the variation of constants formula with these boundary conditions and the splitting into linear and nonlinear part as in (2.5). The solution operator $\mathcal{G}$, on the spaces $\mathcal{X}_{\tilde{L}}$, cf. (2.20),

will be of the form

$$\mathcal{G}(W;W_0,\mu,L) = \mathcal{A}(L)W_0 + \mathcal{N}(W;\mu,L) + \mathcal{B}(L). \tag{2.24}$$

Here $\mathcal{A}$, $\mathcal{N}$ and $\mathcal{B}$ are functions of $\xi_+$ and $\xi_-$ as in (2.17). We denote the evolutions $\Phi_1$ and $\Phi_2$ and nonlinearities of (2.5) projected with the trichotomies by

$$\begin{aligned}\Phi_{+1}^{\mathrm{s/c/u}}(\xi,\zeta) &:= P_{+1}^{\mathrm{s}}(\xi)\Phi_1(\xi,\zeta)\\ \Phi_{-2}^{\mathrm{s/c/u}}(\xi,\zeta) &:= P_{-2}^{\mathrm{s}}(\xi)\Phi_2(\xi,\zeta)\end{aligned}$$

As mentioned above, we take $w_{+1}^{\mathrm{c}}(-L) = 0$ and define, or rather conclude from (2.19) and the variation of constants formula, the three parts of the solution operator respecting the gluing boundary condition. To stress the splitting of growth, decay and center directions, the projections by the trichotomies are written line-wise.

We start by defining a (exponentially small, cf. (2.9)) linear coupling term of $w_1$ and $w_2$

$$\mathfrak{c}_1(W_0,L) := \Phi_{-2}^{\mathrm{u}}(-L,0)\tilde{w}_2 - \Phi_{+1}^{\mathrm{s}}(L,0)\tilde{w}_1\ ,\ \text{and} \tag{2.25}$$

$$\mathcal{A}(L)\begin{pmatrix}\xi_+\\ \xi_-\end{pmatrix}W_0 := \left(\begin{array}{l}\Phi_{+1}^{\mathrm{s}}(\xi_+,0)\tilde{w}_1\\ +\Phi_{+1}^{\mathrm{u}}(\xi_+,L)P_L^{\mathrm{u}}\mathfrak{c}_1(W_0,L)\\ 0\\ \hline \Phi_{-2}^{\mathrm{s}}(\xi_-,-L)P_L^{\mathrm{s}}(-\mathfrak{c}_1(W_0,L))\\ +\Phi_{-2}^{\mathrm{u}}(\xi_-,0)\tilde{w}_2\\ +\Phi_{-2}^{\mathrm{c}}(\xi_-,-L)P_L^{\mathrm{c}}(-\mathfrak{c}_1(W_0,L))\end{array}\right) \tag{2.26}$$

Next, we define a nonlinear coupling term $\mathfrak{c}_2 = \mathfrak{c}_2(W;L,\mu)$ and the nonlinearity $\mathcal{N}$.

$$\mathfrak{c}_2(W;L,\mu) := \int_0^{-L}\Phi_{-2}^{\mathrm{u}}(-L,\zeta)g_2(w_2(\zeta),\zeta;\mu)\mathrm{d}\zeta - \int_0^{L}\Phi_{+1}^{\mathrm{s}}(L,\zeta)g_1(w_1(\zeta),\zeta;\mu)\mathrm{d}\zeta, \tag{2.27}$$

$$
(2.28)\quad \mathcal{N}(W;\mu,L)\begin{pmatrix}\xi_+\\ \xi_-\end{pmatrix} := \left(\begin{array}{l}
\int_0^{\xi_+} \Phi^{\mathrm{s}}_{+1}(\xi_+,\zeta) g_1(w_1(\zeta),\zeta;\mu)\mathrm{d}\zeta \\
+\int_L^{\xi_+} \Phi^{\mathrm{u}}_{+1}(\xi_+,\zeta) g_1(w_1(\zeta),\zeta;\mu)\mathrm{d}\zeta + \Phi^{\mathrm{u}}_{+1}(\xi_+,L)P^{\mathrm{u}}_L \mathfrak{c}_2 \\
+\int_L^{\xi_+} \Phi^{\mathrm{c}}_{+1}(\xi_+,\zeta) g_1(w_1(\zeta),\zeta;\mu)\mathrm{d}\zeta \\
\hline
\int_{-L}^{\xi_-} \Phi^{\mathrm{s}}_{-2}(\xi_-,\zeta) g_2(w_2(\zeta),\zeta;\mu)\mathrm{d}\zeta - \Phi^{\mathrm{s}}_{-2}(\xi_-,-L)P^{\mathrm{s}}_L \mathfrak{c}_2 \\
+\int_0^{\xi_-} \Phi^{\mathrm{u}}_{-2}(\xi_-,\zeta) g_2(w_2(\zeta),\zeta;\mu)\mathrm{d}\zeta \\
+\int_{-L}^{\xi_-} \Phi^{\mathrm{c}}_{-2}(\xi_-,\zeta) g_2(w_2(\zeta),\zeta;\mu)\mathrm{d}\zeta - \Phi^{\mathrm{c}}_{-2}(\xi_-,-L)P^{\mathrm{c}}_L \mathfrak{c}_2
\end{array}\right)
$$

Notice, that $\mathcal{N}(0;0,L)\equiv 0$, because $g_j(0,\cdot;0)\equiv 0$ for $j=1,2$. Finally, the boundary term of the solution operator, which captures the rest of the gluing condition (2.19), is given by

$$
(2.29)\qquad \mathcal{B}(L)\begin{pmatrix}\xi_+\\ \xi_-\end{pmatrix} := \left(\begin{array}{l}
\Phi^{\mathrm{u}}_{+1}(\xi_+,L)P^{\mathrm{u}}_L b_L \\
\hline
-\Phi^{\mathrm{s}}_{-2}(\xi_-,-L)P^{\mathrm{s}}_L b_L \\
-\Phi^{\mathrm{c}}_{-2}(\xi_-,-L)P^{\mathrm{c}}_L b_L
\end{array}\right)
$$

Notice that $\mathcal{G}(\cdot;W_0,\mu,L)$ maps $\mathcal{X}_L$ into itself for any $W_0$, $\mu$ and $L<\infty$.
The following lemma establishes the connection of fixed points of $\mathcal{G}$ with glued solutions.

**Lemma 4** *Assume hypothesis 1 and take $L_0$, $\epsilon_0$ as in lemma 2. Let $W$ be a fixed point of the operator $\mathcal{G}(\cdot;W_0,\mu,L)$, as defined in (2.24) for some $W_0\in E^{\mathrm{s}}_{+1}(0)\times E^{\mathrm{u}}_{-2}(0)$, $\mu\in\Lambda$ and $L\geq L_0$ such that $|L-T_j|\leq\epsilon_0$ for some $j$. Then $W$ solves (2.5) and (2.19).*
*There exists $\rho_0>0$, such that the following holds. Let $u$ be a solution to (2.1) and assume there are $\sigma_0$ and $L\geq L_0$ so that $|L-T_j|\leq\epsilon_0$ for some $j$ and $|w_1(L;\sigma_0)|\leq\rho_0$. There exists a locally unique $C^k$ function $\sigma_L=O(w^{\mathrm{c}}_{+1}(L;\sigma_0))$ which solves $w^{\mathrm{c}}_{+1}(L;\sigma)=0$ such that $W(\sigma_L,L)=\mathcal{G}(W(\sigma_L,L);W_0(\sigma_L,L),\mu,L)$.*

**Proof.** Let $W$ be a fixed point for some $W_0$, $\mu$, $L$, i.e. at $\xi_\pm=\pm L$ we have

$$
W(L,-L)=\mathcal{A}(L)(L,-L)W_0+\mathcal{N}(W;W_0,\mu,L)(L,-L)+\mathcal{B}(L)(L,-L).
$$

To check the gluing (boundary) condition (2.19), we need to compute the difference of the first and second components. The left hand side yields $w_1(L)-w_2(-L)$, hence the

right hand side's difference should be $b_L$. Using lemma 2 it holds that $P^{\mathrm{u}}_{+1}P^{\mathrm{u}}_L = P^{\mathrm{u}}_L$ and $P^{\mathrm{s}}_{-2}P^{\mathrm{s}}_L = P^{\mathrm{s}}_L$ and $P^{\mathrm{c}}_{-2}P^{\mathrm{c}}_L = P^{\mathrm{c}}_L$. So the parts of $\mathcal{G}$ at $\xi_\pm = \pm L$ are

$$\begin{aligned}
\mathcal{A}(L)(L,-L)W_0 &= \begin{pmatrix} \Phi^{\mathrm{s}}_{+1}(L,0)\tilde{w}_1 + P^{\mathrm{u}}_L \mathfrak{c}_1(W_0,L) \\ -P^{\mathrm{sc}}_L \mathfrak{c}_1(W_0,L) + \Phi^{\mathrm{u}}_{-2}(-L,0)\tilde{w}_2 \end{pmatrix} \\
\mathcal{N}(W;W_0,\mu,L)(L,-L) &= \begin{pmatrix} \int_0^L \Phi^{\mathrm{s}}_{+1}(L,\zeta) g_1(w_1(\zeta),\zeta;\mu)\mathrm{d}\zeta + P^{\mathrm{u}}_L \mathfrak{c}_2(W;L,\mu) \\ -P^{\mathrm{sc}}_L \mathfrak{c}_2(W;L,\mu) + \int_0^{-L} \Phi^{\mathrm{u}}_{-2}(-L,\zeta) g_2(w_2(\zeta),\zeta;\mu)\mathrm{d}\zeta \end{pmatrix} \\
\mathcal{B}(L)(L,-L) &= \begin{pmatrix} P^{\mathrm{u}}_L b_L \\ -P^{\mathrm{sc}}_L b_L \end{pmatrix}
\end{aligned}$$

By (2.10), the component's difference in $\mathcal{B}$ yields $b_L$. We see from (2.10) and the definitions of $\mathfrak{c}_1(W_0,L)$ and $\mathfrak{c}_2(W;L,\mu)$ that the components' differences in $\mathcal{A}$ and $\mathcal{N}$ vanish. In particular, this shows that the image of $\mathcal{G}(\cdot,W_0,\mu,L)$ for any function satisfies (2.19). Finally, differentiation shows that a fixed point solves (2.5).

Now assume $W(\sigma,L)$ is a glued solution pair with $w^{\mathrm{c}}_{+1}(L;\sigma) = 0$ and $L \geq L_0$, $|L - T_j| \leq \epsilon_0$ for some $j$. Set $W_0 := (w^{\mathrm{s}}_{+1}(0;\sigma), w^{\mathrm{u}}_{-2}(0;\sigma,L))$, so by definition of $\mathcal{G}$ we have

$$\begin{aligned}
w^{\mathrm{s}}_{+1}(0;\sigma) &= P^{\mathrm{s}}_{+1}(0)\mathcal{G}_1(W(\sigma,L);W_0,\mu,L)(0) \\
w^{\mathrm{u}}_{-2}(0;\sigma,L) &= P^{\mathrm{u}}_{-2}(0)\mathcal{G}_2(W(\sigma,L);W_0,\mu,L)(0).
\end{aligned}$$

Since $W(\sigma,L)$ satisfies (2.19) it follows that $w_1(L;\sigma) - w_2(-L;\sigma,L) = b_L$. By lemma 2 this equation can be decomposed into

$$\begin{aligned}
w^{\mathrm{u}}_{+1}(L;\sigma,L) &= P^{\mathrm{u}}_L(b_L + w^{\mathrm{u}}_{-2}(-L;\sigma,L) - w^{\mathrm{s}}_{+1}(L;\sigma)) \\
w^{\mathrm{c}}_{-2}(-L;\sigma,L) &= P^{\mathrm{c}}_L(b_L + w^{\mathrm{s}}_{+1}(L;\sigma) - w^{\mathrm{u}}_{-2}(-L;\sigma,L)) \\
w^{\mathrm{s}}_{-2}(-L;\sigma,L) &= P^{\mathrm{s}}_L(b_L + w^{\mathrm{s}}_{+1}(L;\sigma) - w^{\mathrm{u}}_{-2}(-L;\sigma,L)).
\end{aligned}$$

At $\xi = L$ the variation of constants for $w_1(\xi;\sigma)$ with initial condition $w_1(0;\sigma)$ gives

$$w_1(L;\sigma) = \Phi(L,0)w_1(0;\sigma) + \int_0^L \Phi(L,\zeta) g_1(w_1(\zeta;\sigma),\zeta,\mu)\mathrm{d}\zeta.$$

Project the right hand side with $P^{\mathrm{s}}_L$, $P^{\mathrm{c}}_L$, $P^{\mathrm{u}}_L$ respectively and use the above decomposition of $w^{\mathrm{u}}_{+1}(L;\sigma)$ as well as the definition of the coupling terms $\mathfrak{c}_1$ and $\mathfrak{c}_2$. This yields precisely

the terms of $\mathcal{G}_1(W(\sigma,L),W_0,\mu,L)(L)$. Similarly, we obtain $\mathcal{G}_2(W(\sigma,L),W_0,\mu,L)(-L)$. Hence, at $\xi_\pm = \pm L$ both $W(\sigma,L)$ and $\mathcal{G}(W(\sigma,L),W_0,\mu,L)$ solve the same initial value problem and therefore coincide.

It remains to solve $w^{\mathrm{c}}_{+1}(L;\sigma)=0$ for $\sigma$ near $\sigma_0$ given $|w^{\mathrm{c}}_{+1}(L;\sigma,L)|$ is sufficiently small. Note $\ker P^{\mathrm{c}}_{+1}(L) = E^{\mathrm{s}}_{+1}(L)\oplus E^{\mathrm{u}}_{+1}(L)$ is a linear $n-1$ dimensional subspace, transverse to the flow, because $\mathrm{Rg}(P^{\mathrm{c}}_{+1}(L)) = \mathrm{span}\{\dot q_1(L)\}$. By continuity there exists $\rho_0>0$ and a constant $C>0$ such that for $|u(L+\sigma_0)-q_1(L)|\le\rho_0$ we have $|\frac{\mathrm{d}}{\mathrm{d}\sigma}|_{\sigma=\sigma_0}u(L+\sigma)|\ge C\min\{\dot q_1(\xi)\,|\,0\le\xi<T_\gamma\}>0$ uniformly in $L$. The implicit function theorem applies and $u(L+\sigma_L)\in q_1(L)+\ker P^{\mathrm{c}}_{+1}(L)$ for a unique $\sigma_L$ near $\sigma_0$. By smoothness of the flow $\sigma_L$ is $O(w^{\mathrm{c}}_{+1}(L;0))$ and $C^k$ in $L$. Since $w_1(L;\sigma_0)=u(L+\sigma_0)-q_1(L)$ the claim follows. □

For the local existence and uniqueness up to time shifts of glued solutions, this lemma allows to assume $w^{\mathrm{c}}_{+1}(L)=0$ without loss of generality, so we focus on the following fixed point equation, which we want to solve by means of theorem 2.1.

$$W = \mathcal{G}(W;W_0,\mu,L) \tag{2.30}$$

We aim to estimate some norm of $\mathcal{G}$ uniformly in $L\in I^0_b(\tilde L)$ for all $\tilde L\in I^0_b$. However, the trichotomy estimates (2.9) do not provide uniform control of the center direction, which is integrated in $\mathcal{N}$. Therefore, we make use of the weighted spaces $\mathcal{X}_L$ introduced in (2.20). Since $\mathcal{G}(W;W_0,\mu,L)-\mathcal{G}(V;W_0,\mu,L)=\mathcal{N}(W;\mu,L)-\mathcal{N}(V;\mu,L)$, differentiability in $W$ and contraction properties of $\mathcal{G}$ depend only on $\mathcal{N}$, and we examine these first.

**Lemma 5** *Assume hypothesis 1 and take $L_0$, $\epsilon_0$ as in lemma 2. For any $\tilde L\ge L\ge L_0$, $|L-T_j|\le\epsilon_0$ for some $j$, the nonlinearity $\mathcal{N}(\cdot;\mu,L):\mathcal{X}_{\tilde L}\to\mathcal{X}_{\tilde L}$ is $C^k$ in $W$, $\mu$ and $L$, and there exists a constant $C$ such that*

$$\begin{aligned}
||\partial_W\mathcal{N}(W;\mu,L)||_{\tilde L} &\le C\mathrm{e}^{(\kappa+\eta)(\tilde L-L)}(||W||_{\tilde L}+\mathrm{e}^{\eta L}|\mu|)\\
||\mathcal{N}(W;\mu,L)||_{\tilde L} &\le C\mathrm{e}^{(\kappa+\eta)(\tilde L-L)}\left(||W||_{\tilde L}||W||^0_{\tilde L}+|\mu|\,||W||_{\tilde L}+|\mu|\right).
\end{aligned}$$

**Proof.** We first find a family of bounded linear operators $\mathcal{I}(L):\mathcal{X}_{\tilde L}\to\mathcal{X}_{\tilde L}$, $C^k$ for any $\tilde L$, $L$ as in the statement, and a family of functions $G(\cdot;\mu):\mathcal{X}_{\tilde L}\to\mathcal{X}_{\tilde L}$ of class $C^k$ in $W$ and

$\mu$ such that $\mathcal{N}(W;\mu,L) = \mathcal{I}(L)G(W;\mu)$. This implies the claimed smoothness of $\mathcal{N}$, and the estimates will follow. Definition (2.28) implies that given any function

$$g = (g_1, g_2) : \mathcal{X}_{\tilde{L}} \to \mathcal{X}_{\tilde{L}},\ g_1 : C_{\eta,\tilde{L}} \to C_{\eta,\tilde{L}},\ g_2 : C_{-\eta,\tilde{L}} \to C_{-\eta,\tilde{L}}$$

we can define the desired linear operator $\mathcal{I}(L)$ to be

$$\begin{aligned}
\mathcal{I}(L)g\begin{pmatrix}\xi_+\\ \xi_-\end{pmatrix} &:= \left(\begin{array}{l}
\int_0^{\xi_+} \Phi^{\mathrm{s}}_{+1}(\xi_+,\zeta)g_1(\zeta)\mathrm{d}\zeta \\
+\int_L^{\xi_+} \Phi^{\mathrm{u}}_{+1}(\xi_+,\zeta)g_1(\zeta)\mathrm{d}\zeta + \Phi^{\mathrm{u}}_{+1}(\xi_+,L)P^{\mathrm{u}}_L\mathfrak{c}(g;L) \\
+\int_L^{\xi_+} \Phi^{\mathrm{c}}_{+1}(\xi_+,\zeta)g_1(\zeta)\mathrm{d}\zeta \\
\hline
\int_{-L}^{\xi_-} \Phi^{\mathrm{s}}_{-2}(\xi_-,\zeta)g_2(\zeta)\mathrm{d}\zeta - \Phi^{\mathrm{s}}_{-2}(\xi_-,-L)P^{\mathrm{s}}_L\mathfrak{c}(g;L) \\
+\int_0^{\xi_-} \Phi^{\mathrm{u}}_{-2}(\xi_-,\zeta)g_2(\zeta)\mathrm{d}\zeta \\
+\int_{-L}^{\xi_-} \Phi^{\mathrm{c}}_{-2}(\xi_-,\zeta)g_2(\zeta)\mathrm{d}\zeta - \Phi^{\mathrm{c}}_{-2}(\xi_-,-L)P^{\mathrm{c}}_L\mathfrak{c}(g;L)
\end{array}\right) \\
\text{where } \mathfrak{c}(g;L) &:= \int_0^{-L} \Phi^{\mathrm{u}}_{-2}(-L,\zeta)g_2(\zeta)\mathrm{d}\zeta - \int_0^{L} \Phi^{\mathrm{s}}_{+1}(L,\zeta)g_1(\zeta)\mathrm{d}\zeta.
\end{aligned}$$

In the following estimates we frequently use the trichotomy estimates (2.9) and that for $0 \le \zeta \le L \le \tilde{L}$ we have the pointwise estimate

$$|g_1(\zeta)| = \mathrm{e}^{-\eta\zeta}\mathrm{e}^{\eta\zeta}|g_1(\zeta)| \le \mathrm{e}^{-\eta\zeta}\sup_{0\le\zeta\le L}\mathrm{e}^{\eta\zeta}|g_1(\zeta)| = \mathrm{e}^{-\eta\zeta}||g_1||_{\eta,\tilde{L}},$$

similarly $|g_2(\zeta)| \le \mathrm{e}^{\eta\zeta}||g_2||_{-\eta,\tilde{L}}$ for $-\tilde{L} \le -L \le \zeta \le 0$. As to the coupling term, we have

$$\begin{aligned}
|\mathfrak{c}(g;L)| &= |\int_0^{-L} \Phi^{\mathrm{u}}_{-2}(-L,\zeta)g_2(\zeta)\mathrm{d}\zeta - \int_0^{L} \Phi^{\mathrm{s}}_{+1}(L,\zeta)g_1(\zeta)\mathrm{d}\zeta| \\
&\le K_2\int_{-L}^{0} \mathrm{e}^{-\kappa(L+\zeta)}|g_2(\zeta)|\mathrm{d}\zeta + K_2\int_0^{L} \mathrm{e}^{-\kappa(L-\zeta)}|g_2(\zeta)|\mathrm{d}\zeta \\
&\le K_2\int_{-L}^{0} \mathrm{e}^{-\kappa(L+\zeta)}\mathrm{e}^{\eta\zeta}||g_2||_{-\eta,\tilde{L}}\mathrm{d}\zeta + K_2\int_0^{L} \mathrm{e}^{-\kappa(L-\zeta)}\mathrm{e}^{-\eta\zeta}||g_1||_{\eta,\tilde{L}}\mathrm{d}\zeta \\
&\le K_2\left(\frac{\mathrm{e}^{-\eta L}-\mathrm{e}^{-\kappa L}}{\kappa-\eta}||g_2||_{-\eta,\tilde{L}} + \frac{\mathrm{e}^{-\eta L}-\mathrm{e}^{-\kappa L}}{\kappa-\eta}||g_1||_{\eta,\tilde{L}}\right) \\
&\le \frac{K_2}{\kappa-\eta}\mathrm{e}^{-\eta L}||g||_{\tilde{L}}. \qquad (2.31)
\end{aligned}$$

Hence the coupling is exponentially small, and applying the projected evolutions we obtain

$$\begin{aligned}\sup_{0\le\xi\le\tilde L}|\Phi^{\mathrm u}_{+1}(\xi,L)P^{\mathrm u}_L\mathfrak c(g;L)| &\le \sup_{0\le\xi\le\tilde L}K_2\mathrm e^{-\kappa(L-\xi)}K_3\frac{K_2}{\kappa-\eta}\mathrm e^{-\eta L}||g||_{\tilde L}\\ &\le C\mathrm e^{\kappa(\tilde L-L)}\mathrm e^{-\eta L}||g||_{\tilde L} \qquad (2.32)\\ \sup_{0\le\xi\le\tilde L}|\Phi^{\mathrm c}_{+1}(\xi,L)P^{\mathrm c}_L\mathfrak c(g;L)| &\le C\mathrm e^{-\eta L}||g||_{\tilde L}. \qquad (2.33)\end{aligned}$$

Now we consider the six parts of $\mathcal I(L)$ without the projected and evolved coupling term aiming at uniform estimates in $\tilde L$, $L$. We emphasize, that constants depend on $\eta$.

i)
$$\begin{aligned}\sup_{0\le\xi\le\tilde L}|\mathrm e^{\eta\xi}\int_0^\xi\Phi^{\mathrm s}_{+1}(\xi,\zeta)g_1(\zeta)\mathrm d\zeta| &\le \sup_{0\le\xi\le\tilde L}\mathrm e^{\eta\xi}\int_0^\xi K_2\mathrm e^{-\kappa(\xi-\zeta)}|g_1(\zeta)|\mathrm d\zeta\\ &\le K_2\sup_{0\le\xi\le\tilde L}\mathrm e^{\eta\xi}\int_0^\xi\mathrm e^{-\kappa(\xi-\zeta)}\mathrm e^{-\eta\zeta}||g_1||_{\eta,\tilde L}\mathrm d\zeta\\ &= K_2\sup_{0\le\xi\le\tilde L}\mathrm e^{\eta\xi}\frac{\mathrm e^{-\eta\xi}-\mathrm e^{-\kappa\xi}}{\kappa-\eta}||g_1||_{\eta,\tilde L}\\ &\le \frac{K_2}{\kappa-\eta}||g_1||_{\eta,\tilde L}\end{aligned}$$

ii)
$$\begin{aligned}\sup_{0\le\xi\le\tilde L}|\mathrm e^{\eta\xi}\int_L^\xi\Phi^{\mathrm u}_{+1}(\xi,\zeta)g_1(\zeta)\mathrm d\zeta| &\le \sup_{0\le\xi\le\tilde L}\mathrm e^{\eta\xi}|\int_L^\xi K_2\mathrm e^{-\kappa(\zeta-\xi)}|g_1(\zeta)|\mathrm d\zeta|\\ &\le K_2\sup_{0\le\xi\le\tilde L}\mathrm e^{\eta\xi}|\int_L^\xi\mathrm e^{-\kappa(\zeta-\xi)}\mathrm e^{-\eta\zeta}||g_1||_{\eta,\tilde L}\mathrm d\zeta|\\ &= K_2\sup_{0\le\xi\le\tilde L}\mathrm e^{\eta\xi}\frac{|\mathrm e^{-\kappa(L-\xi)-\eta L}-\mathrm e^{-\eta\xi}|}{\kappa+\eta}||g_1||_{\eta,\tilde L}\\ &\le C\mathrm e^{(\kappa+\eta)(\tilde L-L)}||g_1||_{\eta,\tilde L}\end{aligned}$$

iii) The following estimate shows the relevance of weighted spaces for uniform estimates:

$$\begin{aligned}\sup_{0\le\xi\le\tilde L}|\mathrm e^{\eta\xi}\int_L^\xi\Phi^{\mathrm c}_{+1}(\xi,\zeta)g_1(\zeta)\mathrm d\zeta| &\le \sup_{0\le\xi\le\tilde L}K_2\mathrm e^{\eta\xi}|\int_L^\xi\mathrm e^{-\eta\zeta}||g_1||_{\eta,\tilde L}\mathrm d\zeta|\\ &= K_2\sup_{0\le\xi\le\tilde L}\mathrm e^{\eta\xi}\frac{|\mathrm e^{-\eta\xi}-\mathrm e^{-\eta L}|}{\eta}||g_1||_{\eta,\tilde L}\\ &\le C\mathrm e^{\eta(\tilde L-L)}||g_1||_{\eta,\tilde L}\end{aligned}$$

$$\text{iv)}\quad \sup_{-\tilde{L}\le\xi\le 0}|\mathrm{e}^{-\eta\xi}\int_{-L}^{\xi}\Phi^{\mathrm{s}}_{-2}(\xi,\zeta)g_2(\zeta)\mathrm{d}\zeta| \;\le\; \sup_{0\le\xi\le\tilde{L}}\mathrm{e}^{-\eta\xi}|\int_{-L}^{\xi}K_2\mathrm{e}^{\kappa(\zeta-\xi)}\mathrm{e}^{\eta\zeta}||g_2||_{-\eta,\tilde{L}}\mathrm{d}\zeta|$$
$$= K_2\sup_{0\le\xi\le\tilde{L}}\mathrm{e}^{-\eta\xi}\frac{|\mathrm{e}^{-\kappa(L+\xi)-\eta L}-\mathrm{e}^{\eta\xi}|}{\kappa+\eta}||g_2||_{-\eta,\tilde{L}}$$
$$\le C\mathrm{e}^{(\kappa+\eta)(\tilde{L}-L)}||g_2||_{-\eta,\tilde{L}}$$

$$\text{v)}\quad \sup_{-\tilde{L}\le\xi\le 0}|\mathrm{e}^{-\eta\xi}\int_{0}^{\xi}\Phi^{\mathrm{u}}_{-2}(\xi,\zeta)g_2(\zeta)\mathrm{d}\zeta| \;\le\; \sup_{-\tilde{L}\le\xi\le 0}K_2\mathrm{e}^{-\eta\xi}\int_{0}^{\xi}\mathrm{e}^{\kappa(\xi-\zeta)}\mathrm{e}^{\eta\zeta}||g_2||_{-\eta,\tilde{L}}\mathrm{d}\zeta$$
$$= K_2\sup_{-\tilde{L}\le\xi\le 0}\mathrm{e}^{-\eta\xi}\frac{\mathrm{e}^{\kappa\xi}-\mathrm{e}^{\eta\xi}}{\kappa-\eta}||g_2||_{-\eta,\tilde{L}}$$
$$\le C||g_2||_{-\eta,\tilde{L}}$$

vi) Again, the center direction's estimate relies on the exponential weights:

$$\sup_{-\tilde{L}\le\xi\le 0}|\mathrm{e}^{-\eta\xi}\int_{-L}^{\xi}\Phi^{\mathrm{c}}_{-2}(\xi,\zeta)g_2(\zeta)\mathrm{d}\zeta| \;\le\; K_2\sup_{-\tilde{L}\le\xi\le 0}\mathrm{e}^{-\eta\xi}|\int_{-L}^{\xi}\mathrm{e}^{\eta\zeta}||g_2||_{-\eta,\tilde{L}}\mathrm{d}\zeta|$$
$$\le K_2\sup_{-\tilde{L}\le\xi\le 0}\frac{\mathrm{e}^{-\eta\xi}}{\eta}|\mathrm{e}^{\eta\xi}-\mathrm{e}^{-\eta L}|\,||g_2||_{-\eta,\tilde{L}}$$
$$\le C\mathrm{e}^{\eta(\tilde{L}-L)}||g_2||_{-\eta,\tilde{L}}$$

Now i) to vi) and (2.33,2.32) yield $\mathcal{I}(L)$ continuous in $\mathcal{X}_{\tilde{L}}$ for $\tilde{L}\ge L\ge L_0$ with

$$||\mathcal{I}(L)||_{\mathcal{L}(\mathcal{X}_{\tilde{L}},\mathcal{X}_{\tilde{L}})}\le C_{\mathcal{I}}\mathrm{e}^{\kappa(\tilde{L}-L)}. \tag{2.34}$$

Notice that $\xi\mapsto P^{\mathrm{s/c/u}}_{+1/-2}(\xi)v$ is $C^k$ for any $v$, cf. proof of lemma 1.1 in [50]. Together with the smoothness of $g_j$, $j=1,2$ we conclude that $\mathcal{I}(L)$ is $C^k$ in $L$. As to the specific Nemitskij operator for $\mathcal{N}(W;\mu,L)$, i.e.

$$G(W;\mu)\begin{pmatrix}\xi_+\\ \xi_-\end{pmatrix}=\begin{pmatrix} g_1(w_1(\xi_+),\xi_+;\mu)\\ g_2(w_2(\xi_-),\xi_-;\mu)\end{pmatrix},$$

it follows e.g. from [50], Lemma 3.1, that $G(W;\mu)$ is $C^k$ in $W$ and $\mu$ on $\mathcal{X}_{\tilde{L}}$. Together, we conclude $\mathcal{N}(W;\mu,L)=\mathcal{I}(L)G(W;\mu,L)$ is $C^k$ in $W$ and $\mu$.

The estimate for $\mathcal{N}$ follows from (2.34) and

$$\begin{aligned}
||G(W;\mu)||_{\tilde{L}} &= ||g_1(w_1(\cdot),\cdot;\mu)||_{\eta,\tilde{L}} + ||g_2(w_2(\cdot),\cdot;\mu)||_{-\eta,\tilde{L}} \\
&\leq \sup_{0\leq\xi\leq\tilde{L}} \mathrm{e}^{\eta\xi}|g_1(w_1(\cdot),\cdot;\mu)| + \sup_{-\tilde{L}\leq\xi\leq 0} \mathrm{e}^{-\eta\xi}|g_2(w_2(\cdot),\cdot;\mu)| \\
&\leq C\left(\sup_{0\leq\xi\leq\tilde{L}} \mathrm{e}^{\eta\xi}(|w_1(\xi)|^2 + |\mu|(|w_1(\xi)| + |q_1(\xi)-\gamma(\xi)|))\right. \\
&\quad \left. + \sup_{-\tilde{L}\leq\xi\leq 0} \mathrm{e}^{-\eta\xi}(|w_2(\xi)|^2 + |\mu|(|w_2(\xi)| + |q_2(\xi)-\gamma(\xi)|))\right) \\
&\leq C\left(\sup_{0\leq\xi\leq\tilde{L}} |w_1(\xi)|||w_1||_{\eta,\tilde{L}} + |\mu|(||w_1||_{\eta,\tilde{L}} + ||q_1-\gamma(\cdot)||_{\eta,\tilde{L}})\right. \\
&\quad \left. + \sup_{-\tilde{L}\leq\xi\leq 0} |w_2(\xi)|||w_2||_{-\eta,\tilde{L}} + |\mu|(||w_2||_{-\eta,\tilde{L}} + ||q_2-\gamma(\cdot)||_{-\eta,\tilde{L}})\right) \\
&\leq C\left(||W||_{\tilde{L}}||W||^0_{\tilde{L}} + |\mu|(||W||_{\tilde{L}} + ||q_1-\gamma||_{\eta,\tilde{L}} + ||q_2-\gamma||_{-\eta,\tilde{L}})\right) \\
&\leq C\left(||W||_{\tilde{L}}||W||^0_{\tilde{L}} + |\mu|\,||W||_{\tilde{L}} + |\mu|\right) \leq C\left(||W||^2_{\tilde{L}} + |\mu|\,||W||_{\tilde{L}} + |\mu|\right). \qquad (2.35)
\end{aligned}$$

Here we used (2.6), and the final constant $C$ absorbed $K_5 := \lim_{\tilde{L}\to\infty} ||q_1-\gamma||_{\eta,\tilde{L}} + ||q_2-\gamma||_{-\eta,\tilde{L}}$ which is bounded by (2.3). Analogously, the estimate for $\partial_W\mathcal{N}$ follows from

$$||\partial_W G(\cdot;\mu)||_{\tilde{L}} = ||\partial_{w_1} g_1(w_1(\cdot),\cdot;\mu)||_{\eta,\tilde{L}} + ||\partial_{w_2} g_2(w_2(\cdot),\cdot;\mu)||_{-\eta,\tilde{L}}$$

and from (2.6) with possibly adjusted $K_1$ so that

$$||\partial_{w_1} g_1(w_1,\cdot;\mu)||_{\eta} + ||\partial_{w_2} g_2(w_2,\cdot;\mu)||_{-\eta} \leq K_1(||W||_{\tilde{L}} + \mathrm{e}^{\eta\tilde{L}}|\mu|).$$

□

As remarked in the definitions of the coupling terms $\mathfrak{c}_1$ and $\mathfrak{c}_2$, the coupling between the components is in fact exponentially small. The estimates of the norms for each component in the lemma could be refined to reflect this. However, for our purposes this is not necessary.

**proof of theorem 2.2.** The theorem follows from the implicit function theorem 2.1 as follows. For the estimates (2.11,2.14) in theorem 2.1, we first consider $\mathcal{A}$ as defined in (2.26). We frequently use the trichotomy estimates (2.9) which immediately give

$$|\mathfrak{c}_1(W_0,L)| = |\Phi^{\mathrm{u}}_{-2}(-L,0)\tilde{w}_2 - \Phi^{\mathrm{s}}_{+1}(L,0)\tilde{w}_1| \leq K_2\mathrm{e}^{-\kappa L}|W_0|, \qquad (2.36)$$

and with $|P_L^{\mathrm{s/c/u}}| \leq K_3$ from lemma 2 we can estimate

$$\begin{aligned}
\sup_{0\leq\xi\leq\tilde{L}} |\mathrm{e}^{\eta\xi}\Phi^{\mathrm{s}}_{+1}(\xi,0)\tilde{w}_1| &\leq \sup_{0\leq\xi\leq\tilde{L}} \mathrm{e}^{(\eta-\kappa)\xi}K_2|\tilde{w}_1| = K_2|\tilde{w}_1| \\
\sup_{0\leq\xi\leq\tilde{L}} |\mathrm{e}^{\eta\xi}\Phi^{\mathrm{u}}_{+1}(\xi,L)P^{\mathrm{u}}_L\mathfrak{c}_1(W_0,L)| &\leq \sup_{0\leq\xi\leq\tilde{L}} \mathrm{e}^{\eta\xi+\kappa(\xi-L)}K_2K_3|\mathfrak{c}_1(W_0,L)| \\
&\leq C\mathrm{e}^{\eta\tilde{L}}\mathrm{e}^{\kappa(\tilde{L}-L)}|\mathfrak{c}_1(W_0,L)| \\
&\leq C\mathrm{e}^{\kappa(\tilde{L}-L)}\mathrm{e}^{(\eta-\kappa)\tilde{L}}|W_0| \\
\sup_{-\tilde{L}\leq\xi\leq 0} |\mathrm{e}^{-\eta\xi}\Phi^{\mathrm{s}}_{-2}(\xi,-L)P^{\mathrm{s}}_L\mathfrak{c}_1(W_0,L)| &\leq \sup_{-\tilde{L}\leq\xi\leq 0} \mathrm{e}^{-\eta\xi-\kappa(\xi+L)}K_2K_3|\mathfrak{c}_1(W_0,L)| \\
&= K_2K_3\mathrm{e}^{\kappa(\tilde{L}-L)}\mathrm{e}^{\eta\tilde{L}}|\mathfrak{c}_1(W_0,L)| \\
&\leq C\mathrm{e}^{\kappa(\tilde{L}-L)}\mathrm{e}^{(\eta-\kappa)\tilde{L}}|W_0| \\
\sup_{-\tilde{L}\leq\xi\leq 0} |\mathrm{e}^{-\eta\xi}\Phi^{\mathrm{u}}_{-2}(\xi,0)\tilde{w}_2| &\leq \sup_{-\tilde{L}\leq\xi\leq 0} \mathrm{e}^{(-\eta+\kappa)\xi}K_2|\tilde{w}_2| = K_2|\tilde{w}_2| \\
\sup_{-\tilde{L}\leq\xi\leq 0} |\mathrm{e}^{\eta\xi}\Phi^{\mathrm{c}}_{-2}(\xi,-L)P^{\mathrm{c}}_L\mathfrak{c}_1(W_0,L)| &\leq \sup_{-\tilde{L}\leq\xi\leq 0} K_2K_3\mathrm{e}^{\eta\xi}|\mathfrak{c}_1(W_0,L)| \\
&\leq C\mathrm{e}^{(\eta-\kappa)\tilde{L}}|W_0|
\end{aligned}$$

For $\tilde{L} \in I_b^0$ and $L \in I_b^0(\tilde{L})$ we have $0 < \tilde{L} - L < \epsilon_0 < T_\gamma/2$, and with $|W_0| = |\tilde{w}_1| + |\tilde{w}_2|$ we obtain a constant $C$ such that

$$||\mathcal{A}(L)W_0||_{\tilde{L}} \leq C|W_0|. \tag{2.37}$$

Together with lemma 5 we obtain the estimates (2.11) needed in theorem 2.1. Now consider the constant boundary term $\mathcal{B}$ and its projections.

$$\begin{aligned}
\sup_{0\leq\xi\leq\tilde{L}} |\mathrm{e}^{\eta\xi}\Phi^{\mathrm{u}}_{+1}(\xi,L)P^{\mathrm{u}}_Lb_L| &\leq \sup_{0\leq\xi\leq\tilde{L}} \mathrm{e}^{-\kappa(L-\xi)+\eta\xi}K_2K_3|b_L| \leq C\mathrm{e}^{\kappa(\tilde{L}-L)}\mathrm{e}^{\eta\tilde{L}}|b_L| \\
\sup_{-\tilde{L}\leq\xi\leq 0} |\mathrm{e}^{-\eta\xi}\Phi^{\mathrm{s}}_{-2}(\xi,-L)P^{\mathrm{s}}_Lb_L| &\leq \sup_{-\tilde{L}\leq\xi\leq 0} \mathrm{e}^{-\eta\xi-\kappa(\xi+L)}C|b_L| \leq C\mathrm{e}^{\kappa(\tilde{L}-L)}\mathrm{e}^{\eta\tilde{L}}|b_L| \\
\sup_{-\tilde{L}\leq\xi\leq 0} |\mathrm{e}^{-\eta\xi}\Phi^{\mathrm{c}}_{-2}(\xi,-L)P^{\mathrm{c}}_Lb_L| &\leq \sup_{-\tilde{L}\leq\xi\leq 0} \mathrm{e}^{-\eta\xi}K_2K_3|b_L| \leq C\mathrm{e}^{\eta\tilde{L}}|b_L|
\end{aligned}$$

For any $\tilde{L} \in I_b^0$ and $L \in I_b^0(\tilde{L})$ we have $\tilde{L} - L \leq T_\gamma/2$ and so lemma 3 implies

$$||\mathcal{B}(L)||_{\tilde{L}} \leq C\mathrm{e}^{\eta\tilde{L}}|b_L| \leq C\mathrm{e}^{(\eta-\kappa)\tilde{L}} \tag{2.38}$$

and in particular $\mathcal{B}(L) \to 0$ as $L \to \infty$.

Let $C_2$ be the sum of the constant $C$ from lemma 5 and that of (2.37), and set $C_1 := 1$. Choose $\tilde{L}_1 \geq L_0$ so that $C_1|\mathcal{B}(L)| \leq 1/(8C_1C_2)$.

These estimates allow to apply theorem 2.1. Fix any $\tilde{L} \in I_b^0 \cap (\tilde{L}_1, \infty)$ and define $I := I_b^0(\tilde{L})$, $X = Y := \mathcal{X}_{\tilde{L}}$ and $Z := \Lambda^1_{\tilde{L}} \times \mathbb{R}^n$ so $y = W$, $z = (\mu, W_0)$. Set $Q(z, L) := \mathrm{Id} : Y \to Y$, $R(y, z, L) := -\mathcal{A}(L)W_0 - \mathcal{N}(y, z, L)$ and $S(L) := \mathcal{B}(L)$.

Theorem 2.1 provides constants $\epsilon_1$, $\tilde{\delta}_1$ and $C$ independent of $\tilde{L}$ and the desired fixed point $W^1(W_0, \mu, L)$ of $\mathcal{G}$. This is unique in[2] $B_{\epsilon_1}(0; \tilde{L})$ and $C^k$ in $\mu$, $W_0$, $L$ for $|W_0| \leq \delta_1/2$, $\tilde{L} \in I_b^0 \cap (\tilde{L}_1, \infty)$, $L \in I_b^0(\tilde{L}) \cap (\tilde{L}_1, \infty)$ and $|\mu| \leq \delta_1/2 \exp(-\eta\tilde{L})$. Note that while the parameter $|\mu|$ needs to be exponentially small to obtain a contraction, the estimate (2.13) holds for $|\mu| + |W_0| \leq \delta$ and $L \in I_b^0 \cap (\tilde{L}_1, \infty)$. Only the estimate for the derivative of $G$ requires exponentially small $\mu$, cf. lemma 5. Later we will derive for 1–homoclinics from the estimate (2.13) that the parameter is exponentially small with rate larger than $\eta$ and thus obtain uniqueness in a uniform neighborhood in parameter space. Here, $|b_L| \leq C\mathrm{e}^{-\kappa\tilde{L}}$ and so (2.13) becomes

$$||W^1(W_0, \mu, L)||_{\tilde{L}} \quad \leq \quad C(|\mu| + |W_0| + \mathrm{e}^{(\eta-\kappa)\tilde{L}}).$$

Concluding the existence statement, take $\delta_1 = \tilde{\delta}_1/2$ and notice lemma 4 implies the fixed point is a glued solution.

As to the uniqueness, assume for the variation of a given solution $W(\sigma, L)$ and $\rho > 0$ that $W(\sigma, L) \in B_\rho^0(0; L)$, i.e. smallness in $\mathcal{X}_L^0$. Recall the shift function $\sigma_L$ from lemma 4 and that for $\rho \leq \rho_0$ we have $W(\sigma_L, L)$ is a fixed point of $\mathcal{G}$. Firstly, we show that if $\rho$ is sufficiently small and $L$ is large enough, then we can find $\ell_L \in I_b^0$ such that $W(\sigma_{\ell_L}, \ell_L)$ is a fixed point of $\mathcal{G}$. Secondly, we prove that if a fixed point of $\mathcal{G}$ is small in $\mathcal{X}_L^0$ then it is small in $\mathcal{X}_L$, i.e. it is the unique $\mathcal{X}_L$-small fixed point $W^1$. Together, we can conclude uniqueness in the sense of the theorem statement.

For $W(\sigma, L) \in B_\rho^0(0; L)$ we have (cf. figure 8)

$$|q_1(L) - q_2(-L)| = |q_1(L) - u(L + \sigma) + u(L + \sigma) - q_2(-L)| = |w_2(-L; \sigma) - w_1(L; \sigma)| \leq \rho.$$

[2]In the application of theorem 2.1 we did not use the full structure of $\mathcal{G}$, and the constants and sizes of neighborhoods are not optimal, but sufficient for our purposes.

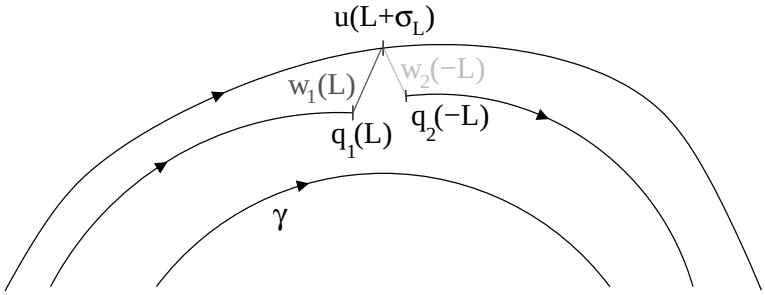


Figure 8: Small glued solutions at the approximate semi-travel-time.

Recall the definition of $T_j$ and $I_j$ from lemma 3. Assume $q_1(\xi_j)-q_2(-\xi_j)\to 0$ as $j\to\infty$ for some sequence of real numbers $\xi_j$. This is equivalent to $\gamma(\xi_j)-\gamma(-\xi_j)\to 0$, which implies $\operatorname{dist}(\xi_j,\{T_i\,|\,i\geq 0\})\to 0$. Hence, for all $\rho>0$ there is a constant $\bar{L}_1\geq\tilde{L}_1$ and locally unique $j_L$ such that for all $L\geq\bar{L}_1$ we have $|L-T_{j_L}|\leq C\rho$ if $W(\sigma,L)\in B^0_\rho(0;L)$. We next define $\ell_L$: if $L\in I_b$ set $\ell_L:=L$, otherwise $\ell_L:=T_{j_L}$. It follows that $W(\sigma,\ell_L)\in B^0_{\rho'}(0;\ell_L)$, where $\rho'\leq C|L-T_{j_L}|$ accounts for shifting $u(\xi+2L+\sigma)$ to $u(\xi+2\ell_L+\sigma)$ relative to $q_2(\xi)$ for $\xi\in[-L,0]$. Here $C$ depends on $\sup\{\dot{q}_2(\xi)\,|\,\xi\geq 0\}$, which is bounded because $q_2(\xi)-\gamma(\xi)\to 0$ as $\xi\to-\infty$. Thus, there are constants $C>0$ and $\rho_1>0$ such that $\rho'\leq C\rho$ for all $0<\rho\leq\rho_1$. Define $\rho_2:=\min\{\rho_1,\rho_0/C\}$ where $\rho_0$ is from lemma 4. If $\rho\leq\rho_2$ then $W(\sigma,\ell_L)\in B^0_{\rho_0}(0;\ell_L)$ and lemma 4 implies $W(\sigma_{\ell_L},\ell_L)$ is a fixed point of $\mathcal{G}$. Since $\sigma_L=O(w^{\mathrm{c}}_{+1}(L,\sigma))$, we can choose $\rho_2$ so that in addition $W(\sigma_{\ell_L},\ell_L)\in B^0_{\rho_1}(0;\ell_L)$.

In the second step we show that a given fixed point which is small in $\mathcal{X}^0_L$ is actually small in $\mathcal{X}_L$ and conclude that $W(\sigma_{\ell_L},\ell_L)$ is identical to one of the unique fixed points found above. Using lemma 5, (2.37) and (2.38) it follows for any fixed point $V(\sigma,L)$ of $\mathcal{G}$ with $L\in I^0_b\cap(\bar{L}_1,\infty)$, $|W_0|+|\mu|\leq\delta_1$ that

$$\begin{aligned} ||V(\sigma,L)||_L &\leq C\left(|V(\sigma,L)(0)|+||V(\sigma,L)||_L(||V(\sigma,L)||^0_L+|\mu|)+|\mu|+\mathrm{e}^{(\eta-\kappa)L}\right)\\ \Rightarrow ||V(\sigma,L)||_L &\leq C\frac{\mathrm{e}^{(\eta-\kappa)L}+\rho_2+|\mu|}{1-C(\rho_2+|\mu|)}=:c(L,\rho_2,\mu). \end{aligned}$$

By definition of $c(L,\rho,\mu)$ we can choose $L_1$, $\delta$ and $\rho_3$ so that $L_1\geq\bar{L}_1$, $\rho_2\geq\rho_3>0$ and such that $\delta_1\geq\delta>0$ and $c(L,\rho,\mu)\leq\epsilon_1$ for any $L\geq L_1$, $\rho\leq\rho_3$ and $|\mu|\leq\delta\exp(-\eta\tilde{L})$. Define $\epsilon:=\min\{\rho_3,\epsilon_1,\delta_1\}$, so $W(\sigma,L)\in B^0_\epsilon(0;L)$ satisfies all conditions simultaneously and we obtain a fixed point $W(\sigma_{\ell_L},\ell_L)\in B_{\epsilon_1}(0;\ell_L)$. By the contraction argument above,

the fixed point of $\mathcal{G}(\cdot; W_0(\sigma_{\ell_L}, \ell_L), \mu, \ell_L)$ in this ball is unique, so $W(\sigma_{\ell_L}, \ell_L)$ is identical to $W^1(W_0(\sigma_{\ell_L}, \ell_L), \mu, \ell_L)$. Therefore this fixed point is actually unique in $B^0_\epsilon(0; \ell_L)$ and $u$ can be written as in the theorem statement. □

### 2.3.2 Matching the glued solutions, homoclinic orbits

We want to find all $W_0$, $\mu$ and $L$ such that the associated glued solution $W^1(W_0, \mu, L)$ yields a homoclinic orbit to $p_0$ by means of (2.18). For this, we now assume the di- and trichotomies from lemma 1 are maximally transverse at $\xi = 0$ and the heteroclinic cycle is codimension–2 or –1.

**Hypothesis 2 (codimension 2)**

$$i_{p_0} = i_\gamma + 1, \quad \dim(E^{\mathrm{u}}_{-1}(0) \cap E^{\mathrm{s}}_{+1}(0)) = 1, \quad \dim(E^{\mathrm{s}}_{+2}(0) + E^{\mathrm{u}}_{-2}(0)) = n - 2$$

**Hypothesis 3 (codimension 1)**

$$i_{p_0} = i_\gamma, \quad \dim(E^{\mathrm{u}}_{-1}(0) \cap E^{\mathrm{s}}_{+1}(0)) = 0, \quad \dim(E^{\mathrm{s}}_{+2}(0) + E^{\mathrm{u}}_{-2})(0) = n - 1$$

We assume that the parameters transversely unfold the intersection of stable and center-unstable manifolds: let $a^j_0$, $j = 1, 2$, be so that $E_2 := (E^{\mathrm{s}}_{+2} + E^{\mathrm{u}}_{-2}) = \mathrm{span}\{a^1_0, a^2_0\}^\perp$ and $a^j$, $j = 1, 2$, be solutions to the adjoint linear equation $\dot{a}^j = -(A_2(\xi))^* a^j$, with $a^j(0) = a^j_0$, $j = 1, 2$.

**Hypothesis 4** *The following linear map $\mathcal{M} : \mathbb{R}^d \to (E_2)^\perp$ is invertible,*

$$\mu \mapsto \sum_{j=1,2} \int_{-\infty}^{\infty} \langle f_\mu(q_2(\zeta); 0)\mu, a^j(\zeta)\rangle \mathrm{d}\zeta a^j_0.$$

We define $E_1 := E^{\mathrm{u}}_{-1}(0) \cap E^{\mathrm{s}}_{+1}(0)$ and $\tilde{Q} : E^{\mathrm{u}}_{-1}(0) \to E_1$ a projection with arbitrary kernel containing $E^{\mathrm{c}}_{+1}(0)$. Notice $E_1 = \{0\}$ and $\tilde{Q} = 0$ under hypothesis 3.

**Theorem 2.3** *Assume hypotheses 2 or 3, and 1, 4. There exist positive constants $\epsilon_4$, $\delta_4$, $L_4$ and $C$ such that for $\tilde{L} \in I^1_b \cap (L_4, \infty)$, $L \in I^1_b(\tilde{L}) \cap (L_4, \infty)$ and $\mathfrak{v} \in B_{\delta_4}(0) \subset E_1$ the following holds. There exists countably infinite families of $C^k$-curves $\mu(L, \mathfrak{v}) \in B_{\delta_4}(0) \subset$*

$\mathbb{R}^d$ *of parameters and* $h_{L,\mathfrak{v}} \in B_{\epsilon_4}(0;\tilde{L})$ *of 1–homoclinic orbits to* $p_0$ *in (2.1) such that*

$$\begin{aligned} |\mu(L,\mathfrak{v})| &\leq C(\mathrm{e}^{-2\kappa L} + |\mathfrak{v}|) \\ ||h_{L,\mathfrak{v}} - q_1||_{\eta,\tilde{L}} + ||h_{L,\mathfrak{v}}(2L+\cdot) - q_2||_{-\eta,\tilde{L}} &\leq C(\mathrm{e}^{(\eta-\kappa)\tilde{L}} + |\mathfrak{v}|) \end{aligned}$$

*Given a 1–homoclinic solution* $h$ *to (2.1) for* $|\mu| \leq \delta_4$ *with variations* $W(\sigma;L) \in B^0_{\epsilon_4}(0;L)$, *there exist* $\ell_L = L + O(\mathrm{dist}(L, I_b^4))$ *and unique* $\sigma_L = O(w^{\mathrm{c}}_{+1}(L;\sigma))$ *which is* $C^k$ *in* $L$, *such that* $h \equiv h_{\ell_L,0}(\cdot + \sigma_L)$ *and* $\mu = \mu(\ell_L, \tilde{Q}w^{\mathrm{u}}_{-1}(0;\sigma_{\ell_L}))$.

We define $I_b^4 := I_b^4 \cap (L_4,\infty)$ and $I_b^4(\tilde{L}) := I_b^1(\tilde{L}) \cap (L_4,\infty)$.

**Remark 6** *For* $\mathfrak{v} = 0$ *the ambiguity in defining the semi travel time of homoclinic solutions from a neighborhood of* $q_1(0)$ *to* $q_2(0)$ *is exponentially small in* $L$, *because* $|h_{L,0}(0) - q_1(0)| + |h_{L,0}(2L) - q_2(0)| \leq C(\mathrm{e}^{(\eta-\kappa)L})$. *The convergence to the heteroclinic cycle consisting of* $q_1$ *and* $q_2$ *as* $L \to \infty$ *is also reflected by* $|\mu(L,0)| \leq C(\mathrm{e}^{-2\kappa L})$.
*The fact that all 1–homoclinic orbits near the heteroclinic cycle consisting of* $q_1$ *and* $q_2$ *are contained in the family* $h_{L,0}$ *implies local uniqueness of these 1–homoclinic orbits up to time shifts. In remark 5 this is expressed more intuitively using sections* $\Sigma_1$, $\Sigma_2$.
*Recall that the set* $I_b^1$ *from theorem 2.2 consists of disjoint intervals* $I_j$ *with length* $|I_j| \leq \mathrm{e}^{-\kappa \sup I_j}$ *and containing the point* $T_j := jT_\gamma/2$, *where* $j \geq j_0$, *cf. lemma 3 and figure 5. Therefore, there is* $j_1 \geq j_0$ *such that the countable family of curves of 1–homoclinics can be parametrized as* $h_{j,r} := h_{T_j+r,0}$ *where* $j \in \mathbb{N}$, $j \geq j_1$ *and* $|r| \leq \mathrm{e}^{-\kappa \sup I_j}$. *With this parametrization,* $j$ *counts the number of times the 1–homoclinic winds around* $\gamma$, *e.g.* $h_{j+1,0}$ *has one more 'hump' than* $h_{j,0}$.
*The disconnectedness of the set* $I_b^4$ *implies that for* $\mathfrak{v} = 0$ *the set of parameter values* $\{\mu(L,\mathfrak{v}) | L \in I_b^1 \cap (L_4,\infty)\}$ *consists of a union of disjoint curve segments near* $\mu = 0$, *i.e. if* $\mu(L,0) = \mu(L',0)$ *for* $L \leq L' \in I_b^4$, *then* $L = L'$. *This follows locally from the implicit function theorem and hypothesis 4, and globally from* $B_{\epsilon_4}(0;L') \subset B_{\epsilon_4}(0;L)$ *and the uniqueness up to time shifts of 1–homoclinic orbits in these balls.*

The disjoint parameter curves may be connected to form a smooth curve with parameter values for homoclinics beyond the reach of theorem 2.3. In section 2.4 we consider

this for the codimension–2 case analytically by essentially pathfollowing solutions in $\mathfrak{v}$. Numerically this has been found even for the codimension–1 case in [65].

**2a) Matching near the transverse heteroclinic**

As a first step, we match $q_1(0) + w_1^1(W_0, \mu, L)(0)$ with the unstable manifold of $p_0$ using that Lemma 1 established exponential dichotomies of the variation about $q_1(\xi)$ for $\xi \leq 0$. The unstable manifold of $p_0$ near $q_1(0)$ is a graph over $q_1(0) + E^{\mathrm{u}}_{-1}(0)$, and there exists $\epsilon_{\mathrm{u}} > 0$ and a $C^k$-function $m_1(\cdot;\mu) : E^{\mathrm{u}}_{-1}(0) \to E^{\mathrm{s}}_{-1}(0)$ such that for $|v| \leq \epsilon_{\mathrm{u}}$, and $\mu \in \Lambda$ where the point $q_1(0) + v + m_1(v;\mu) \in \mathcal{W}^{\mathrm{u}}(p_0;\mu)$ , cf. e.g. [14]. We possibly have to shrink $\Lambda$ for this, keeping an open set. Furthermore, $m_1(0;0) = 0$, $\partial_v m_1(0;0) = 0$ and for a suitable constant $K_6$ we have

$$|m_1(v;\mu)| \quad \leq \quad K_6(|v|^2 + |\mu|). \tag{2.39}$$

Therefore, matching a glued solution $W^1 = (w_1^1, w_2^1)$ from theorem 2.2 with the unstable manifold near the heteroclinic $q_1$ means to solve the equation

$$w_1^1(W_0, \mu, L)(0) \quad = \quad v + m_1(v;\mu). \tag{2.40}$$

This will be achieved in terms of $\tilde{w}_1$ and $v$, leaving $\tilde{w}_2$ and $\mu$, $L$ as parameters to match near the codimension–1 or –2 heteroclinic $q_2$.

**Lemma 6** *Assume hypotheses 1, and 2 or 3. There exist positive constants $C$, $L_2$, $\epsilon_2$, $\delta_2$ such that for all $\tilde{L} \in I_b^1 \cap (L_2, \infty)$, there exist $C^k$ functions $\tilde{w}_1(\tilde{w}_2, \mu, L)$ and $\tilde{v}(\tilde{w}_2, \mu, L, \mathfrak{v})$, for $|\tilde{w}_2| + \mathrm{e}^{\eta \tilde{L}}|\mu| + |\mathfrak{v}| < \delta_2$, $L \in I_b^1(\tilde{L}) \cap (L_2, \infty)$, which solve (2.40) with $W_0 = (\tilde{w}_1(\tilde{w}_2, \mu, L, \mathfrak{v}), \tilde{w}_2)$ and $v = \tilde{v} + \mathfrak{v}$. These are the unique solutions to (2.40) with $|v| + |\tilde{w}_1| \leq \epsilon_2$ for any $\tilde{w}_2, \mu, L, \mathfrak{v}$ as above.*
*Let $u$ be a solution to (2.1) with variations $W(\sigma, L) \in B^0_{\epsilon_2}(0; L)$ which solves (2.40) for $|w^{\mathrm{u}}_{-2}(0; \sigma_{\ell_L}, \ell_L)| + |\tilde{Q} w^{\mathrm{u}}_{-1}(0; \sigma_{\ell_L})| + |\mu| < \delta_2$. Then $W_0(\sigma_{\ell_L}, \ell_L)$ satisfies*

$$|w_1(0; \sigma_{\ell_L})| \quad \leq \quad C \left( |w^{\mathrm{u}}_{-2}(0; \sigma_{\ell_L}, \ell_L)| + |\mu| + \mathrm{e}^{2(\eta - \kappa)L} + |\tilde{Q} w^{\mathrm{u}}_{-1}(0; \sigma_{\ell_L})| \right).$$

**Proof.** Theorem 2.2 applies and yields glued solutions $W^1(W_0, \mu, L)$ for $|W_0| \leq \delta$, $|\mu| \leq \delta \mathrm{e}^{-\eta L}$, $L \in I_b^1$ satisfying

$$W^1(W_0, \mu, L)(0) = \mathcal{A}(L)(0) W_0 + \mathcal{N}(W^1(W_0, \mu, L); \mu, L)(0) + \mathcal{B}(L)(0)$$

whose first component $w_1^1$ as defined in (2.26, 2.28, 2.29) at $\xi = 0$ is

$$\begin{aligned}
\mathcal{A}_1(L)(0)W_0 &= \tilde{w}_1 + \Phi^{\mathrm{u}}_{+1}(0,L)P^{\mathrm{u}}_L \mathfrak{c}_1(W_0, L) \\
\mathcal{N}_1(W^1(W_0,\mu,L);\mu,L)(0) &= \int_L^0 \Phi^{\mathrm{cu}}_{+1}(0,\zeta) g_1(w_1^1(W_0,\mu,L)(\zeta),\zeta;\mu)\mathrm{d}\zeta + \\
&\quad + \Phi^{\mathrm{u}}_{+1}(0,L)P^{\mathrm{u}}_L \mathfrak{c}_2(W^1(W_0,\mu,L);L,\mu) \\
\mathcal{B}_1(L)(0) &= \Phi^{\mathrm{u}}_{+1}(0,L)P^{\mathrm{u}}_L b_L
\end{aligned}$$

With the above notation, the matching equation (2.40) can be viewed as a nonlinear perturbation of $v - \tilde{w}_1 = e$, $e \in \mathbb{R}^n$, $v \in E^{\mathrm{u}}_{-1}(0)$, $\tilde{w} \in E^{\mathrm{s}}_{+1}(0)$. This linear equation is generally solvable by both hypothesis 2 or 3, and the solution is unique up to a component in $E^{\mathrm{u}}_{-1}(0) \cap E^{\mathrm{s}}_{+1}(0)$. We project by $\mathrm{Id} - \tilde{Q}$ to a complement $\tilde{E}^{\mathrm{u}}_{-1}$ of $E^{\mathrm{u}}_{-1}(0) \cap E^{\mathrm{s}}_{+1}(0)$ in $E^{\mathrm{u}}_{-1}(0)$, so that $\mathbb{R}^n = \tilde{E}^{\mathrm{u}}_{-1} \oplus E^{\mathrm{s}}_{+1}(0)$ and view $\mathfrak{v} := \tilde{Q}v$ as a parameter. For any $\mathfrak{v} \in E_1$ the map $\tilde{E}^{\mathrm{u}}_{-1} \times E^{\mathrm{s}}_{+1}(0) \to \mathbb{R}^n; (\tilde{v}, \tilde{w}) \mapsto \tilde{v} - \tilde{w}_1 + \mathfrak{v}$ is invertible. Since $\mathfrak{c}_1(W_0, L)$ is linear in $W_0$ equation (2.40) contains a perturbed linear map $D^1_L(\tilde{v}, \tilde{w}_1) = \tilde{v} - \tilde{w}_1 - \Phi^{\mathrm{u}}_{+1}(0,L)P^{\mathrm{u}}_L \Phi^{\mathrm{s}}_{+1}(L,0)\tilde{w}_1$. If $L \in I^1_b \cap (\bar{L}_2, \infty)$, for sufficiently large $\tilde{L}_2$, then $D^1_L$ is invertible with uniformly bounded norm $C_1 > 0$ of the inverse, because by (2.9,2.36) and remark 3

$$|\Phi^{\mathrm{u}}_{+1}(0,L)P^{\mathrm{u}}_L \Phi^{\mathrm{s}}_{+1}(L,0)| \leq C\mathrm{e}^{-3\kappa L}|\tilde{w}_1|.$$

We can write (2.40) as

$$\begin{aligned}
D^1_L(\tilde{v}, \tilde{w}_1) &= \mathcal{N}_1(W^1((\tilde{w}_1, \tilde{w}_2),\mu,L);\mu,L)(0) + \mathcal{B}_1(L)(0) - m_1(\tilde{v} + \mathfrak{v};\mu) \\
&\quad - \Phi^{\mathrm{u}}_{+1}(0,L)P^{\mathrm{u}}_L \Phi^{\mathrm{u}}_{-2}(-L,0)\tilde{w}_2 - \mathfrak{v}.
\end{aligned}$$

Using lemma 5 and (2.23) there is a constant $C_2 > 0$ such that for $\tilde{L} \in I^1_b \cap (\tilde{L}_2, \infty)$ and $L \in I^1_b(\tilde{L})$ we have

$$\begin{aligned}
|\mathcal{N}_1(W^1((\tilde{w}_1, \tilde{w}_2),\mu,L);\mu,L)(0)| &\leq C_2(||W^1||^2_{\tilde{L}} + |\mu|\,||W^1||_{\tilde{L}} + |\mu|) \\
&\leq C_2\left(|(\tilde{w}_1,\tilde{w}_2)|\left(|(\tilde{w}_1,\tilde{w}_2)| + |\mu| + \mathrm{e}^{(\eta-\kappa)\tilde{L}}\right)\right. \\
&\quad \left. + |\mu| + \mathrm{e}^{2(\eta-\kappa)\tilde{L}}\right),
\end{aligned}$$

and analogously for the derivative of $\mathcal{N}_1(W^1)$ with respect to $\tilde{w}_1$. Including the linear term from $\mathcal{N}_1(W^1)$, the linear part of (2.40) is of the form $D^1_L + O(\mathrm{e}^{(\eta-\kappa)L} + |\mu|)$. There exist constants $\bar{L}_2 \geq \tilde{L}_2$ and $0 < \bar{\delta} \leq \min\{\epsilon_{\mathrm{u}}, \delta\}$, where $\delta > 0$ is from theorem 2.2, such

that for all $L \in I_b^1 \cap (\bar{L}_2, \infty)$ and $|\mu| \leq \bar{\delta}$ this linear map is invertible with uniform bounded norm $C_1 > 0$ of the inverse. By virtue of (2.9), we can estimate

$$|\mathcal{B}_1(L)(0)| \quad \leq \quad C\mathrm{e}^{-2\kappa L},$$

and therefore choose $L_2 \geq \bar{L}_2$ so that $|\mathcal{B}_1(L)(0)| + C_2\mathrm{e}^{2(\eta-\kappa)L} \leq 1/(8C_1^2C_2)$. The implicit function theorem 2.1 applies with the following choices for any $\tilde{L} \in I_b^1 \cap (\bar{L}_2, \infty)$: $X = \mathbb{R}^n$, $Y = B_{\delta_*}(0) \subset \tilde{E}^{\mathrm{u}}_{-1} \times E^{\mathrm{s}}_{+1}(0)$, $y = (\tilde{w}_1, \tilde{v})$. For $B_{\delta_*}(0) \subset E^{\mathrm{u}}_{-2}(0) \times E_1$ define $Z = B_{\delta_*}(0) \times \Lambda_{\tilde{L}}^{\delta_*}$, $z = (\tilde{w}_2, \mathfrak{v}, \mu)$, and $I := I_b^1(\tilde{L}) \cap (L_2, \infty)$. Using the terms contained in $\mathcal{N}_1$ we set $Q(z, L) := D_L^1 + O(\mathrm{e}^{(\eta-\kappa)L})$, $R(y, z, L) := m_1(\tilde{v} + \mathfrak{v}; \mu) + O(|z| + |y|(|y| + |z|))$, and $S(L) := \mathcal{B}_1(L)(0) + O(\mathrm{e}^{2(\eta-\kappa)L})$. As in the proof of theorem 2.2, all constants are independent of $\tilde{L}$, hence the estimates and constants from theorem 2.1 are.
In conclusion, we obtain constants $\epsilon'$, $\delta_2$ and unique solutions $(\tilde{v}, \tilde{w}_1)(\tilde{w}_2, \mu, L, \mathfrak{v}) \in B_{\epsilon'}(0) \subset Y$, where $\tilde{v}$, $\tilde{w}_1$ are $C^k$ in $L$, $\mu$, $\mathfrak{v}$ and $\tilde{w}_2$ for all $\tilde{L} \in I_b^1 \cap (L_2, \infty)$, $L \in I_b^1(\tilde{L}) \cap (L_2, \infty)$ and $\mathrm{e}^{\eta\tilde{L}}|\mu| + |\tilde{w}_2| + |\mathfrak{v}| < \delta_2$. In addition, theorem 2.1 and theorem 2.2 imply that the following estimate also holds for $|\mu| + |\tilde{w}_2| + |\mathfrak{v}| < \delta_2$:

$$\begin{aligned} |\tilde{w}_1| + |\tilde{v}| \quad &\leq \quad C\left(|\tilde{w}_2| + |\mu| + \mathrm{e}^{2(\eta-\kappa)L} + \mathrm{e}^{-2\kappa L} + |\mathfrak{v}|\right) \\ &\leq \quad C\left(|\tilde{w}_2| + |\mu| + \mathrm{e}^{2(\eta-\kappa)L} + |\mathfrak{v}|\right). \end{aligned}$$

Let $W(\sigma, L)$ be the variations for a given solution and let $\epsilon$ be from theorem 2.2. For any $\epsilon_2 \leq \min\{\epsilon', \epsilon\}$, the unique solution obtained from $W(\sigma, L) \in B^0_{\epsilon_2}(0; L)$ by theorem 2.2 is $W^1(W_0(\sigma_{\ell_L}, \ell_L), \mu, \ell_L)$. For $\epsilon_2$ sufficiently small the smoothness then implies $|w^{\mathrm{s}}_{+1}(0; \sigma_{\ell_L})| + |w^{\mathrm{u}}_{-1}(0; \sigma_{\ell_L})| \leq \epsilon'$. Hence, these coincide with the solutions found above for $\mathfrak{v} = \tilde{Q}w^{\mathrm{u}}_{-1}(0; \sigma_{\ell_L})$, if $\mu \in \Lambda_{\tilde{L}}^{\delta_2}$. □

We now have obtained solutions $w_1^1((\tilde{w}_1(\tilde{w}_2, \mu, L, \mathfrak{v}), \tilde{w}_2), \mu, L) \in C_{\eta,\tilde{L}}$ which lie in the unstable manifold of the equilibrium $p_0$ and pass close to the periodic orbit $\gamma$. Note that we have existence and local uniqueness only for $|\mu| \leq \delta_2\mathrm{e}^{-\eta L}$, but the estimate holds already for such solutions if $|\mu| \leq \delta_2$. We denote $I_b^2 := I_b^1 \cap (L_2, \infty)$, $I_b^2(\tilde{L}) := I_b^1(\tilde{L}) \cap (L_2, \infty)$ and

$$\begin{aligned} W_0^2(\tilde{w}_2, \mu, L, \mathfrak{v}) \quad &:= \quad (\tilde{w}_1(\tilde{w}_2, \mu, L, \mathfrak{v}), \tilde{w}_2) \\ W^2(\tilde{w}_2, \mu, L, \mathfrak{v}) \quad &:= \quad W^1(W_0^2(\tilde{w}_2, \mu, L, \mathfrak{v}), \mu, L). \end{aligned}$$

From (2.23) and lemma 6 we conclude the estimates

$$
\begin{aligned}
|W_0^2(\tilde{w}_2,\mu,L,\mathfrak{v})| &\leq C\left(|\tilde{w}_2|+|\mu|+\mathrm{e}^{2(\eta-\kappa)L}+|\mathfrak{v}|\right)\\
||W^2(\tilde{w}_2,\mu,L,\mathfrak{v})||_{\tilde{L}} &\leq C\left(|\tilde{w}_2|+|\mu|+\mathrm{e}^{(\eta-\kappa)\tilde{L}}+|\mathfrak{v}|\right).
\end{aligned}
\tag{2.41}
$$

**2b) Matching near the codim–d heteroclinic, Ljapunov-Schmidt reduction**

To complete the homoclinic to $p_0$, we want to find $\tilde{w}_2$, $\mu$ and $L$ such that $w_1^2(\tilde{w}_2,\mu,L,\mathfrak{v})\in\mathcal{W}^{\mathrm{s}}(p_0;\mu)$. Analogous to the previous step, we use the dichotomy $P^{\mathrm{s}}_{+2}(\xi)$ and $P^{\mathrm{u}}_{+2}(\xi)$ from lemma 1 for the variation about $q_2$ towards $p_0$. The stable manifold near $q_2(0)$ is a graph over $q_2(0)+E^{\mathrm{s}}_{+2}(0)$ given by a $C^k$ function $m_2(\cdot;\mu):B_{\epsilon_{\mathrm{s}}}(0)\subset E^{\mathrm{s}}_{+2}(0)\to E^{\mathrm{u}}_{+2}(0)$ with suitable $\epsilon_{\mathrm{s}}$, and for $\mu\in\Lambda$, possibly shrunken, and it satisfies, cf. [14], the estimate

$$
|m_2(v;\mu)|\leq C(|v|^2+|\mu|).
\tag{2.42}
$$

As before, this allows to formulate matching through the equation

$$
w_2^2(\tilde{w}_2,\mu,L,\mathfrak{v})(0) \;=\; v+m_2(v;\mu)
\tag{2.43}
$$

where the left hand side satisfies

$$
\begin{aligned}
w_2^2(\tilde{w}_2,\mu,L,\mathfrak{v})(0) \;=\;& \mathcal{A}_2(L)(0)W_0^2(\tilde{w}_2,\mu,L,\mathfrak{v})+\mathcal{N}_2(W^2(\tilde{w}_2,\mu,L,\mathfrak{v});\mu,L)(0)\\
&+\mathcal{B}_2(L)(0)
\end{aligned}
$$

and from (2.26, 2.28, 2.29) at $\xi=0$ the details are

$$
\begin{aligned}
\mathcal{A}_2(L)(0)W_0^2(\tilde{w}_2,\mu,L,\mathfrak{v}) &= \tilde{w}_2-\Phi^{\mathrm{sc}}_{-2}(0,-L)P^{\mathrm{sc}}_L\mathfrak{c}_1(W_0^2(\tilde{w}_2,\mu,L,\mathfrak{v}),L)\\
\mathcal{N}_2(W^2(\tilde{w}_2,\mu,L,\mathfrak{v});\mu,L)(0) &= \int_{-L}^0\Phi^{\mathrm{sc}}_{-2}(0,\zeta)g_2(w_2^2(\tilde{w}_2,\mu,L,\mathfrak{v}),\zeta;\mu)\mathrm{d}\zeta-\\
&\quad -\Phi^{\mathrm{sc}}_{-2}(0,-L)P^{\mathrm{sc}}_L\mathfrak{c}_2(W^2(\tilde{w}_2,\mu,L,\mathfrak{v}),L)\\
\mathcal{B}_2(L)(0) &= -\Phi^{\mathrm{sc}}_{-2}(0,-L)P^{\mathrm{sc}}_Lb_L
\end{aligned}
\tag{2.44}
$$

We will see below, that the linear part of (2.43) is a small perturbation of $\tilde{w}_2-v$. By hypothesis 2 or 3, $\dim(E^{\mathrm{s}}_{+2}(0)+E^{\mathrm{u}}_{-2}(0))=n-d$, whence we use Ljapunov-Schmidt reduction to solve (2.43) first for $(v,\tilde{w}_2)$ in $E_2:=E^{\mathrm{s}}_{+2}(0)+E^{\mathrm{u}}_{-2}(0)\sim\mathbb{R}^{n-d}$ and then in the complement $(E_2)^{\perp}\sim\mathbb{R}^d$. Let $P_2$ denote the projection $P^{\mathrm{u}}_{-2}(0)+P^{\mathrm{s}}_{+2}(0)$ onto $E_2$ with kernel $(E_2)^{\perp}$ in $\mathbb{R}^n$ and $\kappa'=\min\{2(\kappa-\eta),\kappa\}$.

**Lemma 7** *Assume hypothesis 1, and 2 or 3. There exist strictly positive constants $\epsilon_3$, $L_3$ and $\delta_3$, such that for all $\tilde{L} \in I_b^2 \cap (L_3, \infty)$, there exist smooth functions $\tilde{w}_2(\mu, L)$ and $v(\mu, L, \mathfrak{v})$ for $|\mu| < \mathrm{e}^{-\eta \tilde{L}} \delta_3$, $L \in I_b^2(\tilde{L}) \cap (L_3, \infty)$, which solve (2.43) in $E_2$:*

$$P_2 w_2^2(v_2^{\mathrm{u}}(\mu, L, \mathfrak{v}), \mu, L)(0) \quad = \quad P_2(v + m_2(v(\mu, L, \mathfrak{v}); \mu)).$$

*These are the unique solutions in $B_{\epsilon_3}(0) \subset E_2$. Let $u$ be a solution to (2.1) with variations $W(\sigma, L) \in B^0_{\epsilon_3}(0; L)$ which solve (2.40, 2.43) for $|\mu| + |\tilde{Q} w_{-1}^{\mathrm{u}}(0; \sigma_{\ell_L})| < \delta_3$. Then*

$$|w_{-2}^{\mathrm{u}}(0; \sigma_{\ell_L})| + |w_{+2}^{\mathrm{s}}(0; \sigma_{\ell_L}, \ell_L)| \quad \leq \quad C(|\mu| + \mathrm{e}^{-\kappa' \tilde{L}} + |\tilde{Q} w_{-1}^{\mathrm{u}}(0; \sigma_{\ell_L})|).$$

**Proof.** By the assumptions, theorem 2.2 and lemma 6 apply. In $E_2$ the linear map $D_L^2 : E_{+2}^{\mathrm{s}}(0) \times E_{-2}^{\mathrm{u}}(0) \to E_2 \sim \mathbb{R}^{n-d}$, $(v, \tilde{w}_2) \mapsto v - \tilde{w}_2$ is invertible by both hypothesis 2 or 3. In $E_2$, (2.43) is of the form

$$\begin{aligned} D_L^2(v, \tilde{w}_2) \quad = \quad & P_2 \left( -\Phi_{-2}^{\mathrm{sc}}(0, -L) P_L^{\mathrm{sc}} \mathfrak{c}_1(W_0^2(\tilde{w}_2, \mu, L, \mathfrak{v}), L) + \right. \\ & \left. + \mathcal{N}_2(W^2(\tilde{w}_2, \mu, L, \mathfrak{v}); \mu, L)(0) + \mathcal{B}_2(L)(0) - m_2(v; \mu) \right). \end{aligned}$$

Using remark 3, (2.9) and (2.41) we can estimate

$$\begin{aligned} |\Phi_{-2}^{\mathrm{sc}}(0, -L) P_L^{\mathrm{sc}} \mathfrak{c}_1(W_0^2(\tilde{w}_2, \mu, L, \mathfrak{v}), L)| \quad & \leq \quad C \mathrm{e}^{-2\kappa L}(|\tilde{w}_2| + |\mu| + \mathrm{e}^{2(\eta - \kappa)L} + |\mathfrak{v}|) \\ |\mathcal{N}_2(W^2(\tilde{w}_2, \mu, L, \mathfrak{v}); \mu, L)(0)| \quad & \leq \quad C(||W^2||_{\tilde{L}}^2 + |\mu| ||W^2||_{\tilde{L}} + |\mu|) \\ & \leq \quad C \Big( |\tilde{w}_2|(|\tilde{w}_2| + |\mu| + \mathrm{e}^{(\eta - \kappa)\tilde{L}} + |\mathfrak{v}|) \\ & \quad + |\mathfrak{v}|(|\mathfrak{v}| + |\mu| + \mathrm{e}^{(\eta - \kappa)\tilde{L}}) + |\mu| + \mathrm{e}^{2(\eta - \kappa)\tilde{L}} \Big) \\ \text{and} \qquad |\mathcal{B}_2(L)(0)| \quad & \leq \quad C \mathrm{e}^{-\kappa \tilde{L}}. \end{aligned}$$

We proceed as in the proof of lemma 6 and omit some details.

The parts of these estimates linear in $|\tilde{w}_2|$ are $O(\mathrm{e}^{(\eta - \kappa)\tilde{L}} + |\mathfrak{v}| + |\mu|)$, and we find $L_3 \geq L_2$, $\bar{\delta}_3 \leq \delta_2$ such that for $L \geq L_3$ and $|\mathfrak{v}| + |\mu| \leq \bar{\delta}_3$ the perturbed linear map $D_L^2 + O(\mathrm{e}^{(\eta - \kappa)L} + |\mathfrak{v}| + |\mu|)$ is invertible with uniformly bounded norm of the inverse.

Now let $\epsilon' := \min\{\epsilon_2, \bar{\delta}_3\}$ and $\delta' := \min\{\epsilon_{\mathrm{s}}, \bar{\delta}_3\}$. Together with (2.42), the above estimates allow to apply theorem 2.1 for any $\tilde{L} \in I_b^2 \cap (L_3, \infty)$ with $I := I_b^2(\tilde{L})$, $X = E_2$, $Y = B_{\epsilon'}(0) \subset E_2$ and $Z = \Lambda_{\tilde{L}}^{\delta'} \times B_{\delta'}(0) \subset \Lambda \times E_1$. So $y = v$, $z = (\mu, \mathfrak{v})$ and we take $Q(z, L) := D_L^2 + O(\mathrm{e}^{(\eta - \kappa)L} + |\mathfrak{v}| + |\mu|)$, $R(y, z, L) := m_2(v; \mu) + O(|z| + |y|(|z| + |y|))$, and

$S(L) := \mathcal{B}_2(L)(0) + O(\mathrm{e}^{2(\eta-\kappa)\tilde{L}})$. Again all constants are uniform in $\tilde{L}$, so are the resulting constants and estimates[3].

We obtain constants $\epsilon_3 > 0$, $\delta_3 > 0$, $C$ and unique solutions $(v, \tilde{w}_2)(\mu, L, \mathfrak{v}) \in B_{\epsilon_3}(0) \subset E_2$ which are $C^k$ functions for $\mathrm{e}^{\eta\tilde{L}}|\mu| + |\mathfrak{v}| < \delta_3$, and $\tilde{L} \in I_b^2 \cap (L_3, \infty)$, $L \in I_b^2(\tilde{L}) \cap (L_3, \infty)$ and satisfy for $|\mu| \leq \delta_3$ that

$$|\tilde{w}_2(\mu, L, \mathfrak{v})| + |v(\mu, L, \mathfrak{v})| \quad \leq \quad C\left(|\mu| + \mathrm{e}^{2(\eta-\kappa)\tilde{L}} + \mathrm{e}^{-\kappa\tilde{L}} + |\mathfrak{v}|\right) \leq C\left(|\mu| + \mathrm{e}^{-\kappa' L} + |\mathfrak{v}|\right).$$

The local uniqueness statement follows analogous to the one in lemma 6 by possibly decreasing $\epsilon_3 > 0$. □

Thus, we obtained glued solution, matched everywhere except in a complement of $E_2$ and denote $I_b^3 := I_b^2 \cap (L_3, \infty)$, $I_b^3(\tilde{L}) := I_b^2(\tilde{L}) \cap (L_3, \infty)$ and

$$\begin{aligned} W_0^3(\mu, L, \mathfrak{v}) &:= W_0^2(\tilde{w}_2(\mu, L, \mathfrak{v}), \mu, L) \\ W^3(\mu, L, \mathfrak{v}) &:= W^2(\tilde{w}_2(\mu, L, \mathfrak{v}), \mu, L). \end{aligned}$$

From (2.23) and lemma 7 we conclude the estimates

$$\begin{aligned} |W_0^3(\mu, L, \mathfrak{v})| &\leq C\left(|\mu| + \mathrm{e}^{-\kappa' L} + |\mathfrak{v}|\right) \\ ||W^3(\mu, L, \mathfrak{v})||_{\tilde{L}} &\leq C\left(|\mu| + \mathrm{e}^{(\eta-\kappa)\tilde{L}} + |\mathfrak{v}|\right). \end{aligned} \tag{2.45}$$

**2c) Matching in the complement, Melnikov's method, proof of theorem 2.3**

To solve (2.43) in the $d$-dimensional complement $(E_2)^\perp$, we use the basis $\{a_0^1, a_0^2\} \subset \mathbb{R}^n$ of $(E_2)^\perp$ introduced at the beginning of this section. Throughout this subsection $j$ takes on both values $j = 1$ and $j = 2$. The matching is complete, if

$$\langle w_2^3(\mu, L, \mathfrak{v})(0), a_0^j \rangle \quad = \quad \langle m_2(v(\mu, L, \mathfrak{v}); \mu), a_0^j \rangle. \tag{2.46}$$

Let $\tilde{L} \in I_b^3$, $L \in I_b^3(\tilde{L})$. Again, we exploit the fixed point equation

$$w_2^3(\mu, L, \mathfrak{v})(0) \quad = \quad \mathcal{A}_2(L)(0) W_0^3(\mu, L, \mathfrak{v}) + \mathcal{N}_2(w_2^3(\mu, L, \mathfrak{v}), \mu)(0) + \mathcal{B}_2(L)(0)$$

[3]Note that we did not make use of the better estimates with respect to $\mathfrak{v}$.

with details analogous to (2.44). Since $\tilde{w}_2(\mu, L, \mathfrak{v}) \in E_2$, it follows that $\langle \tilde{w}_2(\mu, L, \mathfrak{v}), a_0^j \rangle = 0$ and $\dot{q}_2(0) \in E^{\mathrm{s}}_{+2}(0) \subset E_2$, so $\langle P^{\mathrm{c}}_{-2}(0)\cdot, a_0^j \rangle \equiv 0$. Hence, the center direction is not visible in this matching and (2.46) is in fact equivalent to

$$\begin{aligned}(2.47)\quad &\langle \int_{-L}^{0} \Phi^{\mathrm{s}}_{-2}(0,\zeta) g_2(w_2^3(\mu, L, \mathfrak{v})(\zeta), \zeta; \mu) \mathrm{d}\zeta + m_2(v(\mu, L, \mathfrak{v}); \mu), a_0^j \rangle \\ &\qquad = -\langle \Phi^{\mathrm{s}}_{-2}(0,-L) P^{\mathrm{s}}_L \left( \mathfrak{c}_1(W_0^3(\mu, L, \mathfrak{v}), L) + \mathfrak{c}_2(W^3(\mu, L, \mathfrak{v}), L) + b_L \right), a_0^j \rangle.\end{aligned}$$

For later reference, we single out the expected leading order term in $L$ on the right hand side. From the estimates (2.31), (2.35), (2.36) and (2.45), we obtain that

$$\begin{aligned}&|\langle \Phi^{\mathrm{s}}_{-2}(0,-L) P^{\mathrm{s}}_L \left( \mathfrak{c}_1(W_0^3(\mu, L, \mathfrak{v}), L) + \mathfrak{c}_2(W^3(\mu, L, \mathfrak{v}), L) \right), a_0^j \rangle| \\ &\quad \leq \ \mathrm{e}^{-\kappa L} \left( \mathrm{e}^{-\kappa L}(|\mu| + \mathrm{e}^{-\kappa' L} + |\mathfrak{v}|) + \mathrm{e}^{-\eta L}(\mathrm{e}^{2(\eta-\kappa)L} + |\mathfrak{v}|(|\mathfrak{v}| + |\mu| + \mathrm{e}^{(\eta-\kappa)L}) + |\mu|) \right) \\ &\quad \leq \ \mathrm{e}^{(\eta-3\kappa)L} + \mathrm{e}^{-(\kappa+\eta)L} \left( |\mathfrak{v}|(|\mathfrak{v}| + |\mu| + \mathrm{e}^{(\eta-\kappa)L}) + |\mu| \right).\end{aligned}$$

The full right hand side of (2.47) thus satisfies (roughly estimated in $\mathfrak{v}$)

$$(2.48)\quad -\langle \Phi^{\mathrm{s}}_{-2}(0,-L) P^{\mathrm{s}}_L b_L, a_0^j \rangle + O\left( \mathrm{e}^{(\eta-3\kappa)L} + \mathrm{e}^{-(\kappa+\eta)L}(|\mathfrak{v}| + |\mu|) \right) \ = \ O(\mathrm{e}^{-2\kappa L}).$$

Since $0 < \eta < \kappa$ it holds that $\eta - 3\kappa < -2\kappa$ and so the leading order term in $L$ is expected to be $\langle \Phi^{\mathrm{s}}_{-2}(0,-L) P^{\mathrm{s}}_L b_L, a_0^j \rangle$. In particular the right hand side is exponentially small in $L$. For the left hand side of (2.47), we set up a Melnikov-type integral. Since the image of the trichotomy projection $P^{\mathrm{s}}_{-2}(0)$ is arbitrary, as long as different from $\mathrm{Rg}(P^{\mathrm{u}}_{-2}(0))$, cf. [16], we may assume for the adjoint projection $(E_2)^\perp \subset \mathrm{Rg}((P^{\mathrm{s}}_{-2}(0))^*)$. Hence, we have $a_0^j = (P^{\mathrm{s}}_{-2}(0))^* a_0^j$ and

$$a^j(\zeta) = (\Phi^{\mathrm{s}}_{-2}(0,\zeta))^* a_0^j = (\Phi_2(0,\zeta))^* (P^{\mathrm{s}}_{-2}(0))^* a_0^j = (\Phi_2(0,\zeta))^* a_0^j.$$

Inspecting the linearization of the left hand side of (2.47) with respect to $\mu$ at $\mu = 0$, recall the definition of $g_2$ in (2.5), we obtain on the one hand for $j = 1, 2$ that

$$\begin{aligned}&\langle \int_{-L}^{0} \Phi^{\mathrm{s}}_{-2}(0,\zeta) f_\mu(q_2(\zeta) + w_2^3(0, L, \mathfrak{v})(\zeta); 0) \mu \mathrm{d}\zeta, a_0^j \rangle = \\ &\qquad\qquad \langle \int_{-L}^{0} f_\mu(q_2(\zeta) + w_2^3(0, L, \mathfrak{v})(\zeta); 0) \mu \mathrm{d}\zeta, a^j(\zeta) \rangle.\end{aligned}$$

From (2.45), $||w_2^3(0, L, \mathfrak{v})||_{-\eta} \leq C(\mathrm{e}^{(\eta-\kappa)\tilde{L}} + |\mathfrak{v}|)$ and, since the trichotomy estimates hold for the adjoint equation, it follows $|a^j(\zeta)| \leq C\mathrm{e}^{\kappa\zeta}|a_0^j|$ for $\zeta \leq 0$. Hence, for $\tilde{L} \in I_b^3$, $L \in I_b^3(\tilde{L})$ we can approximate by the $w_2^3$ independent integral

$$
\begin{aligned}
&|\langle \int_{-L}^{0} \left(f_\mu(q_2(\zeta)+w_2^3(0,L)(\zeta);0)-f_\mu(q_2(\zeta);0)\right)\mu\,\mathrm{d}\zeta, a^j(\zeta)\rangle| \\
&\qquad \leq C\int_{-L}^{0} \sup_{\substack{s\in[0,1]\\ \zeta\in[-L,0]}} |f'_\mu(q_2(\zeta)+sw_2^3(0,L,\mathfrak{v})(\zeta);0)|\,|w_2^3(0,L,\mathfrak{v})(\zeta)|\,|\mu|\,|a^j(\zeta)|\mathrm{d}\zeta \\
&\qquad \leq C|\mu|\int_{-L}^{0} \mathrm{e}^{\eta\zeta}||w_2^3(0,L,\mathfrak{v})||_{-\eta,\tilde{L}}\mathrm{e}^{-\kappa\zeta}|a_0^j|\mathrm{d}\zeta \leq C|\mu|||w_2^3(0,L,\mathfrak{v})||_{-\eta,\tilde{L}} \\
&\qquad \leq C(\mathrm{e}^{(\eta-\kappa)L}+|\mathfrak{v}|)|\mu|.
\end{aligned}
$$

The difference of the $w_2^3$ independent to the infinite integral satisfies for $j=1,2$ that

$$
\begin{aligned}
|\langle \int_{-\infty}^{-L} f_\mu(q_2(\zeta);0)\mu\mathrm{d}\zeta, a^j(\zeta)\rangle| &\leq \int_{-\infty}^{-L}|f_\mu(q_2(\zeta);0)\mu||a^j(\zeta)|\mathrm{d}\zeta \leq C|\mu|\int_{-\infty}^{-L}|a^j(\zeta)|\mathrm{d}\zeta \\
&\leq C|\mu|\mathrm{e}^{-\kappa L}
\end{aligned}
$$

On the other hand, the graph $m_2$ satisfies, cf. e.g. [39],

$$
\left(\frac{\mathrm{d}}{\mathrm{d}\mu}\Big|_{\mu=0} m_2(v(\mu,L);\mu)\right)\mu = \int_0^\infty P^{\mathrm{u}}_{+2}(0)\Phi_2(0,\zeta)f_\mu(q_2(\xi);0)\mu\mathrm{d}\zeta.
$$

As above for the trichotomy near $\gamma$, we may adjust $\mathrm{Rg}(P^{\mathrm{u}}_{+2}(0))$ so that $(P^{\mathrm{u}}_{+2}(0))^* a_0^j = a_0^j$ and therefore

$$
\begin{aligned}
\int_{-\infty}^{\infty}\langle f_\mu(q_2(\zeta);0)\mu, a^j(\zeta)\rangle\mathrm{d}\zeta &= \int_{-L}^{0}\langle f_\mu(q_2(\zeta)+w_2^3(0,L,\mathfrak{v})(\zeta);0)\mu, a^j(\zeta)\rangle\mathrm{d}\zeta + \\
&\quad + \int_0^\infty \langle f_\mu(q_2(\xi);0)\mu, a^j(\zeta)\rangle\mathrm{d}\zeta + O\left((\mathrm{e}^{(\eta-\kappa)L}+|\mathfrak{v}|)|\mu|\right).
\end{aligned}
$$

All in all (2.47) is of the form (again $\mathfrak{v}$ in a rough estimate)

$$
\begin{aligned}
\int_{-\infty}^{\infty}\langle f_\mu(q_2(\zeta);0)\mu, a^j(\zeta)\rangle\mathrm{d}\zeta &= -\langle b_L, a^j(-L)\rangle \\
&\quad + O\left(|\mu|(\mathrm{e}^{(\eta-\kappa)L}+|\mathfrak{v}|+|\mu|)+\mathrm{e}^{(\eta-3\kappa)L}+|\mathfrak{v}|\right)
\end{aligned} \tag{2.49}
$$

By hypothesis 4, the Melnikov-integral linear map $\mathcal{M}$ on the left hand side is invertible. The perturbed map $\mathcal{M}+O(\mathrm{e}^{(\eta-\kappa)L}+|\mathfrak{v}|)$ is invertible with uniformly bounded norm of the inverse if $L\in I_b^3\cap(\bar{L}_4,\infty)$, $|\mathfrak{v}|\leq\delta_{\mathfrak{v}}$ for sufficiently large $\bar{L}_4$ and small $\delta_{\mathfrak{v}}\leq\delta_3$.

To obtain a fully matched solution pair, i.e. a 1–homoclinic orbit, we can apply theorem 2.1 in the same way as in the proof of lemma 6: We find a constant $L_4\geq\bar{L}_4$ and fix any $\tilde{L}\in I_b^3\cap(L_4,\infty)$. Then set $I:=I_b^3(\tilde{L})$, $X:=Y:=\Lambda^{\delta_3}_{\tilde{L}}(0)$, so $y=\mu$, $Z:=$

$B_{\delta_\mathfrak{v}}(0) \subset E_1$, and $Q(L) := \mathcal{M} + O(\mathrm{e}^{(\eta-\kappa)\tilde{L}} + |\mathfrak{v}|)$, $R(y,L) := O(|\mu|(|\mu| + |\mathfrak{v}|) + |\mathfrak{v}|)$, and $S(L) := \sum_{j=1,2}\langle -b_L, a^j(-L)\rangle a_0^j + O(\mathrm{e}^{(\eta-3\kappa)L})$. Note $|S(L)| \leq C\mathrm{e}^{-2\kappa L}$ by (2.48). As in the proofs before, all constants are independent of $\tilde{L}$.

This yields positive constants $\epsilon_4$, $\delta_4$ and $C$, uniform in $\tilde{L}$, and a countably infinite family of $C^k$ curves $\mu(L,\mathfrak{v})$ for all $\tilde{L} \in I_b^3 \cap (L_4,\infty)$, $L \in I_b^3(\tilde{L}) \cap (L_4,\infty)$, $|\mathfrak{v}| \leq \delta_4$, which provide the unique solutions in $\Lambda_{\tilde{L}}^{\epsilon_4}$. Now $W^4(L,\mathfrak{v}) := W^3(\mu(L,\mathfrak{v}),L,\mathfrak{v})$, $W_0^4(L,\mathfrak{v}) := W_0^3(\mu(L,\mathfrak{v}),L,\mathfrak{v})$ is a family of curves of 1–homoclinic solution $h_{L,\mathfrak{v}}$ by means of (2.18). These 1–homoclinic orbits and the parameter curve $\mu(L,\mathfrak{v})$ satisfy

$$\begin{aligned} |\mu(L,\mathfrak{v})| &\leq C(\mathrm{e}^{-2\kappa L} + |\mathfrak{v}|) \\ |W_0^4(L,\mathfrak{v})| &\leq C(\mathrm{e}^{-\kappa' L} + |\mathfrak{v}|) \\ ||W^4(L,\mathfrak{v})||_{\tilde{L}} &\leq C(\mathrm{e}^{(\eta-\kappa)\tilde{L}} + |\mathfrak{v}|) \end{aligned}$$

and in particular

$$|h_{L,\mathfrak{v}}(0) - q_1(0)| + |h_{L,\mathfrak{v}}(2L) - q_2(0)| \leq C(\mathrm{e}^{(\eta-\kappa)L} + |\mathfrak{v}|).$$

The local uniqueness in the statement of theorem 2.3 follows from its analogue in theorem 2.2, the uniqueness statements in lemmas 6, 7 and for $\mu(L,\mathfrak{v})$ above by possibly decreasing $\epsilon_4 > 0$. The estimate $|\mu| \leq C(\mathrm{e}^{-2\kappa L} + |\mathfrak{v}|)$ follows from theorem 2.1 already without the existence proof, similar to the estimates in lemmas 6, 7. Hence, while the existence proof needed $|\mu| \leq \delta_4 \mathrm{e}^{-\eta L}$, the local uniqueness for 1–homoclinics holds for example if $|\mathfrak{v}| \leq C\mathrm{e}^{-\kappa L}$ and $\mu \in B_{\delta_4}(0) \subset \Lambda$. Taken together we obtain the claimed uniqueness up to time shifts in $B_{\delta_4}(0) \subset \Lambda$ for $\mathfrak{v} = 0$, i.e. uniform in $L$. □

Recall that the set $I_b^3$ consists of disconnected open intervals, see remark 6, and $h_{L,\mathfrak{v}}$, $\mu(L,\mathfrak{v})$ consist of disjoint curve segments for any fixed small $\mathfrak{v}$. In section 2.4 the role of $\mathfrak{v}$ in connecting these pieces is investigated. See remark 6 concerning the meaning of the enumeration of the countably infinite families.

**Remark 7** *We could now translate these homoclinics into ones that have semi travel time $L$ between section $\Sigma_1$ and $\Sigma_2$ as indicated in remark 4. While we do not pursue this in our discussion, we outline the approach. For simplicity consider $\mathfrak{v} = 0$ in the*

*codimension–2 case. Since $h_{L,0}(0)$ and $h_{L,0}(2L)$ lie exponentially close to $q_1(0)$ and $q_2(0)$ respectively, we can find exponentially small unique $\xi_L^1$ and $\xi_L^2$ so that $h_{L,0}(\xi_L^1) \in \Sigma_1$ and $h_{L,0}(\xi_L^1 + 2L + \xi_L^2) \in \Sigma_2$, hence the semi travel time is $(\xi_L^1 + 2L + \xi_L^2)/2$. We can take $L^* = \xi_L^1 + 2L + \xi_L^2$ and define $h_{L^*}^*(\xi) := h_{L,0}(\xi - \xi_L^1)$ to obtain homoclinics that are parameterizes by the unique semi-travel-times between the sections.*

## 2.4 Extending the curves of 1–homoclinic orbits

In the codimension–2 case the 1–homoclinics found in theorem 2.3 have the additional parameter $\mathfrak{v}$ due to the two-dimensionality of $E^{\mathrm{u}}_{-1}(0) \cap E^{\mathrm{s}}_{+1}(0)$ and $\mathcal{W}_1 = \mathcal{W}^{\mathrm{u}}(p_0) \cap \mathcal{W}^{\mathrm{cs}}(\gamma)$. This creates a one-parameter family of distinct *heteroclinic* orbits in $\mathcal{W}_1$, i.e. not related by time shifts. Theorem 2.3 may be applied to any one of these heteroclinics with asymptotic phase zero, if all other hypotheses hold. In the following, we will reparametrize $h_{L,\mathfrak{v}}$ in terms of these distinct heteroclinic orbits and draw global conclusions about connected curves of 1–homoclinics.

Let $q_{1,\alpha}$ be a heteroclinic from $p_0$ to $\gamma$ such that $q_{1,\alpha}(0) \in \mathcal{W}^{\mathrm{ss}}_\alpha(\gamma)$. Then $q_{1,\alpha}(\cdot - \alpha)$ has asymptotic phase zero and under the assumptions of theorem 2.3 we obtain a family of 1–homoclinic orbits, which we denote by $h^\alpha_{L,\mathfrak{v}}$. The set of approximate semi-travel-times associated to $q_{1,\alpha}$ (not $q_{1,\alpha}(\cdot - \alpha)$) will be identified as $I_\alpha := I_b^4 - \alpha/2$ in the following theorem.

Let $\Phi(\xi)$ denote the flow to $\dot{u} = f(u;0)$, cf. (2.1), and given a set $S \subset \mathbb{R}^n$ denote its orbit by $\mathcal{O}(S) := \{\Phi(\xi)v \,|\, v \in S, \xi \in \mathbb{R}\}$. For an interval $J$ formally set $\Gamma_J := \{q_{1,\alpha}(0) \in \mathcal{W}^{\mathrm{ss}}_\alpha(\gamma) \,|\, \alpha \in J\}$.

**Lemma 8** *Assume hypothesis 1, 2 and 4. There exists a $C^k$ curve $\Gamma \subset \mathcal{W}_1$ which contains $q_1(0)$ and is transverse to the flow and strong stable fibers of $\gamma$. Any such bounded curve can be parametrized so that $\Gamma = \Gamma_J$ for a bounded nontrivial interval $J \subset \mathbb{R}$.*

**Proof.** By hypothesis 2 the intersection of unstable and center-stable manifolds is transverse at $q_1(0)$ and $\mathcal{W}_1$ is two-dimensional. By the implicit function theorem smoothness of stable and unstable manifolds implies that a neighborhood of $q_1(0)$ is a two-dimensional $C^k$ manifold. Let $\alpha_0$ be so that $q_1(0) \in \mathcal{W}^{\mathrm{ss}}_{\alpha_0}(\gamma) \cap \mathcal{W}_1$. Since $\mathcal{W}_1$ is flow invariant, the

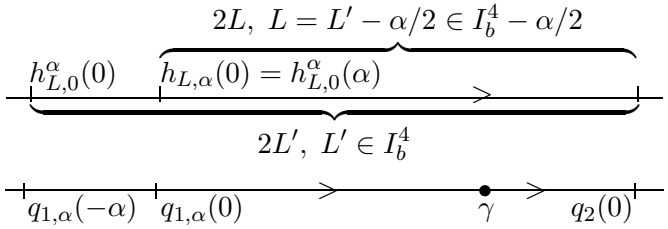


Figure 9: Schematic picture of shifting the approximate semi-travel-time by $\alpha/2$.

tangent space $T_{q_1(0)}\mathcal{W}_1$ is spanned by $E_1$ and $\dot{q}_1(0)$, which is transverse to the strong stable fibers. This allows to find a $C^k$ curve $\Gamma$ through $q_1(0)$, which is simultaneously transverse to the flow and the strong stable fibers. Since $\mathcal{W}^{\rm s}(\gamma)$ is fibered by $\mathcal{W}^{\rm ss}_\alpha(\gamma)$, $0 \le \alpha < T_\gamma$, we can parametrize any such $\Gamma$ as claimed. □

**Theorem 2.4** *Assume hypotheses 1, 2 and 4. Let $\Gamma = \Gamma_J$ as in lemma 8. There exist constants $\epsilon_\Gamma > 0$ and $j_0$ and countably infinite $C^k$ families of curves $\mu^j_\Gamma(L)$ of parameters and $h^j_\Gamma(\xi; L)$ of 1–homoclinic orbits to $p_0$, for $L \in I_\Gamma$ and $j \ge j_0$ such that for each $j$ the estimates of theorem 2.3 hold.*

*The interval $J$ can be extended so that there exists an interval $J' \subset J$ such that the following holds. For any 1–homoclinic $h$ which lies in the $\epsilon_\Gamma$–neighborhood of $\mathcal{O}(\Gamma_{J'}) \cup \mathcal{O}(\{q_2(0)\})$ there exist $j \ge j_0$, $L \in I_\Gamma$ and $\sigma_L = O(\epsilon_\Gamma)$ such that $h(\cdot - \sigma_L) \equiv h^j_\Gamma(\cdot, L)$ and for $\alpha \in J'$ we have $\{h^\alpha_{L,\mathfrak{v}}(\xi) \mid \xi \in \mathbb{R}, |\mathfrak{v}| \le \delta_4, L \in I_\alpha\} \subset \{h^j_\Gamma(\xi) | \xi \in \mathbb{R}, L \in I_\Gamma, j \ge j_0\}$.*

**Proof.**

As noted previously $q_{1,\alpha}(-\alpha) \in \mathcal{W}^{\rm ss}_0(\gamma)$, so existence of an $\alpha$ dependent family of curves of 1–homoclinics $h^\alpha_{L,\mathfrak{v}}$ and parameters $\mu(L, \alpha, \mathfrak{v})$ follows from theorem 2.3. The 1–homoclinics $h^\alpha_{L,0}$ for parameter $\mu(L, \alpha, 0)$ have any approximate semi-travel-time $L \in I_b^4$. Define $\mu(L, \alpha) := \mu(L, \alpha, 0)$ and $h_{L,\alpha} := h^\alpha_{L,0}(\cdot + \alpha)$ for $\alpha \in J$, i.e. $h_{L,\alpha}(0) - q_{1,\alpha}(0) = O(\mathrm{e}^{(\eta-\kappa)L})$ with any approximate semi-travel-times $L \in I_\alpha$, see figure 9, and associated parameters $\mu(L, \alpha)$. Recall $I_b$ has been derived in lemma 3 by slightly 'thickening' the sequence $T_j = jT_\gamma/2$, which has the property $|q_{1,\alpha}(T_j - \alpha) - q_2(-T_j)| \le C\mathrm{e}^{-\kappa T_j}$. By definition of $I_\alpha$ we conclude for $\alpha, \alpha' \in I_\Gamma$ that $I_\alpha = I_{\alpha'} + (\alpha' - \alpha)/2$, and so varying $\alpha$ extends the available approximate semi-travel-times $I_\Gamma := \cup_{\alpha \in J} I_\alpha \subset \mathbb{R}$. Smoothness of $h^\alpha_{L,0}$ in $\alpha$ follows from

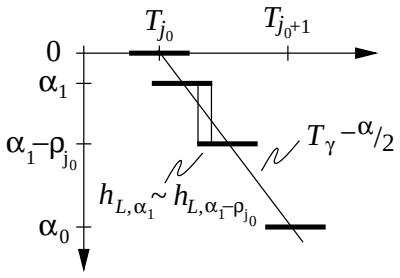


Figure 10: Patching curves of 1–homoclinic orbits.

smoothness of $\Gamma$, the heteroclinic and the trichotomies with respect to parameters, cf. e.g. [50].

For each $q_{1,\alpha}(\cdot-\alpha)$ theorem 2.3 provides a constant $\epsilon(\alpha)=\epsilon_4$. Continuous dependence and boundedness of $J$ yield uniform $0<\epsilon:=\min\{\epsilon(\alpha)\,|\,\alpha\in J\}$. Each interval in $I_\alpha$ is open, so there are $\rho_j>0$ such that for $\alpha,\alpha'\in J$, $|\alpha-\alpha'|\le\rho_j$ we have $T_j\in I_\alpha\cap I_{\alpha'}$ and the intersection is open. Note that $I_\alpha\cap I_{\alpha'}$ is bounded, because the intervals constituting $I_\beta$ are exponentially short for any $\beta$. Let $I_L$ be the connected component of $I_\alpha$ containing $L$. By continuity in $\beta$ of $h_{L,\beta}$ we may decrease the $\rho_j>0$ such that for any $L\in I_\alpha\cap I_{\alpha'}$ and $\beta=\alpha$, $\beta=\alpha'$ it holds that

$$(h_{L,\beta}(\cdot-\beta)-q_{1,\alpha}(\cdot-\alpha),h_{L,\beta}(2L-\beta+\cdot)-q_2)\in B^0_\epsilon(0;\sup I_L). \tag{2.50}$$

Theorem 2.3 provides a unique $\sigma_L(\alpha)=O(\alpha-\alpha')$, $C^k$ in $L$ and $\alpha$ such that the overlapping parts can be patched together smoothly (note $\ell_L=L$, because $L\in I_\alpha$), i.e.

$$\begin{aligned} h_{L,\alpha} &\equiv h_{L,\alpha'}(\cdot+\alpha-\alpha'+\sigma_L(\alpha)) \\ \mu(L,\alpha) &= \mu(L,\alpha',\tilde{Q}P^{\mathrm{u}}_{-1}(0)(h_{L,\alpha'}(\sigma_L-\alpha)-q_{1,\alpha}(-\alpha))). \end{aligned} \tag{2.51}$$

Therefore, we can define extended curves of parameters and 1–homoclinics, cf. figure 10, as follows. Define $\alpha_0:=\inf J$, $\alpha_1:=\sup J$, $j_0:=\min\{j\,|\,T_j\in I_\Gamma\}$ and for $j\ge j_0$ set

$$\alpha(j,L):=\begin{cases} -\alpha_1/2 & L<T_j-\alpha_1/2 \\ -2(L-T_j) & L\in[T_j-\alpha_1/2,T_j-\alpha_0/2] \\ -\alpha_0/2 & L>T_j-\alpha_0/2 \end{cases}$$

Due to (2.51) we can define $C^k$ curves for $j\ge j_0$ by

$$\begin{aligned} h^j_\Gamma(\xi;L) &:= h_{L,\alpha(L,j)} \\ \mu^j_\Gamma(L) &:= \mu(L,\alpha(L,j)). \end{aligned}$$

These contain all 1–homoclinics $h_{L,\alpha}$ and parameters $\mu(L,\alpha)$, because by definition

$$\bigcup_{L\in I_\Gamma, j\geq j_0} \alpha(L,j) = I_\Gamma$$

We emphasize that for $\alpha \neq \alpha'$ and $\alpha - \alpha' < T_\gamma$ we have $q_{1,\alpha}(0) \neq q_{1,\alpha'}(0)$, and $|h_{L,\alpha}(0) - q_{1,\alpha}(0)| \leq \mathrm{e}^{(\eta-\kappa)L}$. Hence, for $L$ sufficiently large $h_{L,\alpha'}(\cdot+\tau) \neq h_{L,\alpha}$ for any $\tau$, i.e. we can separate 1–homoclinics by fixing $\alpha$, $\alpha'$ and choosing $L$ large, while we can patch them in (2.51) by choosing $\alpha$ and $\alpha'$ close to each other.

As to the claimed local uniqueness, let $E^{\mathrm{u}}_{-1}(0;\alpha)$, $P^{\mathrm{u}}_{-1}(0;\alpha)$ and $E^{\mathrm{s}}_{+1}(0;\alpha)$, $P^{\mathrm{s}}_{+1}(0;\alpha)$ as well as $E_1(\alpha)$, $\tilde{Q}_\alpha$ denote the spaces and projections from theorem 2.3 with respect to the heteroclinic $q_{1,\alpha}(\cdot-\alpha)$. Given a 1–homoclinic $h$ with variations $W(\sigma,L) \in B^0_\epsilon(0;L)$, the local uniqueness statement of theorem 2.3 implies that from $\tilde{Q}_\alpha P^{\mathrm{u}}_{-1}(0;\alpha)w_1(0;\sigma) = 0 \in E_1(\alpha)$ it follows $h$ is a time shift of $h^\alpha_{L,0}$. Let $\beta \in J$, and set $q := q_{1,\beta}(0)$. The tangent space $T_q\mathcal{W}_1 = \mathrm{span}\{E_1(\beta), \dot{q}_{1,\beta}(0))\}$, and by choice of $\Gamma$ it follows $T_q\mathcal{W}_1 = \mathrm{span}\{\frac{\mathrm{d}}{\mathrm{d}\alpha}|_{\alpha=\beta} q_{1,\alpha}(\alpha), \dot{q}_{1,\beta}(0)\}$. Therefore, we can solve $\tilde{Q}_\alpha P^{\mathrm{u}}_{-1}(0;\alpha)w_1(0;\sigma) = 0$ locally by the implicit function theorem. By the same argument, $J$ can be extended so that for $\Gamma = \Gamma_J$ we have $\{h^j_{L,\Gamma}(\xi) \mid \xi\in\mathbb{R}, L\in I_\Gamma, j\geq j_0\} \supset \{h^{\alpha_0}_{L,\mathfrak{v}}(\xi) \mid |\mathfrak{v}| \leq \delta_4, \xi\in\mathbb{R}\}$. For a set $S\subset\mathbb{R}^n$ define $B_\epsilon := \{v\in\mathbb{R}^n \,|\, \mathrm{dist}(v,S)\leq\epsilon\}$. By continuity, there are $J'\subset J$ and $\epsilon_\Gamma \in (0,\epsilon)$, such that for $\Gamma' := \Gamma'$ we have

$$B_{\epsilon_\Gamma}(\{h^j_{L,\Gamma'}(\xi) \mid \xi\in\mathbb{R}, L\in I_\Gamma, j\geq j_0\}) \subset \{h_{L,\Gamma}(\xi) \mid \xi\in\mathbb{R}, L\in I_\Gamma\}.$$

Together with the local uniqueness statement in theorem 2.3 we conclude the claimed uniqueness for any 1–homoclinic with variations in $B^0_{\epsilon_\Gamma}(0;L)$ with respect to $q_{1,\alpha}$, $\alpha\in\Gamma_{J'}$ and any $L\in I_{\Gamma'_J}$. □

If $\Gamma_J$ is so that $I_\alpha \cap I_{\alpha'} \neq \emptyset$ implies $\alpha-\alpha' < T_\gamma$, then $\alpha\in J_\Gamma$ uniquely identifies $h_{L,\alpha}$. However, if $J=(\alpha_0,\alpha_1)$ and $|\alpha_0-\alpha_1| \geq T_\gamma$, then the 1–homoclinics $h_{1,\alpha_0}$ and $h_{1,\alpha_1}$ may or may not be related by time shifts as we will see in the next theorem.

Suppose that $I_\Gamma = (L_*,\infty)$ for some $L_*$ so there exist 1–homoclinics in the family $h^j_\Gamma$ for an unbounded interval of approximate semi-travel-times. However, it is not clear this yields a connected curve of 1–homoclinics and parameters, i.e. a bifurcation from the

heteroclinic cycle. As pointed out in remark 6 the uniqueness has the effect that the set of parameter values $\{\mu(L,\alpha)|L \in I_\alpha\}$ consists of disjoint curve segments for each $\alpha$ and the curves $\mu^j_\Gamma(L)$ do not necessarily connect these. Consider for instance a curve $\Gamma = \Gamma_{(\alpha_0,\alpha_1)}$ for $0 < \alpha_0 - \alpha_1 < T_\gamma/2$. Since the orbit of a curve $\Gamma$ is contained in $\mathcal{W}_1$ by invariance, there exists an unbounded curve $\Gamma' \subset O(\Gamma)$, which is transverse to the flow and intersects all strong stable fibers transversely. However, this curve is not closed, and while for any bounded piece theorem 2.4 applies, we cannot expect that the homoclinic orbits associated to any two heteroclinic orbits starting at distinct points in $\Gamma$ are the same, i.e. related by time shifts. Furthermore, $\Gamma = \Gamma_J$ for unbounded $J$ is tangent to the flow as $\beta \to \infty$ for $\beta \in J$. Therefore heteroclinics for large $\beta \in J$ are 'almost' related by time shifts. Hence, we expect that a curve of 1–homoclinics obtained from $\Gamma$ does not bifurcate from the heteroclinic cycle.

From this perspective, the only general condition that could guarantee a smooth connected curve of 1–homoclinics appears to be the existence of a *closed* curved that intersects all strong stable fibers.

**Hypothesis 5** *The intersection $\mathcal{W}_1$ between the equilibrium's unstable manifold $\mathcal{W}^{\mathrm{u}}(p_0)$ and the periodic orbit's center-stable manifold $\mathcal{W}^{\mathrm{cs}}(\gamma)$ contains a nontrivial $C^k$ Jordan curve $\Gamma$, which transversely intersects all strong stable fibers $\mathcal{W}^{\mathrm{ss}}_\alpha(\gamma)$, $0 \le \alpha < T_\gamma$. Any heteroclinic orbit in $\mathcal{W}_1$ intersects $\Gamma$ and those starting in $\Gamma$ satisfy hypotheses 2 and 4.*

Here, Jordan curve means a non self-intersecting, closed curve and the part concerning hypothesis 2 means that the unstable manifold of $p_0$ intersects the center-stable manifold of $\gamma$ transversely at every point. The intersection of any heteroclinic with $\Gamma$ means that the orbit of $\Gamma$ is surjective on $\mathcal{W}_1$, so $\mathcal{W}_1$ is a two-dimensional $C^k$ manifold with boundary $p_0 \cup \gamma$. Note that as the intersection of two manifolds $\mathcal{W}_1$ may a priori have several connected components.

As mentioned previously, this hypothesis is for instance satisfied when $\gamma$ stems from a 'nearby' Hopf-bifurcation of $p_0$. In this case the union of $p_0$ with its center manifold contains a disc which has $\gamma$ as its boundary, cf. e.g. chapters 6.4 and 8 in [31]. Circles in this disc which wind around $p_0$ once can be chosen for $\Gamma$, and for counter-examples to hypothesis 5 we can insert a saddle-node bifurcation into this disc, see figure 11.

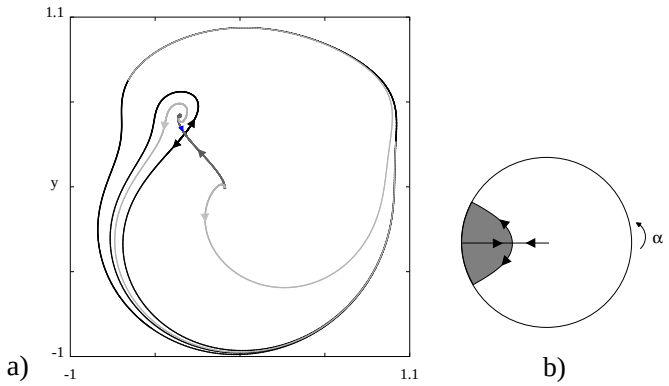


Figure 11: a) Example for winding number zero: $x' = x - x(x^2+y^2) - y + 0.7\exp(-10(y-0.5)^2)$, $y' = y - y(x^2+y^2) + x$. The saddle's unstable manifold (black) separates heteroclinic sets from the central and the outer focus; computed with dstool [4]. b) schematic picture for 'cutting out' strong stable fibers with a saddle's unstable manifold.

We expect Hypothesis 5 can be derived from more abstract topological assumptions, such as: *There is a curve in $\mathcal{W}_1$, which is homotopic in $\mathcal{W}_1 \cup \mathcal{O}(\gamma(0))$ to $\gamma$, but not to single point,* or alternatively, *it has nonvanishing, but finite (appropriately defined) winding number with respect to $p_0$ in $\mathcal{W}_1$.*

Let $\Gamma$ be a curve that satisfies hypothesis 5. As shown in theorem 2.4, transversality to strong stable fibers yields a parametrization $\Gamma = \{q_{1,\alpha}(0) \in \mathcal{W}^{\mathrm{ss}}_\alpha(\gamma) \,|\, \alpha \in [0, T^*)\}$. Since $\Gamma$ is closed and nontrivial there is $m \in \mathbb{N} \setminus \{0\}$ such that $T^* = mT_\gamma$ and we call $m$ the winding number of $\Gamma$. By surjectivity the flow provides a pointwise defined diffeomorphism between any two curves that satisfy hypothesis 5, so $m$ is the same and counts how often the set of heteroclinic points $\mathcal{W}_1$ 'winds around' $\gamma$ and $p_0$. If $\mathcal{W}_1 \cup \mathcal{O}(\gamma(0))$ is a Möbius band near $\gamma$, then $m = 2$.

The proof of following theorem mainly uses that the "uniqueness neighborhoods" from theorem 2.3 are uniform for all heteroclinics in $\Gamma$. We conjecture that for infinite winding number a countably infinite number of curves of 1–homoclinics bifurcates.

**Theorem 2.5** *Assume hypotheses 1 and 5, and let $m$ be the winding number of $\Gamma$. There are positive constants $\epsilon$, $L_*$ and $C$, such that the following holds. There exist $m$ curves $h^j_L$ of 1–homoclinic orbits to $p_0$ of (2.1) and $\mu^j(L)$ of associated parameters for $L \geq L_4$.*

*The curves are of class $C^k$, bifurcate from the heteroclinic cycle and satisfy*

$$\begin{aligned} |\mu^j(L)| &\leq C\mathrm{e}^{-2\kappa L} \\ ||h_L - q_1||_{0,\tilde{L}} + ||h_L^j(2L - \cdot) - q_2||_{-0,\tilde{L}} &\leq C\mathrm{e}^{-\kappa\tilde{L}}. \end{aligned}$$

*Let $h$ be a 1–homoclinic solution to (2.1) for $|\mu| \leq \delta$ such that $h(\xi) \in B_\epsilon(\mathcal{W}_1 \cup \{q_2(\xi) | \xi \in \mathbb{R}\}) \subset \mathbb{R}^n$ for all $\xi$. There exists unique $\sigma \in \mathbb{R}$, $L \geq L_4$ and $j \in \{0, \ldots, m-1\}$ such that $h \equiv h_L^j(\cdot + \sigma)$ and $\mu = \mu^j(L)$.*

**Proof.** Let $\Gamma$ satisfy hypothesis 5 with winding number $m$. Parametrize $\Gamma = \{q_{1,\alpha}(0) \in \mathcal{W}_\alpha^{\mathrm{ss}}(\gamma) \,|\, \alpha \in [0, T^*]\}$ as in theorem 2.4 so that $q_{1,0} \equiv q_{1,T^*}$. Then $T^* = mT_\gamma$ and using the estimates and notation from theorem 2.3 as well as (2.50) we get for $L \in I_\Gamma$ that

$$\begin{aligned} ||(h_{L,T^*}(\cdot - T^*) - q_{1,T^*}(\cdot - T^*), h_{L,T^*}(2L - T^* + \cdot) - q_2)||_L &\leq C\mathrm{e}^{(\eta-\kappa)L} \\ \Rightarrow ||(h_{L,T^*} - q_{1,T^*}, h_{L,T^*}(2L - T^* + \cdot) - q_2)||_L &\leq C\mathrm{e}^{\eta T^*}\mathrm{e}^{(\eta-\kappa)L} \\ \Leftrightarrow ||(h_{L,T^*} - q_{1,0}, h_{L,T^*}(2(L - T^*/2) + \cdot) - q_2)||_L &\leq C\mathrm{e}^{\eta T^*}\mathrm{e}^{(\eta-\kappa)L}. \end{aligned}$$

For sufficiently large $\bar{L}_4$ and using $\epsilon_\Gamma$ from theorem 2.4 we have $C\mathrm{e}^{T^*}\mathrm{e}^{(\eta-\kappa)L} \leq \epsilon_\Gamma$ for any $L \geq \bar{L}_4$. Hence, by uniqueness $h_{L+T^*/2,0} \equiv h_{L,T^*}$. Here $L = \ell_L$ and $\sigma_L = 0$, because both vary with respect to the same heteroclinic and are fixed points of $\mathcal{G}$, cf. lemma 4. Therefore, the curves found in theorem 2.4 consist of $m$ curves, which we can parametrize by $j = 0, \ldots, m-1$ and $\alpha(L) := -2L \bmod T^*$ as

$$\begin{aligned} h_L^j &:= h_{(L+jT_\gamma/2),\alpha(L)} \\ \mu^j(L) &:= \mu(L + jT_\gamma/2, \alpha(L)). \end{aligned} \tag{2.52}$$

We next show that $h_L^j$ is not a time shift of any $h_{L'}^{j'}$ if $j \neq j'$ and $L, L'$ are large enough, and that any 1–homoclinic near the heteroclinic cycle is captured. It follows that there are precisely $m$ curves of 1–homoclinics bifurcating from the heteroclinic cycle, as indicated in figure 12, and precisely $m$ connected associated parameter curves $\mu^j(L)$ bifurcate from $\mu = 0$.

Since 1–homoclinics in a uniform neighborhood of $q_{1,\alpha}$ and $q_2$ for each $\alpha$ are locally unique by theorem 2.3, it suffices to show that none of the heteroclinic orbits $q_{1,\alpha}$ are related by time shifts.

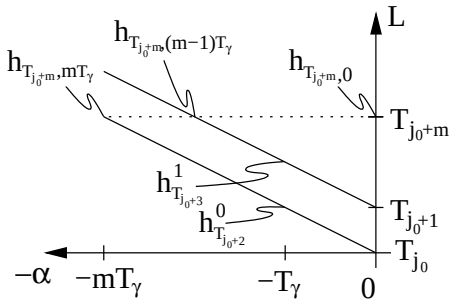


Figure 12: Paths of the 1–homoclinics in the parameters $\alpha$ and $L$ using the sequence $T_j := jT_\gamma/2$ and $j_0$ so that $T_{j_0} \in I_b^4$. The homoclinics associated to $L = (m + j_0)T_\gamma/2$, and $\alpha = 0$, $\alpha = mT_\gamma$ coincide, while the one for $\alpha = (m-1)T_\gamma$ is different.

To show the heteroclinics are distinct in this sense, assume for a contradiction first, that there are $\xi_0 > 0$ and $\alpha_0, \alpha_1 \in I_\Gamma$ such that $0 < \alpha_0 - \alpha_1 < mT_\gamma$ and $q_{1,\alpha_0}(\xi_0) = q_{1,\alpha_1}(0)$. Define the partial orbit $O_1 := \{q_{1,\alpha_0}(\xi) \,|\, 0 \le \xi \le \xi_0\}$ and the closed curve $\Gamma_0 := O_1 \cup \{q_{1,\alpha}(0) \,|\, \alpha \in (\alpha_0, \alpha_1)\}$. We may assume $\xi_0 > 0$ is the smallest $\xi$ so that $q_{1,\alpha_0}(\xi) = q_{1,\alpha_1}(0)$. Since $\Gamma$ is non self-intersecting this implies that $\Gamma_0$ is non self-intersecting.

The curves $\Gamma$ and $\Gamma_0$ are bounded, so we can find $\xi_+ > \xi_- > \xi_0$ such that the partial orbits $\{\Phi(\xi)\Gamma_0 \,|\, -\xi_+ \le \xi \le -\xi_-\}$ and $\{\Phi(\xi)\Gamma_0 \,|\, \xi_- \le \xi \ge \xi_+\}$ have empty intersection with $\Gamma$ and $\Gamma_0$. Therefore, the partial orbit $O := \{\Phi(\xi)\Gamma_0 \,|\, -\xi_+ \le \xi \le \xi_+\} \subset W_1$ is a $C^k$ manifold which is homeomorphic to an annulus, because $\Phi(\xi)\Gamma_0$ is homeomorphic to $S^1$ for any $\xi$. Hence, $O$ is separated by $\Gamma_0$ into an 'interior' containing $\Phi(\xi_+)\Gamma$, and an 'exterior' containing $\Phi(-\xi_+)\Gamma$. Any connected curve in $\mathcal{W}_1$ that has parts inside and outside has to cross $\partial O$ or $\Gamma_0$.

The parametrization induces an orientation on $\Gamma$ for increasing $\alpha$, and smoothness yields tangent vectors $\partial_\alpha q_{1,\alpha}(0) \neq 0$. Since $\Gamma$ is transverse to the flow, the angle $s(\alpha)$ from $\partial_\alpha q_{1,\alpha}(0)$ to $f(q_{1,\alpha}(0); 0)$ in the two-dimensional tangent space $T_{q_{1,\alpha}(0)}\mathcal{W}_1$ is never a multiple of $\pi$. By assumption, this angle always lies in $(\pi, 2\pi)$, see figure 13. Therefore, for increasing $\alpha$ the curve $\Gamma$ can cross the tangent vectors to the flow line $O_1$ only at angles $s(\alpha) \in (\pi, 2\pi)$, i.e. from outside $\Gamma_0$ to inside. Hence, for any sufficiently small $\beta > 0$ we have $q_{1,\alpha_1+\beta}(0)$ and $q_{1,\alpha_0-\beta}(0)$ lie on opposite sides of $\Gamma_0$ in $O$, see figure 13. Since $\Gamma$ is closed and does not intersect $\partial O$, it has to cross $\Gamma_0$ from interior to exterior for increasing $\alpha$. This would have to occur at $O_1$, because $\Gamma$ is non self-intersecting, which contradicts

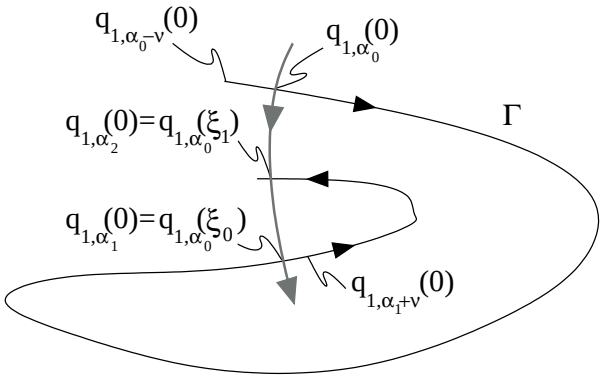


Figure 13: Configuration in the case that $\mathcal{O}(\Gamma)$ intersects $\Gamma$ (black) along a flow line (gray).

$s(\alpha) \in (\pi, 2\pi)$. Hence such an intersection along a flow line cannot occur for $\xi_0 > 0$ and $0 < \alpha_0 < \alpha_1 < mT_\gamma$. Similarly, the case $\xi_0 < 0$ is ruled out, so the set of heteroclinics is distinct. As noted above, it follows that the 1–homoclinics $h_L^j$ are distinct.

The constants $C$, $L_4$ and $\delta_4$ from theorem 2.3 may be chosen uniform in $\alpha$ due to continuity and the boundedness of $[0, T_\gamma]$. We denote by $L_*$ the uniform $L_4$ and set $\epsilon := \epsilon_\Gamma$ from theorem 2.4.

Let $u$ be a solution to (2.1) with $u(0) \in B_\epsilon(\Gamma) \subset \mathbb{R}^n$ and $L$ so that $u(2L) \in B_\epsilon(q_2(0))$. Then $L \to \infty$ as $\epsilon \to 0$. Since $\mathcal{O}(\Gamma \cup q_2(0))$ is bounded and the vector field continuous, there is a uniform lower bound $L_\epsilon$ such that for all solutions $u$ and times $L$ with $u(0)$ and $u(2L)$ as above we have $L \geq L_\epsilon$, and $L_\epsilon \to \infty$ as $\epsilon \to 0$. Now let $h$ be a 1–homoclinic orbit that lies in $B_\epsilon(\mathcal{W}_1 \cup \{q_2(\xi) | \xi \in \mathbb{R}\}) \subset \mathbb{R}^n$. There is $L$ and, by hypothesis 5, there are $\alpha$ and $\sigma$ such that $|h(\sigma) - q_{1,\alpha}(0)| \leq \epsilon$ and $|h(2L + \sigma) - q_2(0)| \leq \epsilon$. Therefore $L \geq L_\epsilon$ and we may assume $\epsilon$ is so small that $L_\epsilon \geq L_4$ and $\epsilon \leq \epsilon_\Gamma$, where $\epsilon_\Gamma > 0$ is from theorem 2.4. It follows from theorem 2.4 for unique $\sigma_L$ and $j \in \{0, \ldots, m-1\}$ that $h \equiv h_L^j(\cdot + \sigma_L)$. □

Note that the extension of curves of $n$–homoclinic orbits works the same way, given an existence and uniqueness theorem like theorem 2.3, but we do not pursue this here.

## 2.5 Expansion of parameter curves

In this section, we investigate the leading order geometry of any connected parameter curve $\mu(L)$ from theorem 2.5. Let $\Gamma = \{q_{1,\alpha}(0) \in \mathcal{W}^{\text{ss}}_\alpha(\gamma) \,|\, \alpha \in [0, mT_\gamma)\}$ be a curve which

satisfies hypothesis 5 and has winding number $m$. Theorem 2.5 and (2.52) imply that initial conditions for the heteroclinic orbits that are exponentially close to the 1–homoclinics at parameter values $\mu(L)$ can be chosen $q_{1,\alpha(L)}(0)$ with $\alpha(L) = -2L \mod mT_\gamma$.
By theorem 2.5 we have $\mu(L) = O(\mathrm{e}^{-2\kappa L})$ and so (2.49), note $\mathfrak{v} = 0$, yields

$$\mathcal{M}\mu(L) = -\langle b_L, a^1(-L)\rangle a_0^1 - \langle b_L, a^2(-L)\rangle a_0^2 + O(\mathrm{e}^{(\eta-3\kappa)L}). \tag{2.53}$$

We expect that the parameter curve is determined to leading order as $L \to \infty$ by the scalar products in this expression. Recall $b_L = q_2(-L) - q_{1,\alpha(L)}(L)$, hence the scalar products in (2.53) are, for $j = 1, 2$, given by

$$\langle -b_L, a^j(-L)\rangle \;=\; \langle q_{1,\alpha(L)}(L) - \gamma(-L), a^j(-L)\rangle - \langle q_2(-L) - \gamma(-L), a^j(-L)\rangle. \tag{2.54}$$

Recall the Floquet representation $A_{\mathrm{per}}(\xi)\mathrm{e}^{R\xi}$ of the evolution $\Phi_\gamma(\xi, 0)$ of $v' = \partial_u f(\gamma(\xi))v$, where $A_{\mathrm{per}}(\xi)$ is $T_\gamma$-periodic and invertible, $A_{\mathrm{per}}(0) = \mathrm{Id}$. By hypothesis 1, the matrix $R$ has an algebraically simple eigenvalue zero, and no other eigenvalues lie on the imaginary axis. Let $E_j$ be the generalized eigenspace of $R$ to the eigenvalues $\nu_j$, $j = 1, \dots n$, and $\nu^{\mathrm{s}} \neq 0$ be so that $\Re(\nu^{\mathrm{s}}) < 0$ and $\Re(\nu_j) < 0 \Rightarrow \Re(\nu_j) \leq \Re(\nu^{\mathrm{s}})$. We define the strong stable, leading stable and center-unstable generalized eigenspaces of $R$:

$$E_R^{\mathrm{ss}} := \sum_{\{j \,|\, \Re(\nu_j) < \Re(\nu^{\mathrm{s}})\}} E_j \quad , \quad E_R^{\mathrm{s}} := \sum_{\{j \,|\, \Re(\nu_j) = \Re(\nu^{\mathrm{s}})\}} E_j \quad , \quad E_R^{\mathrm{u}} := \sum_{\{j \,|\, \Re(\nu_j) > \Re(\nu^{\mathrm{s}})\}} E_j$$

Notice that $E_R^{\mathrm{ss}} \oplus E_R^{\mathrm{s}} \oplus E_R^{\mathrm{u}} = \mathbb{R}^n$ and let $P_R^{\mathrm{ss}}$ be the projection onto $E_R^{\mathrm{ss}}$ with kernel $E_R^{\mathrm{s}} \oplus E_R^{\mathrm{u}}$, and $P_R^{\mathrm{s}}$ the projection onto $E_R^{\mathrm{s}}$ with kernel $E_R^{\mathrm{ss}} \oplus E_R^{\mathrm{u}}$, as well as $P_R^{\mathrm{u}}$ the projection onto $E^{\mathrm{u}}$ with kernel $E_R^{\mathrm{ss}} \oplus E^{\mathrm{s}}$.
In the following $A^*$ denotes the adjoint of $A$ and $E^\perp$ the ortho-complement of a linear space $E$ with respect to the standard scalar product. Furthermore, $\bar{z}$ denotes the complex conjugate of $z \in \mathbb{C}$, and direct sums as well as spans are over $\mathbb{R}$.
Since we did not distinguish leading stable and unstable rates in our analysis, but only considered the joint rate $\kappa$, we need to assume that the stable spectrum of $R$ is closest to the imaginary axis in the following. We expect from a refined analysis that this assumption can be dropped.

**Hypothesis 6 (real leading eigenvalue)** *There is a real algebraically and geometrically simple eigenvalue $\nu^{\rm s} < 0$ such that there is a $\delta > 0$ so $|\Re(\nu)| - |\nu^{\rm s}| \geq \delta$ for all other eigenvalues $\nu$ of $R$.*

**Hypothesis 7 (complex leading eigenvalues)** *There is a pair of complex conjugate algebraically and geometrically simple eigenvalues $\nu^{\rm s}$, $\bar{\nu}^{\rm s}$ with $\Re(\nu^{\rm s}) < 0$ such that there is a $\delta > 0$ so $|\Re(\nu)| - |\Re(\nu^{\rm s})| \geq \delta$ for all other eigenvalues $\nu$ of $R$.*

Let $\mathcal{W}_\rho \subset \mathcal{W}_1$ be such that for $q(0) \in \mathcal{W}_\rho$ the solution $q(\xi)$ satisfies $\limsup_{\xi\to\infty} \frac{\ln(q(\xi))}{-\xi} = \rho$.

**Lemma 9** *Assume hypotheses 1 and 5 with winding number $m$, and hypothesis 6 or 7. Let $\Re(\nu^{\rm s}) = -\rho < 0$. It holds that $q_2(\xi) = \gamma(\xi) + O(\mathrm{e}^{-(\rho+\delta)|\xi|})$ for $\xi \leq 0$ and there exists $j \geq 1$ and a $(mT_\gamma/j)$–periodic $C^k$ function $v : \mathbb{R} \to \Re(E^{\rm s}_R)$ such that for $\xi \geq 0$*

$$q_{1,\alpha}(\xi) \;=\; \gamma(\xi+\alpha) + A_{\rm per}(\xi+\alpha)\mathrm{e}^{R\xi}v(\alpha) + O(\mathrm{e}^{-(\rho+\delta)\xi}). \tag{2.55}$$

*If $\mathcal{W}_\rho \neq \emptyset$ then there is $\alpha \in [0, mT_\gamma)$ such that $v(\alpha) \neq 0$.*

**Proof.** We first show the expansion for $q_{1,\alpha}(\xi)$. Consider $v = q_{1,\alpha} - \gamma(\cdot + \alpha)$, which solves the variational equation

$$\begin{aligned} v' &= \partial_u f(\gamma(\xi+\alpha);0)v + g(v,\xi,\alpha) \quad \text{where} \\ g(v,\xi,\alpha) &= f(v+\gamma(\xi+\alpha);0) - f(\gamma(\xi+\alpha)) - \partial_u f(\gamma(\xi+\alpha);0)v. \end{aligned}$$

Analogous to (2.5) and (2.6) we obtain $g(v,\xi,\alpha) = O(|v|^2)$, because of the periodicity in $\alpha$. We now consider $w = A_{\rm per}(\xi+\alpha)^{-1}v$. It holds for general Floquet representation, cf. e.g. [14], that $\partial_u f(\gamma(\xi);0)A_{\rm per}(\xi) = A_{\rm per}(\xi)' + A_{\rm per}(\xi)R$ and so $w$ solves

$$w' = Rw + A^{-1}_{\rm per}(\xi+\alpha)g(A_{\rm per}(\xi+\alpha)w,\xi,\alpha).$$

Since $v(\xi) = O(\mathrm{e}^{-\rho\xi})$ for $\xi \geq 0$, it follows $w(\xi) = O(\mathrm{e}^{-\rho\xi})$ by periodicity. Therefore, for any fixed $\alpha$, the proof of Theorem 4.5 from chapter 13 in [14] implies that there is a vector $v(\alpha) \in \Re(E^{\rm s}_R) \oplus \Im(E^{\rm s}_R)$ such that $w(\xi) = \mathrm{e}^{R\xi}v(\alpha) + O(\mathrm{e}^{-(\rho+\delta)\xi})$ for $\xi \geq 0$. Moreover, $v(\alpha)$ satisfies

$$v(\alpha) = P^{\rm s}\left((P^{\rm ss}_R - \mathrm{Id})w(0) + \int_0^\infty \mathrm{e}^{-R\zeta}(P^{\rm s}_R + P^{\rm u}_R)A^{-1}_{\rm per}(\zeta+\alpha)g(A_{\rm per}(\zeta+\alpha)w(\zeta),\zeta,\alpha)\mathrm{d}\zeta\right).$$

Since $P_R^{\rm ss} + P_R^{\rm u} + P_R^{\rm s} = {\rm Id}$ and $w(\zeta) = A_{\rm per}^{-1}(\alpha+\zeta)(q_{1,\alpha}(\zeta) - \gamma(\zeta+\alpha))$ we obtain

$$v(\alpha) = -P_R^{\rm s} A_{\rm per}^{-1}(\alpha)(q_{1,\alpha}(0) - \gamma(\alpha)) + \int_0^\infty {\rm e}^{-R\zeta} P_R^{\rm s} A_{\rm per}^{-1}(\zeta+\alpha) g(q_{1,\alpha}(\zeta) - \gamma(\zeta+\alpha), \zeta, \alpha) {\rm d}\zeta \tag{2.56}$$

By periodicity in $\alpha$ the integral converges uniformly in $\alpha$ and so $v(\alpha)$ is $C^k$. Since $q_{1,\alpha}(0)$ has minimal period $mT_\gamma$ uniqueness of the solutions imply that $q_{1,\alpha}(\xi)$ has minimal period $mT_\gamma$ for any $\xi \in \mathbb{R}$. Hence, (2.56) implies that $v(\alpha)$ has period $mT_\gamma/j$ for some $j \geq 1$. The claimed expansion follows from changing coordinates back to $u$.

As to the expansion of $q_2(\xi)$ which lies in the unstable manifold, hypothesis 6 or 7 imply that the unstable eigenvalues have real parts larger than $\rho + \delta$. A similar coordinate change as above and application of theorem 4.3 from chapter 13 in [14] implies $q_2(\xi) = \gamma(\xi) + O({\rm e}^{-(\rho+\delta)|\xi|})$ for $\xi \leq 0$.

As to roots of $v(\alpha)$, if $\mathcal{W}_\rho \neq \emptyset$ then by hypothesis 5 there are $\sigma \in \mathbb{R}$ and $\alpha \in [0, mT_\gamma)$ such that $q(0) = q_{1,\alpha}(\sigma)$, and so (2.55) implies that $v(\alpha) \neq 0$. □

We emphasize, that this lemma does not exclude the possibility that $v(\alpha)$ is constant. However, it shows that if $\mathcal{W}_1$ contains a "leading order strong stable fiber", i.e. $W_\rho \neq \emptyset$, then the leading order term in the expansion (2.55) does not vanish identically.

Next we prove a leading order expansion as $L \to \infty$ of the parameter curve $\mu(L)$. Let $\tilde{E}_\rho \subset (E_2)^\perp$ be the set of points such that for solutions $a(\xi)$ to the adjoint linear equation $a' = -(\partial_u f(q_2(\xi)))^* a$ with $a(0) \in \tilde{E}_\rho$ it holds that

$$\limsup_{\xi \to -\infty} \frac{\ln(a(\xi))}{\xi} = \rho.$$

Since the equation is linear it follows that $E_\rho := \tilde{E}_\rho \cup \{0\}$ is a linear subspace of $(E_2)^\perp$.

**Theorem 2.6** *Assume hypotheses 1, 2, 4, 5. Let $m$ be the winding number of $\Gamma$ and $\mu(L)$ a parameter curve of 1–homoclinic orbits to $p_0$ from theorem 2.5.*

*Assume hypothesis 6 and write $\nu^{\rm s} = -\rho$ for some $\rho > 0$. If $\tilde{E}_\rho \neq \emptyset$, then there exist $b_0 \in \tilde{E}_\rho$, $\epsilon > 0$ and a $C^k$ function $s_0 : \mathbb{R} \to \mathbb{R}$, which is constant or has minimal period $(mT_\gamma/(2\ell))$ for some $\ell \in \mathbb{N} \setminus \{0\}$ and*

$$\mu(L) = {\rm e}^{-2\rho L} s_0(L) b_0 + O({\rm e}^{(-(2\rho+\epsilon)L}).$$

*Assume hypothesis 7 and write* $\nu^{\rm s} = -\rho + {\rm i}\sigma$ *for some* $\rho > 0$ *and* $\sigma \in \mathbb{R}$. *If* $\dim(E_\rho) = 2$, *then there exist* $\epsilon > 0$ *and* $C^k$ *functions* $b_j : \mathbb{R} \to E_\rho$, $j = 1, 2$, *which are constant or have minimal period* $(mT_\gamma/(2\ell))$ *for some* $\ell \in \mathbb{N} \setminus \{0\}$ *and*

$$\mu(L) \;\; = \;\; {\rm e}^{-2\rho L}\left(\sin(2L\sigma)b_1(L) + \cos(2L\sigma)b_2(L)\right) + O({\rm e}^{-(2\rho+\epsilon)L}).$$

*If* $\dim(E_\rho) = 1$ *then the same holds and there are* $\tilde{b}_0 \in \tilde{E}_\rho$, $s_j : \mathbb{R} \to \mathbb{R}$ *such that* $b_j(L) = s_j(L)\tilde{b}$ *for* $j = 1, 2$.
*Assume* $\mathcal{W}_\rho \neq \emptyset$, $\tilde{E}_\rho \neq \emptyset$ *and set* $L_r := -\alpha/2 + rmT_\gamma/(2\ell)) \neq 0$ *for all* $r \in \mathbb{Z}$. *There exists* $\alpha \in [0, mT_\gamma)$ *such that* $q_{1,\alpha}(0) \in \mathcal{W}_\rho$ *and if* $v(\alpha) \notin (\Re(E^{\rm s}_{R^*})^\perp$ *then* $s_j(L_r) \neq 0$ *or* $b_j(L_r) \neq 0$ *for all* $r \in \mathbb{Z}$ *and* $j = 0$ *or* $j = 1, 2$ *respectively.*

**Proof.** We first derive expansions under hypothesis 6 and 7 alternatively and let $\Re(\nu^{\rm s}) = -\rho < 0$. Consider the scalar product in (2.54) involving $q_2(-L)$. Since $a^j(\xi) = O({\rm e}^{-\rho|\xi|})$ for $\xi \leq 0$ lemma 9 implies

$$\langle q_2(-L) - \gamma(-L), a^j(-L)\rangle \;\; = \;\; O({\rm e}^{-(2\rho+\delta)L}). \tag{2.57}$$

Next we address the scalar product in (2.54) involving $q_{1,\alpha(L)}(-L)$. Substituting $\alpha = \alpha(L) = -2L \mod mT_\gamma$ into (2.55) at $\xi = L$, we obtain

$$q_{1,\alpha(L)}(L) \;\; = \;\; \gamma(-L) + A_{\rm per}(-L){\rm e}^{RL}v(-2L) + O({\rm e}^{-(\rho+\delta)L}). \tag{2.58}$$

Now consider the adjoint solution $a^j(\xi)$. Notice that $(P^{\rm s}_R)^*$ is the projection onto the leading unstable eigenspace of $R^*$, and denote $E^{\rm u}_{R^*} := {\rm Rg}((P^{\rm s}_R)^*)$. We can write

$$(a^j)' = -(\partial_u f(\gamma(\alpha + \xi))^* + B(\xi)^*)a^j$$

where $B(\xi) := \partial_u f(q_2(\xi)) - \partial_u f(\gamma(\xi)) = O({\rm e}^{-\rho\xi})$, because $\nu^{\rm s}$ is algebraically simple and so we may choose $\kappa = \rho$, cf. (2.2). The proof of theorem 4.5 in chapter 13 of [14] shows there is a constant vector $c(a^j) \in \Re(E^{\rm u}_{R^*})$ such that, as $\xi \to -\infty$,

$$a^j(\xi) \;\; = \;\; (\Phi_\gamma(0, \xi))^* c(a^j) + O({\rm e}^{-(\rho+\delta)|\xi|}).$$

Using the Floquet representation $(\Phi_\gamma(0, \xi))^* = (A^*_{\rm per}(\xi))^{-1}{\rm e}^{-R\xi}$ for the adjoint evolution we obtain

$$a^j(-L) \;\; = \;\; {\rm e}^{R^*L}(A^{-1}_{\rm per}(-L))^* c(a^j) + O({\rm e}^{-(\rho+\delta)L}). \tag{2.59}$$

Application of (2.57), (2.58) and (2.59) to the terms in (2.54) implies

$$\begin{aligned}(2.60)\ \langle -b_L, a^j(-L)\rangle &= \langle A_{\rm per}(-L)\mathrm{e}^{RL}v(-2L), (A_{\rm per}(-L)^*)^{-1}\mathrm{e}^{R^*L}c(a^j)\rangle + O(\mathrm{e}^{-(2\rho+\delta)L}) \\ &= \langle v(-2L), \mathrm{e}^{2R^*L}c(a^j)\rangle + O(\mathrm{e}^{-(2\rho+\delta)L}).\end{aligned}$$

To obtain an expansion for $\mu(L)$ from (2.53) we compare $-(2\rho+\delta)$ and $\eta - 3\kappa$, where $0 < \eta < \kappa$. We may choose $\kappa = \rho$, because $\nu^{\rm s}$ is algebraically simple. Therefore, $\epsilon := \min\{\rho - \eta, \delta\}$ satisfies $\epsilon > 0$ and $\eta - 3\kappa = -2\rho + \eta - \rho \le -(2\rho + \epsilon)$, as well as $-(2\rho+\delta) \le -2(\rho+\epsilon)$. Upon substituting (2.60) into (2.53) it thus follows that

$$(2.61)\qquad \mu(L) = \sum_{j=1,2} \langle v(-2L), \mathrm{e}^{2R^*L}c(a^j)\rangle \mathcal{M}^{-1}a_0^j + O(\mathrm{e}^{-(2\rho+\epsilon)L}),$$

We next determine the form of the claimed expansions for real or complex leading stable eigenvalues. Note that $v(\alpha)$ does not depend on $a_0^1$ or $a_0^2$.

If $\tilde{E}_\rho \neq \emptyset$ then we may choose $a_0^1 \in \tilde{E}_\rho$, whence $c(a^1) \neq 0$, because of (2.59), and under hypothesis 6 $c(a^1)$ is an eigenvector. We define $s_0(L) := \langle v(-2L), c(a^1)\rangle$, $b_0 := \mathcal{M}^{-1}a_0^1$ and substitution into (2.61) implies the expansion in this case.

Under hypothesis 7, $E^{\rm s}_{R^*}$ is the direct sum of complex eigenspaces to $\nu^{\rm s}$ and $\bar{\nu}^{\rm s}$. Let $w^*$ be an arbitrary eigenvector to $\nu^{\rm s}$. There are $x_j, y_j \in \mathbb{R}$ such that $c(a_0^j) = x_j w^* + y_j \bar{w}^*$ for $j = 1, 2$. If $\dim(E_\rho) = 2$ then $E_\rho = \mathrm{span}\{a_0^1, a_0^2\}$ so $c(a_0^j) \neq 0$ for $j = 1, 2$ and we define

$$\begin{aligned}b_1(L) &:= \sum_{j=1,2} \langle v(-2L), (y_j - x_j)\Re(w^*) - (x_j + y_j)\Im(w^*)\rangle \mathcal{M}^{-1}a_0^j \\ b_2(L) &:= \sum_{j=1,2} \langle v(-2L), (x_j + y_j)\Re(w^*) + (y_j - x_j)\Im(w^*)\rangle \mathcal{M}^{-1}a_0^j.\end{aligned}$$

Upon substituting these into (2.61) the claimed terms in the expansion follow from a straight-forward computation using $R^*\Re(w^*) = \cos(\sigma)\Re(w^*) - \sin(\sigma)\Im(w^*)$ and $R^*\Im(w^*) = \sin(\sigma)\Re(w^*) + \cos(\sigma)\Im(w^*)$.

In case $\dim(E_\rho) = 1$ we choose $a_0^1 \in \tilde{E}_\rho$. Then $c(a_0^1) \neq 0$ and we set $s_j(L) := \langle v(-2L), (y_j - x_j)\Re(w^*) - (x_j + y_j)\Im(w^*)\rangle$ for $j = 1, 2$ as well as $b_1 = b_2 := \mathcal{M}^{-1}a_0^1$. The previously mentioned computation proves the claimed expansion for this case.

Regarding periodicity, lemma 9 shows the minimal period of $v(-2L)$ in $L$ is 0 or $mT_\gamma/(2\ell)$ for some integer $\ell \ge 1$. Therefore the period of $s_j$, $b_j$ for $j = 0$, $j = 1, 2$ respectively is as claimed.

If $\mathcal{W}_\rho \neq \emptyset$ and $\tilde{E}_\rho \neq \emptyset$ then hypothesis 5 implies that there exists $\alpha \in [0, mT_\gamma)$ such that $q_{1,\alpha}(0) \in \mathcal{W}_\rho$ and lemma 9 yields $v(\alpha) \neq 0$. If $s_j(L) = 0$ or $b_j(L) = 0$ then $\langle v(-2L), \Re(w^*)\rangle = 0$ and $\langle v(-2L), \Im(w^*)\rangle = 0$ because $\Re(w^*)$, $\Im(w^*)$ and $a_0^1$, $a_0^1$ are pairwise linearly independent. Therefore, if $v(\alpha) \notin (\Re(E^{\mathrm{s}}_{R^*}))^\perp$ then by periodicity $s_j(L_r) \neq 0$, $b_j(L_r) \neq 0$ for all $r \in \mathbb{Z}$ and $j = 0$ or $j = 1, 2$ respectively. □

We close this discussion with some remarks and conclusions concerning the expansions.
If $v(-2L) = 0$ for some $L$, then $s(L) = 0$ or $b_j(L) = 0$ and the heteroclinic set intersects a non-leading stable fiber of $\gamma$. We expect that a bifurcation similar to the orbit flip homoclinic bifurcation occurs, cf. e.g. [50]. Such an intersection with non-leading fibers may structurally stable in these heteroclinic cycles, which is not the case for heteroclinic cycles between equilibria. In addition, if $s(L)$ is not constant then we suspect that countably infinite such bifurcations would occur.
Since $v(\alpha)$ is given in (2.56) by projections of objects with minimal period $mT_\gamma$ and (2.55) contains higher order periodic corrections, it does not seem possible to conclude a nontrivial minimal period of $v(\alpha)$ in general. Concerning dimensions in which $v(\alpha)$ varies, the ambient space dimension is $n \geq 4$ and the Morse index difference is $i(p_0) - i(\gamma) = 1$, hence we obtain $n - i(\gamma) = n + 1 - i(p_0) \geq n + 1 - (n - 1) = 2$. Therefore, the strong stable fibers are at least two-dimensional.
Let $\tau$ be the minimal period of $v(-2L)$. If $\Im(2\nu^{\mathrm{s}}) \neq \tau$, then the parameter curve $\mu(L)$ 'spirals' into $\mu = 0$ along a more or less complicated path depending on the frequency ratio. However, in the one-to-one resonance the curve possibly does not spiral, and along a non-spiraling curve there are no generic saddle-nodes of the homoclinic orbits. This is in contrast to codimension–2 heteroclinic cycles between two equilibria with one transverse heteroclinic orbit ('T-points', cf. [28]). The analogue of $v(\alpha)$ is constant and spiraling is generically equivalent to leading complex conjugate eigenvalues. In anticipation of the next chapter, for complex conjugate leading eigenvalues, the absolute spectrum is unstable, which typically forces infinitely many eigenvalues of the homoclinic to cross the imaginary axis as $L \to \infty$, cf. theorem 3.4 cited from [52]. We suspect that in a non-spiraling case these eigenvalues only come in complex conjugate pairs or a condition assumed in that

theorem is violated.

On the other hand, for the real leading case, the vector $v$ may be so that saddle-nodes occur despite the monotone approach in one direction in parameter space. Since this is a stable phenomenon and the absolute spectrum may be stable, we suspect that eigenvalues stabilize and destabilize periodically.

# 3 Stability of travelling waves in reaction-diffusion equations

This section establishes a framework for subsequent numerical investigations and bridges the results of chapter 2 to an application in chapter 4. We mainly report known results, but occasionally augment them and give new ones geared towards our purposes.

The general class of equations for the models referred to in chapter 4 are reaction-diffusion equations in one space dimension. These are systems of $N$ 'species' $U_1, \dots U_N \in \mathbb{R}$ with parameter dependent pointwise reaction kinetics $F : \mathbb{R}^N \times \mathbb{R} \to \mathbb{R}^N$ spatially coupled by diffusion with rates $d_j \geq 0$, $D := \mathrm{diag}(d_1, \dots, d_N)$ in the reaction-diffusion system

$$U_t = DU_{xx} + F(U). \tag{3.1}$$

We pose this equation on a function space $X$ so that $D\partial_{xx}$ can be cast as a closed and densely defined operator, and assume the Nemitskij operator $F_{\mathrm{N}}$ derived from $F$ satisfies $F_{\mathrm{N}} \in C^1(X, X)$. For example $X = BC^0_{\mathrm{unif}}(\mathbb{R}, \mathbb{R}^N)$, $\mathrm{dom}(D\partial_{xx}) = BC^2_{\mathrm{unif}}(X, X)$ and $F \in C^1(\mathbb{R}^N, \mathbb{R}^N)$, cf. chapter 2 in [70].

In a comoving frame with speed $c$, in the variable $\xi = x - ct$, (3.1) becomes

$$U_t = DU_{\xi\xi} + cU_\xi + F(U) \tag{3.2}$$

and we call $t$-independent solutions *travelling waves*, i.e. solutions to the 2nd order ODE

$$DU^*_{\xi\xi} + cU^*_\xi + F(U^*) = 0. \tag{3.3}$$

To analyze travelling waves in more detail and for numerical purposes, we consider (3.2) also on bounded domains, i.e. intervals $(-L, L)$ with various Robin as well as periodic boundary conditions. The space $X$ and the domain of the linear part are then adapted accordingly.

If $d_j > 0$, $j = 1, \dots, N$ the linear parts in (3.1) and (3.2) generate analytic semigroups on $X$, and the evolution yields differentiable solutions in time which are given by the variations of constants formula, cf. e.g. [60].

*In the following an asymptotically periodic travelling wave refers to a solution to (3.3), which approaches nontrivial hyperbolic periodic orbits as $\xi \to \pm\infty$. An asymptotically constant travelling wave is a solution to (3.3), which approaches hyperbolic steady states.*

In many applications some species do not diffuse, e.g. in the Oregonator model (4.1) $d_3 = 0$. In section 3.2 we show that travelling waves and their spectral properties can be recovered as the weak diffusion limit $d_3 \to 0$. Hence, we can rely on the PDE framework for $d_3 > 0$, while analyzing solutions and their spectra in the case $d_3 = 0$.
For applications it is important to distinguish stable and unstable solutions, and we focus on this question in the remainder of this chapter. Since (3.3) is an ODE which determines the existence of travelling waves, the results of chapter 2 can be interpreted as bifurcation results for travelling waves.

## 3.1 Spectra and stability of travelling waves

Stability properties of a travelling wave $U^*$ are largely determined by the spectrum of the linearization of (3.2) in $U^*$. Denote $F' = \partial_U F$ and consider the spectrum of the operator

$$L_* := D\partial_{\xi\xi} + c\partial_\xi + F'(U^*). \tag{3.4}$$

**Definition 4** *The spectrum of $U^*$, $\mathrm{spec}(U^*)$ is the set of $\lambda \in \mathbb{C}$ for which the operator $L_* - \lambda$ is not boundedly invertible in $X$. The point spectrum of $U^*$, $\mathrm{spec}_{\mathrm{pt}}(U^*)$, is the set of all $\lambda$ in the spectrum of $U^*$ for which $L_* - \lambda$ is a Fredholm operator with index zero. The essential spectrum of $U^*$ is $\mathrm{spec}_{\mathrm{ess}}(U^*) := \mathrm{spec}(U^*) \setminus \mathrm{spec}_{\mathrm{pt}}(U^*)$. We call the point, essential and full spectrum (strictly) stable respectively, if they lie in the (open) left half plane, $\Re(\mathrm{spec}(U^*)) \leq 0$ ($< 0$), and unstable, if parts lie in the open right half plane.*

The essential spectrum of asymptotically constant or periodic travelling waves only depends on the asymptotic states, as will be discussed below, and we frequently focus on these states. In general, $\lambda$ lies in the spectrum of $U^*$, if the following eigenvalue problem has a bounded solution $V$, cf. the review paper [51] and the references therein.

$$\lambda V = L_* V \tag{3.5}$$

The derivative $\partial_\xi U^*$ solves this eigenvalue problem, and so zero lies in the spectrum of $U^*$. This corresponds to spatial translations of $U^*$ and is sometimes called 'Goldstone mode'. From a symmetry perspective, (3.2) is equivariant under spatial translations, and the one-dimensional group orbit generated by a solution's derivative causes spectrum at zero.

Therefore, we cannot expect asymptotic stability of any travelling wave on unbounded domains. Nevertheless, the following theorem gives conditions for nonlinear stability with asymptotic phase and we shall refer to stability in this sense.
We say that $\lambda \in \mathrm{spec}_{\mathrm{pt}}(U^*)$ is simple, if there is $U_\lambda \in X$ such that $\ker(L^* - \lambda) = \mathrm{span}\{U_\lambda\}$ and $L^*V \neq \lambda V + U_\lambda$ for all $V \in X$, i.e. there is no 'Jordan block', cf. e.g. [51].

**Theorem 3.1 (chapter 5.1 in [31])** *Suppose zero is a simple eigenvalue of $L_*$ on $X$, and $\Re(\mathrm{spec}(L_*) \setminus \{0\}) < -\delta < 0$, for some $\delta > 0$. Then there exists $\epsilon > 0$, $C > 0$ such that for all $U_0 \in X$ with $|U_0 - U^*| < \epsilon$ there exists $\phi_0 \in \mathbb{R}$ such that the solution $U$ of (3.1) with initial condition $U_0$ satisfies $|U(t,\cdot) - U^*(\cdot + \phi_0)| \leq C\mathrm{e}^{-\delta t}$ in $X$ as $t \to \infty$.*
*If the spectrum of $L_*$ is strictly stable then the above conclusion holds for $\phi_0 = 0$.*

The spectral gap used in this theorem can arise for instance in spatially uniform steady states or solutions whose spatial asymptotics are constant, e.g. pulses or fronts. For spatially periodic travelling waves, nonlinear stability on unbounded domains is more involved. In these cases, the Goldstone mode belongs to the essential spectrum, which typically comes in curves and then necessarily touches the imaginary axis ('marginal stability'). Therefore, the spectral gap needed in the above theorem does not exist on the real line, but it may on bounded domains, or in weighted spaces. In an amplitude equation description, nonlinearities are often 'irrelevant', which sometimes allows to conclude nonlinear (diffusive) stability from marginally stable spectrum, see e.g. the review in [40] and the references therein.

On the other hand, unstable spectrum causes nonlinear instability for any travelling wave, cf. [31]. Note that for a nonlinearly stable solution on a bounded domain, the basin of attraction may be exponentially small compared to the domain size [56].

**Notation** *Throughout this chapter, we assume $c \neq 0$ if $N \neq M := \dim(\mathrm{Rg}(D))$.*

### 3.1.1 The asymptotically constant case

If $U^*(\xi) \to U_\pm$, as $\xi \to \infty$, then the essential spectrum is characterized by the (linear) *dispersion relations*

$$d_\pm(\lambda, \nu) \quad = \quad \det(D\nu^2 + c\nu + F'(U_\pm) - \lambda) = 0. \tag{3.6}$$

We refer to solutions $\lambda, \nu \in \mathbb{C}$ of (3.6) as temporal and spatial eigenvalues respectively. For each temporal eigenvalue $\lambda$, we find $N + M$ spatial eigenvalues $\nu$ for each dispersion relation and solutions $\lambda_j^\pm(k)$ for $\nu = \mathrm{i}k$ are called *dispersion curves*, i.e. they solve

$$\lambda_j^\pm(k) := \{\lambda | \exists k \in \mathbb{R} : d_+(\lambda, \mathrm{i}k) d_-(\lambda, \mathrm{i}k) = 0\}.$$

The etymology can be understood using the ansatz $U = \mathrm{e}^{\lambda t + \nu \xi} U_0$. The numbers of spatial eigenvalues $\nu$ with positive real part are called the *spatial Morse-indices* denoted by $i_\pm(\lambda)$. A spatial Morse-index can only change when $\lambda$ crosses a dispersion curve, and the following lemma shows that these indices are asymptotically constant in $\Re(\lambda)$. Moreover, we collect some (probably) known properties in lack of conclusive references.

**Lemma 10** *Let $U^*$ be an asymptotically constant travelling wave of (3.1), then $\lambda$ is in the essential spectrum $\mathrm{spec}_{\mathrm{ess}}(U^*)$, if and only if $\lambda$ lies in one of the dispersion curves, or $i_-(\lambda) \neq i_+(\lambda)$. The essential spectrum and spatial eigenvalues of an uniform steady state $U_0$ of (3.1) have the following properties*

*i) Each point on a dispersion curve $\lambda(\mathrm{i}k)$ lies in a circle with radius $\sum_{j=1;j\neq i}^N |\partial_j F_i(U_0)|$ and center $-d_i k^2 + c\mathrm{i}k + \partial_i F_i(U_0)$. Furthermore, there is $R \in \mathbb{R}$, such that for any $\lambda$ with $\Re(\lambda) > R$ and $c > 0$ ($c < 0$) the spatial Morse-index is $i(\lambda) = N$ ( $i(\lambda) = M$).*

*ii) The essential spectrum is connected in the Riemann sphere $\mathbb{C} \cup \{\infty\}$.*

*iii) Let $\lambda(\mathrm{i}k)$ be a dispersion curve. If $\Im(\frac{\mathrm{d}}{\mathrm{d}k}\lambda(\mathrm{i}k)) > 0$ ($\Im(\frac{\mathrm{d}}{\mathrm{d}k}\lambda(k)) < 0$) for some $k \in \mathbb{R}$, then the spatial Morse-index increases (decreases) when $\lambda$ crosses through $\lambda(\mathrm{i}k)$ from left to right (see also [25]). If $k = 0$, then $\Im(\frac{\mathrm{d}}{\mathrm{d}k}\lambda(\mathrm{i}k)|_{k=0}) = c$.*

**Proof.** The relation between dispersion curves and essential spectrum can be found e.g. in [31]. For a constant steady state $U_0$ the dispersion functions $d_\pm$ coincide and we define $d(\lambda, \nu) := d_\pm(\lambda, \nu)$, but count solutions only once.

i) Consider the matrix $D\nu^2 + c\nu + A$. From Gershgorin's theorem, cf. e.g. [68], the eigenvalue $\lambda_i$, $i = 1, \dots, N$, lies in a circle with radius $\rho_i := \sum_{j\neq i} |a_{ij}|$ and center $d_i\nu^2 + c\nu + a_{ii}$. Since only the circle centers depend on $\nu$, we conclude that $\lambda \in \mathbb{C} \setminus B_R(0)$, $R > 0$ implies $\lambda \in B_{\rho_i}(d_i\nu^2 + c\nu + a_{ii})$ for some $i$ where $d_i\nu^2 + c\nu + a_{ii} \in \mathbb{C} \setminus B_{R-\rho_i}(0)$. Since then also $B_{\rho_i}(d_i\nu^2 + c\nu + a_{ii}) \subset B_{2\rho_i}(\lambda)$ we obtain for $d_i > 0$ that $\nu = \nu_i^{\pm}$ where $\nu_i^{\pm} \in B_{2\rho_i}\left(\frac{-c\pm\sqrt{c^2-4d_i(a_{ii}-\lambda)}}{2d_i}\right)$. For $d_i = 0$ we conclude $\nu \in B_{2\rho_i}\left(\frac{\lambda-a_{ii}}{c}\right)$. Hence there is $R > 0$ such that for $\Re(\lambda)) > R$ we can label the solutions $\nu$ to $d(\lambda, \nu) = 0$ so that $\Re(\nu_i^-) < 0 < \Re(\nu_i^+)$ for $i = 1, \dots, M$ and $0 < \Re(\nu_i)$ for $i = M + 1, \dots, N + M$.

ii) From i) we know that for $k \to \infty$, all $\lambda \to \infty$ that solve $d(\lambda, \mathrm{i}k)$. Therefore, it suffices to extend any dispersion curve continuously for all $k \in \mathbb{R}$. If $\partial_\lambda d(\lambda(\mathrm{i}k_0, \mathrm{i}k_0) \neq 0$ we can extend the curve $\lambda(\mathrm{i}k)$ uniquely for $k$ in a neighborhood of $k_0$ by the implicit function theorem. Generally, let $\lambda(\mathrm{i}k_0)$ be a solution to $d(\lambda(\mathrm{i}k_0), \mathrm{i}k_0) = 0$ and note $d(\lambda, \mathrm{i}k)$ contains the term $(-1)^N\lambda$ so $d(\lambda, \mathrm{i}k) \neq 0$ for any $k$. Then Rouché's theorem, cf. e.g. [15], guarantees that for any sufficiently small $\epsilon > 0$ and any $k \in (k_0, k_0 + \epsilon)$ there is at least one solution $\lambda(\mathrm{i}k) = \lambda(\mathrm{i}k_0) + O(\epsilon)$ to $d(\lambda, \mathrm{i}k) = 0$ which can be chosen continuously in $k$. Hence, the set of $k$ for a dispersion curve $\lambda(\mathrm{i}k)$ is open; if it was bounded, define $\lambda(\mathrm{i}k)$ for $k_0$ in the boundary as $\lim_{k\to k_0} \lambda(\mathrm{i}k)$ and extend as above. Therefore, we obtain a continuous unbounded curve $\lambda(\mathrm{i}k)$ for all $k \in \mathbb{R}$.

iii) If $\frac{\mathrm{d}\Im(\lambda(\nu))}{\mathrm{d}\Im(\nu)} \neq 0$ at some $\nu_0$ and $\lambda_0 = \lambda(\nu_0)$ for a solution curve to $d(\lambda, \nu) = 0$, then we can solve for the inverse $\nu(\lambda)$ by the implicit function theorem and the Cauchy-Riemann equations imply

$$\left.\frac{\mathrm{d}\Im(\lambda(\nu))}{\mathrm{d}\Im(\nu)}\right|_{\nu_0} = \left.\frac{\mathrm{d}\Re(\lambda(\nu))}{\mathrm{d}\Re(\nu)}\right|_{\nu_0} = \left(\left.\frac{\mathrm{d}\Re(\nu(\lambda))}{\mathrm{d}\Re(\lambda)}\right|_{\lambda_0}\right)^{-1}.$$

Therefore, when crossing a dispersion curve from left to right with $\lambda$, the associated spatial eigenvalue $\nu(\lambda)$ crosses the imaginary axis from left to right if $\Im(\frac{\mathrm{d}}{\mathrm{d}k}\lambda(\mathrm{i}k)) > 0$. If $\Im(\frac{\mathrm{d}}{\mathrm{d}k}\lambda(\mathrm{i}k)) < 0$, then it crosses from right to left, which cause the claimed changes in Morse indices.

Since $d(\lambda, \nu) = \det(D\nu^2 + c\nu - \lambda + F'(U_0)) = \det(c\nu - \lambda + F'(U_0)) + O(\nu^2)$ we obtain $\frac{\mathrm{d}}{\mathrm{d}\nu}d(\lambda, \nu) = cD(\det)(c\nu - \lambda + F'(U_0)) + O(\nu)$ and $\frac{\mathrm{d}}{\mathrm{d}\lambda}d(\lambda, \nu) = -D(\det)(c\nu - \lambda + F'(U_0))$,

where $D(\det)$ is the total derivative. Therefore, by implicit differentiation

$$\left.\frac{\mathrm{d}}{\mathrm{d}k}\right|_{k=0} \lambda(\mathrm{i}k) = -\frac{\frac{\mathrm{d}}{\mathrm{d}k}|_{k=0} d(\lambda, \mathrm{i}k)}{\frac{\mathrm{d}}{\mathrm{d}\lambda}|_{\lambda=\lambda(0)} d(\lambda, \mathrm{i}k)} = \mathrm{i}c.$$

□

A connection between the essential spectrum and dispersion curves as well as Morse and Fredholm indices of $L_* - \lambda$ can be found e.g. in [25, 51].

By item ii) of this lemma, the complement of dispersion curves consists of connected components of $\mathbb{C}$ where $i_\pm(\lambda)$ are constant. We denote by $\Omega_\infty$ the connected component which contains an unbounded set in $\mathbb{R}^+$. By lemma 10 this is well-defined, nonempty and the spatial Morse-index $i(\lambda)$ for $\lambda \in \Omega_\infty$ is $N$ if $c > 0$ and $M$ for $c < 0$.

Lemma 10 i) implies that for spatial Morse-index different from $N$ for some $\lambda$, there is essential spectrum to the right of this $\lambda$, i.e. at larger real part. We order the spatial eigenvalues $\nu_j^\pm$, $j = 1, \dots N + M$, for each $\lambda$ so that $\Re(\nu_1^\pm) \geq \Re(\nu_2^\pm) \geq \dots \geq \Re(\nu_{N+M}^\pm)$.

**Definition 5 ([53])** *Notation and ordering as above. The absolute spectrum of an asymptotically constant travelling wave with $N = M$ or $c > 0$ (for $c < 0$ replace $N$ by $M$) is*

$$\mathrm{spec}_{\mathrm{abs}} := \{\lambda \in \mathbb{C} | \Re(\nu_N^+) = \Re(\nu_{N+1}^+) \text{ or } \Re(\nu_N^-) = \Re(\nu_{N+1}^-)\}.$$

The absolute spectrum plays a decisive role for the nature of an instability caused by unstable essential spectrum. On bounded domains or in weighted spaces the spectrum may be strictly stable and then yield nonlinear stability. In a *convective instability*, the solution is unstable on the real line, but on a bounded domain perturbations may be convected through the boundary. However, unstable absolute spectrum causes a so-called *absolute instability*, where perturbations grow pointwise, cf. e.g. [53].

To compute the absolute spectrum, one generally has to rely on pathfollowing software. Possible starting points for the computation are then double zeros of the dispersion relation, which may be computed by means of the resultant.

**Lemma 11 ([46])** *The number of isolated double roots in $\nu$ of a dispersion relation of*

*the form (3.6), i.e.* $d(\lambda,\nu) = \partial_\nu d(\lambda,\nu) = 0$*, for* $N$ *species is at most*

$$\begin{pmatrix} 2N \\ 2 \end{pmatrix} - (\dim(\ker(D)))^2.$$

A class of spaces for refined spectral analyses of (3.5) are exponentially weighted spaces with weight $\eta$, i.e. subsets of $X$, where an exponentially weighted norm is finite, e.g. $\sup_{\xi\in\mathbb{R}} \mathrm{e}^{\eta\xi}|u(\xi)|$. On a fixed bounded domain, exponential weights yield equivalent spaces and spectra of linear operators do not change, which is in contrast to an unbounded domain. Therefore, a relevant question is, how spectra for operators arising from linearizing (3.2) in travelling waves on bounded and unbounded domains relate. Neglecting some technical details, the main results can be summarized as follows.

**Definition 6 ([53])** *The essential spectrum of a constant travelling wave is called reducible, if hypothesis 6 in [53] is satisfied. This states that the set of points where imaginary and (geometrically and algebraically) simple spatial eigenvalues have nonzero derivative with respect to* $\lambda$ *is dense in the essential spectrum.*

**Theorem 3.2 ([53])** *Assume* $F$ *satisfies certain genericity conditions. Suppose the point spectrum of a travelling wave* $U^*$ *with speed* $c$ *and asymptotically constant states* $U^\pm$ *is strictly stable up to a simple eigenvalue at zero. The linearization of 3.2 in* $U^*$ *can be posed on a bounded domain of length* $L$ *as an operator* $\mathcal{L}_L$*. As* $L\to\infty$*, the spectrum of* $\mathcal{L}_L$ *converges in symmetric Hausdorff-distance to the set* $\Sigma\cup\mathrm{spec}_{\mathrm{pt}}(U^*)\cup\mathrm{spec}_{\mathrm{bc}}(U^*)\cup\mathrm{spec}_{\mathrm{res}}(U^*)$*. Here* $\mathrm{spec}_{\mathrm{res}}(U^*) \subset \mathrm{spec}_{\mathrm{ess}}(U^*)$ *consists of isolated eigenvalues called resonance poles and the set* $\mathrm{spec}_{\mathrm{bc}}(U^*)$ *depends only on the asymptotic states and the boundary conditions. Suppose* $\mathrm{spec}_{\mathrm{ess}}(U^*)$ *is reducible and* $U^+ = U^-$*. Then under generic separated b.c.* $\Sigma = \mathrm{spec}_{\mathrm{abs}}(U^*)$*, but under periodic b.c.* $\Sigma = \mathrm{spec}_{\mathrm{ess}}(U^*)$*.*

We emphasize, that the absolute spectrum is in general different from the essential spectrum, but e.g. for $c = 0$ these sets coincide, cf. [53]. The set $\mathrm{spec}_{\mathrm{res}}(U^*)$ consists of eigenvalues arising in exponentially weighted spaces from essential spectrum.
A relevant example for the boundary spectrum $\mathrm{spec}_{\mathrm{bc}}(U^*)$, which appears in this theorem is the following. Suppose a solution on a bounded domain is only unstable with respect to

spatially uniform perturbations, e.g. through a Hopf bifurcation of the reaction kinetics $F(U^*)$. Then Neumann boundary conditions will cause unstable boundary spectrum, while the solution may be stable under Dirichlet boundary conditions. To investigate this and for later reference, we insert a brief digression on spatial dynamics.

We may cast the second order ODE (3.3) in $\xi$ as a first order system, called the travelling wave ODE; its dynamics in $\xi$ is referred to as spatial dynamics. Let $\cdot = \frac{\mathrm{d}}{\mathrm{d}\xi}$, and $P_M : \mathbb{R}^N \to \mathbb{R}^M$ denote the projection onto the first $M$ components. Reorder variables so that $D_M := P_M D = \mathrm{diag}(d_1, \ldots, d_M)$ is invertible, and $d_{M+1}, \ldots d_N = 0$. With $U, V \in \mathbb{R}^M$, $W \in \mathbb{R}^{N-M}$ equation (3.3) can be written as

$$\begin{aligned} \dot{U} &= V \\ \dot{V} &= -D_M^{-1}\left(cV + P_M F((U,W))\right) \\ \dot{W} &= -c^{-1}(\mathrm{Id} - P_M)F((U,W)). \end{aligned}$$

For shorthand we take $u \in \mathbb{R}^{N+M}$, $f : \mathbb{R}^{N+M} \to \mathbb{R}^{N+M}$ and write this system as

$$\dot{u} = f(u; c). \tag{3.7}$$

Existence of travelling waves is now a finite dimensional problem concerning bounded solutions of (3.7), notably heteroclinic and homoclinic orbits, e.g. as in chapter 2.
Stability for the PDE (3.2) on the real line cannot generally be determined through (3.7). However, for asymptotically constant solutions $U_\pm$ the dispersion relation (3.6) shows that solutions to $d_\pm(\lambda, 0) = 0$ are the eigenvalues of $F'(U_\pm)$, while solutions to $d_\pm(0, \nu) = 0$ are the eigenvalues of $f'(u_\pm; c)$, $u_\pm := (P_M U_\pm, 0, \ldots 0, (\mathrm{Id} - P_M)U_\pm)$. This shows how local bifurcations in the finite dimensional kinetics $U_t = F(U)$ typically cause an essential instability with wavenumber $k = 0$ and local bifurcations of $u_\pm$ correspond to essential instabilities with frequency $\omega = 0$. Since the spatial Morse-indices $i_\pm(0)$ are the Morse indices of $f'(u_\pm; c)$, we can conclude instability of $U^*$ using only $f$ if $i_\pm(0) \neq N$, for $c > 0$ or $M$ for $c < 0$, see lemma 10 i). The relation to spatial eigenvalues can also allow to conclude an absolute instability, if the absolute spectrum has a curve extending through $\lambda = 0$, which we refer to as a *real-type absolute instability*, cf. [52].

Notice that asymptotically constant travelling waves by our definition correspond to heteroclinic orbits $u$ between hyperbolic equilibria $u_\pm$ in (3.7).

**Remark 8** *Lemma 10 implies that a stable asymptotically constant travelling wave has Morse index $N$ ($M$) at $\lambda = 0$ for $c > 0$ ($c < 0$), hence a heteroclinic connection between two stable steady states is codimension–1 in the travelling wave ODE. On the other hand, consider a heteroclinic cycle between a stable steady state and an unstable one. Suppose $\lambda = 0 \in \mathbb{C}$ is separated from $\Omega_\infty$ by one dispersion curve $\lambda(\mathrm{i}k)$. If $\lambda(0)$ is a simple solution to $d(\lambda, 0) = 0$, then by lemma 10 the Morse index changes by $1$ ($-1$) for $c > 0$ ($c < 0$) along any curve connecting $\lambda = 0$ to $\Omega_\infty$ via $\lambda(0)$. In addition, the heteroclinic cycle is codimension–(2,0), which is also called a 'T-point', cf. [28]. Note however, that unstable essential spectrum does not necessarily have an effect at $\lambda = 0$.*

Linear boundary conditions can be cast a subspaces in $\mathbb{R}^n$, e.g. Dirichlet b.c. correspond to $\{(U, V, W) \,|\, U = 0, W = 0, V \in \mathbb{R}^N\}$. On sufficiently large bounded domains $(-L, L) \subset \mathbb{R}$ with such boundary conditions, we can typically find locally unique, in $L$ exponentially close solutions $u_L$ which satisfies these boundary conditions, cf. e.g. [52]. In this sense, we refer to travelling waves on comoving, bounded domains. However, essential and absolute spectra only depend on the asymptotic states.

We next consider the case $N = M$. Recall the order of spatial eigenvalues $\nu_j^\pm(\lambda)$, $j = 1, \ldots, N$ by decreasing real parts. Denote by $E_+(\lambda)$ the sum of the generalized eigenspaces of $f'(u_+)$ associated to the $N$ eigenvalues $\nu_j^+(\lambda)$, $j = 1, \ldots, N$ with largest real part, and $E_-(\lambda)$ the sum of generalized eigenspaces of $f'(u_-)$ for the $N$ eigenvalues $\nu_j^-(\lambda)$, $j = N + 1, \ldots, 2N$ with smallest real part.

**Definition 7 ([53])** *The boundary spectrum of an asymptotically constant travelling wave $U^*$ with boundary conditions cast as linear subspaces $Q_\pm \subset \mathbb{R}^n$ is ($\pm$ denotes alternatives)*

$$\mathrm{spec}_{\mathrm{bc}}^\pm(U^*) := \{\lambda \,|\, \lambda \notin \mathrm{spec}_{\mathrm{abs}}(U^*) \text{ and } E_\pm(\lambda) \cap Q_\pm \neq \{0\}\}.$$

Let $\mathrm{spec}_{\mathrm{Neu}}^\pm(U^*)$ and $\mathrm{spec}_{\mathrm{Dir}}^\pm(U^*)$ denote boundary spectra stemming from Neumann and Dirichlet boundary conditions on the left (-) and right (+), and $\mathrm{spec}_{\mathrm{Neu}}(U^*) = \mathrm{spec}_{\mathrm{Neu}}^+(U^*) \cup \mathrm{spec}_{\mathrm{Neu}}^-(U^*)$, as well as $\mathrm{spec}_{\mathrm{Dir}}(U^*) = \mathrm{spec}_{\mathrm{Dir}}^+(U^*) \cup \mathrm{spec}_{\mathrm{Dir}}^-(U^*)$. By definition, these spectra do not contain absolute spectrum.

**Lemma 12** *Assume $D$ is invertible, and $U^*$ is a travelling wave with asymptotically constant states $U_\pm$ restricted to a bounded domain. Then*

$$\mathrm{spec}^{\pm}_{\mathrm{Neu}}(U^*) \setminus \mathrm{spec}(F'(U_\pm)) \;=\; \mathrm{spec}^{\pm}_{\mathrm{Dir}}(U^*) \setminus (\mathrm{spec}(F'(U_\pm) \setminus \bar{\Omega}_\infty)$$

*and for $c > 0$ (for $c < 0$ interchange '+' and '−')*

$$\begin{aligned} \mathrm{spec}(F'(U_+)) \cap \bar{\Omega}_\infty &\subset \mathrm{spec}^{+}_{\mathrm{Neu}}(U^*) \\ \mathrm{spec}^{-}_{\mathrm{Neu}}(U^*) \cap \bar{\Omega}_\infty &= \emptyset. \end{aligned}$$

**Proof.** Since we assume $D$ to be invertible, there is no $W$ component in (3.7) and the eigenvalue problem (3.5) can be cast as

$$\text{(3.8)} \quad \begin{pmatrix} \dot{U} \\ \dot{V} \end{pmatrix} = \begin{pmatrix} 0 & \mathrm{Id} \\ -D^{-1}(F'(U_\pm) - \lambda) & -D^{-1}c \end{pmatrix} \begin{pmatrix} \dot{U} \\ \dot{V} \end{pmatrix} =: A_\pm(\lambda) \begin{pmatrix} \dot{U} \\ \dot{V} \end{pmatrix}.$$

By the block structure it holds that $d_\pm(\lambda, 0) = \det(A_\pm(\lambda)) = \det(F'(U_\pm - \lambda))$, in particular $\mathrm{spec}(F'(U_\pm)) = \{\lambda \mid \ker(A_\pm(\lambda)) \neq \{0\}\} \subset \mathrm{spec}_{\mathrm{ess}}(U_\pm)$.

Neumann boundary conditions are $Q_{\mathrm{Neu}} := \{(U, V) \,|\, V = 0,\ U \in \mathbb{R}^N\}$, while Dirichlet b.c. correspond to $Q_{\mathrm{Dir}} := \{(U, V) \,|\, U = 0,\ V \in \mathbb{R}^N\}$. Note that the spaces are complementary. Assume first $\lambda \notin \mathrm{spec}(F'(U_\pm)) \cup \mathrm{spec}_{\mathrm{abs}}(U^*)$, so $A_\pm(\lambda)$ is invertible. From the form of $A_\pm(\lambda)$ we conclude $A_\pm(\lambda)Q_{\mathrm{Neu}} \subset Q_{\mathrm{Dir}}$. Since $A_\pm(\lambda)$ are invertible for these $\lambda$ we obtain $A_\pm(\lambda)Q_{\mathrm{Neu}} = Q_{\mathrm{Dir}}$. The space $E_+(\lambda)$ is a sum of eigenspaces and therefore invariant under $A_+(\lambda)$. Hence, a nontrivial intersection of $Q_{\mathrm{Neu}}$ with $E_+(\lambda)$ implies one for $Q_{\mathrm{Dir}} = A_+(\lambda)Q_{\mathrm{Dir}}$ with $E_+(\lambda)$ and vice versa. This proves $\mathrm{spec}^{+}_{\mathrm{Neu}}(U^*) \setminus \mathrm{spec}(F'(U_+)) = \mathrm{spec}^{+}_{\mathrm{Dir}}(U^*) \setminus \mathrm{spec}(F'(U_+))$, and the same holds with '+' replaced by '−'.

Let $\lambda_0 \in \mathrm{spec}(F'(U_+)) \cap \bar{\Omega}_\infty$ and $e_0$ an eigenvector of $F'(U_+)$ to $\lambda_0$. Since $i(\Omega_\infty) = N$ it follows from lemma 10 i) that $i(\lambda_0 + \epsilon) = N$ for sufficiently small $\epsilon > 0$. Now, if $c > 0$ then the direction of Morse index change given in lemma 10 iii) implies $\nu^+_N = 0$. Now $(e_0, 0) \notin Q_{\mathrm{Dir}}$ but $(e_0, 0) \in Q_{\mathrm{Neu}}$ and $(e_0, 0) \in E_+(\lambda_0)$. Thus $\mathrm{spec}(F'(U_+)) \cap \bar{\Omega}_\infty \subset \mathrm{spec}^{+}_{\mathrm{Neu}}(U^*)$. The same argument shows for $c > 0$ and $\lambda_0 \in \mathrm{spec}(F'(U_-)) \cap \bar{\Omega}_\infty$ that $(e_0, 0) \notin E_-(\lambda_0)$, and so $\mathrm{spec}^{-}_{\mathrm{Neu}}(U^*) \cap \bar{\Omega}_\infty = \emptyset$. The case $c < 0$ follows analogously. □

The second statement of the lemma means that under Neumann boundary conditions, for positive speed, the critical modes with wavenumber zero do not destabilize from the left boundary, but only from the right. Hence, Dirichlet boundary conditions on the right stabilize those. Even though the suppression of homogeneous oscillations has the expected effect, the tight relation of Neumann and Dirichlet boundary spectra is nontrivial. In particular, Dirichlet b.c. do not introduce spectrum beyond that of Neumann b.c.
We emphasize, that e.g. resonance poles may cause an instability despite stable point, absolute and boundary spectrum, cf. theorem 3.2 cited from [53].
If $D$ is not invertible, then boundary conditions cannot be freely chosen Dirichlet or Neumann. A typical choice are Dirichlet b.c. for the non diffusing species on the right (left) for $c > 0$ ($c < 0$). However, this suppresses for instance spatially uniform oscillations and therefore does not capture the dynamics from the unbounded domain or the weak diffusion limit, see section 3.2. To avoid this problem, one can try to mimic the underlying dynamics using Neumann b.c. for the diffusing species $U$ and 'kinetic' boundary conditions for the non diffusing species $W$: $W_t = P_M(U, W)$ at $\xi = \pm L$ for $\mathrm{sgn}(c) = \pm 1$. We use this and Dirichlet boundary conditions in chapter 4.

The point spectrum on the unbounded domain is in general hard to locate, but can be characterized by Evans functions, cf. e.g. [1]. We do not further pursue its analysis here.

### 3.1.2 The asymptotically periodic case

In this section, we consider travelling waves for which one or both asymptotic states are periodic. In particular, we collect properties of the essential spectra and locate absolute spectrum in some cases.
Again, the essential spectrum only depends on the asymptotic states, cf. e.g. [51]. However, the essential spectrum of a periodic orbit does not have the convenient formulation through a determinant of explicitly given matrices. As mentioned in the discussion of nonlinear stability, zero always lies in the essential spectrum, which typically yields a curve of essential spectrum touching the imaginary axis. For wave trains close to a pulse, i.e. periodic orbits close to a homoclinic in spatial dynamics, there are small circles of essential spectrum around each element in the point spectrum of the pulse, cf. [55]. Hence, we

can expect that finding essential spectrum generally is generally of the same difficulty as finding point spectrum. In particular, lemma 10 ii) fails in general for periodic travelling waves.

In analogy to (3.7) and (3.8), the eigenvalue problem (3.5) for a periodic travelling wave $U^*$ can be cast as a non-autonomous, linear first order ODE in $\mathbb{R}^{N+M}$

$$\dot{v} = A(\xi;\lambda)v \tag{3.9}$$

with $L$-periodic matrix in $\xi$ for some $L > 0$ given by $A(\xi;\lambda) =$

$$f'(u^*;c) - \lambda \begin{pmatrix} 0 & 0 \\ D_M^{-1} & 0 \\ c^{-1}(\mathrm{Id} - P_M) & 0 \end{pmatrix} = \begin{pmatrix} 0 & \mathrm{Id} \\ D_M^{-1}(P_M F'(U^*(\xi)) - \lambda) & -D_M^{-1}c \\ c^{-1}(\mathrm{Id} - P_M)(F'(U^*(\xi)) - \lambda) & 0 \end{pmatrix}$$

where $u^* = (P_M U^*, P_M((U^*)'), (\mathrm{Id} - P_M)U^*)$ and we denote the evolution by $\Phi_\lambda(\xi,\zeta)$. The linear maps $\Phi_\lambda(\xi,0)$ have a Floquet representation $S_\lambda(\xi)\mathrm{e}^{R(\lambda)\xi}$ with $L$-periodic matrix $S_\lambda(\xi)$, $S_\lambda(0) = \mathrm{Id}$. The eigenvalues of $R(\lambda)$ are called spatial Floquet exponents of $U^*$ denoted by $\nu$ and are unique modulo $2\pi\mathrm{i}$. The Morse index (counting center unstable dimensions) of $R(\lambda)$ is referred to as the spatial Morse-index $i(\lambda)$. In analogy to the asymptotically constant case, we may characterize the relation of $\lambda$ and $\nu$ by a determinant, cf. e.g. [25] (note that $R(\lambda)$ is in general not explicitly computable)

$$d_{\mathrm{per}}(\lambda,\nu) = \det(R(\lambda) - \nu).$$

Similar to the asymptotically constant case, where the essential spectrum is characterized by purely imaginary spatial eigenvalues, we have

**Lemma 13 ([27])** *Let $U^*$ be an $L$-periodic travelling wave of (3.1). A complex number $\lambda$ lies in the essential spectrum of $U^*$, if and only if a spatial Floquet exponent is purely imaginary.*

Floquet exponents $\nu \in \mathbb{C}$ may also be characterized by solvability of

$$\begin{aligned} \dot{v} &= A(\xi;\lambda)v \quad 0 < \xi < L \\ v(L) &= \mathrm{e}^{\nu L}v(0). \end{aligned} \tag{3.10}$$

This allows to set up a pathfollowing algorithm, e.g. for the curve of essential spectrum through zero, which may be part of the critical spectrum in applications. We then pathfollow $\nu = \mathrm{i}k$, $k \in \mathbb{R}$ and start e.g. at $k = 0$ and $v = \frac{\mathrm{d}}{\mathrm{d}\xi}u^*$. We apply this numerical method in chapter 4.

Akin to the constant case, the spatial Morse-index for periodic travelling waves is constant for all large $\Re(\lambda)$, as will be shown below. Hence, we can define an absolute spectrum for these waves ordering spatial Floquet exponents $\nu_j$ for each fixed $\lambda$ by their real parts: $\Re(\nu_1) \geq \Re(\nu_2) \geq \ldots \geq \Re(\nu_{N+M})$. The absolute spectrum is then precisely given as in definition 5, and we find a unique connected component $\Omega_\infty \subset \mathbb{C} \setminus \mathrm{spec}_{\mathrm{ess}}(U^*)$, which contains an unbounded interval of $\mathbb{R}^+$ by virtue of the following lemma.

**Lemma 14** *Let $U^*$ be a periodic travelling wave. There is $R \in \mathbb{R}$ such that for $\Re(\lambda) > R$ the spatial Morse-index is $i(\lambda) = N$ if $c > 0$ and $i(\lambda) = M$ if $c < 0$.*
*For asymptotically constant or periodic travelling waves, $\lambda \in \mathrm{spec}_{\mathrm{abs}}(U^*)$ is separated from the set $\Omega_\infty$ by a curve of essential spectrum.*

**Proof.** Consider $D\ddot{V} + c\dot{V} + \tilde{A}(\xi)V - \lambda V = 0$, where $\tilde{A}(\xi) = F'(U_*(\xi))$. Rescaling to fast 'spatial time' $\xi = \epsilon\zeta$, $\cdot\ = \frac{\mathrm{d}}{\mathrm{d}\zeta}$ and $\lambda \to \lambda/\epsilon^2$ we obtain

$$D\ddot{V}/\epsilon^2 + c\dot{V}/\epsilon + \tilde{A}(\epsilon\zeta)V - \lambda/\epsilon^2 V = 0$$
$$(\epsilon \neq 0) \Leftrightarrow D\ddot{V} + \epsilon c\dot{V} + \epsilon^2\tilde{A}(\epsilon\zeta)V - \lambda V = 0$$

For $\epsilon = 0$ the latter equation is autonomous, and by lemma 10 ii) the spatial Morse-index is $N$ for $\Re(\lambda) > R$ and some $R \in \mathbb{R}$. For such $\lambda$, the fast system has exponential dichotomies with Morse index $N$, or $M$ which persist for small bounded perturbation, cf. [16], i.e. for $\epsilon$ sufficiently small.

The second claim follows for $\mathrm{spec}_{\mathrm{abs}}(U^*) \cap \mathrm{spec}_{\mathrm{ess}}(U^*)$, because $\Omega_\infty$ is open and $\mathrm{spec}_{\mathrm{ess}}(U^*)$ closed. Consider any curve $\Gamma$ starting in $\mathrm{spec}_{\mathrm{abs}}(U^*) \setminus \mathrm{spec}_{\mathrm{ess}}(U^*)$ and ending in $\Omega_\infty$. The matrix $R(\lambda)$ and its eigenvalues are continuous in $\lambda$, whence there is a point $\lambda_0 \in \Gamma$ for which a spatial Floquet exponent is purely imaginary, and $\lambda_0 \in \mathrm{spec}_{\mathrm{ess}}(U^*)$. □

The essential spectrum of a periodic wave may contain isolas, for example each element of a pulse's point spectrum creates a small circle of essential spectrum for nearby wave trains,

cf. [55]. Unstable essential spectrum of the wave train might 'only' cause a convective instability, cf. [53], however an instability of the point spectrum of a pulse should influence nearby wave trains. The next new theorem establishes that certain regular isola of essential spectrum to the right of other essential spectrum necessarily contain absolute spectrum. In general these contain iso-real spectrum, which we define first.

**Definition 8 (iso-real spectra)** *Consider the eigenvalues or Floquet exponents $\nu_j$, $j = 1, \dots, N+M$ of $A(\xi;\lambda)$ associated with an asymptotically constant or periodic travelling wave $U^*$, ordered by decreasing real parts, cf. (3.8) or (3.9). The $j$-iso-real spectrum is*

$$\mathrm{spec}^j_{\mathrm{iso}}(U^*) := \{\lambda \,|\, \Re(\nu_j) = \Re(\nu_{j+1})\}.$$

*The iso-real spectrum is the union of the $j$-iso-real spectra for $j = 1, \dots N+M-1$.*

If the essential spectrum of an asymptotically periodic travelling wave contains a self-intersecting curve, i.e. $\lambda(\mathrm{i}k_1) = \lambda(\mathrm{i}k_2)$ for $k_1 \neq k_2$, then this point lies in the iso-real spectrum. This point lies in the $j$-iso-real spectrum, where $j$ is the Morse index of a connected component of the essential spectrum whose boundary contains the intersection point.

**Theorem 3.3** *Assume a dispersion curve $\lambda(\mathrm{i}k)$ satisfies $\frac{\mathrm{d}}{\mathrm{d}k}\lambda(\mathrm{i}k) \neq 0$, $k \in [0, 2\pi)$ and parametrizes a Jordan curve $\gamma = \{\lambda(\mathrm{i}k) \mid k \in [0, 2\pi)\}$ in the essential spectrum of an asymptotically periodic travelling wave. Assume $\gamma$ is isolated in the essential spectrum, such that in the exterior of $\gamma$ close to $\gamma$ the Morse index is a constant $j$. Assume in addition that the interior of $\gamma$, $\mathrm{int}(\gamma)$, does not contain essential spectrum, and that $\partial_\lambda d_{\mathrm{per}}(\lambda, \nu) \neq 0$ for $\lambda \in \mathrm{int}(\gamma)$. Then $\overline{\mathrm{int}(\gamma)}$ contains $j$-iso-real spectrum.*

**Proof.** Since $\frac{\mathrm{d}}{\mathrm{d}k}\lambda(\mathrm{i}k) \neq 0$ the implicit function theorem applies and $\lambda(\nu)$ is defined in an open neighborhood of $\gamma$. By the Cauchy-Riemann equations $\frac{\mathrm{d}}{\mathrm{d}k}\lambda(\mathrm{i}k) \neq 0$ implies that $\frac{\mathrm{d}\lambda(\nu)}{\mathrm{d}\Re(\nu)}|_{\nu=\mathrm{i}k}$ are nonvanishing normal vectors to $\gamma$ for any $k \in [0, 2\pi)$. By continuity in $k$ these are either all interior or all exterior normals. We assume these are interior normals; the case of exterior normals is treated essentially the same, and we include comments to clarify this. Together with boundedness of $\gamma$, there is $\eta_0 > 0$ such that $\lambda(-\eta + \mathrm{i}k)$ lies in

the exterior of $\gamma$ and

$$\lambda(\eta + \mathrm{i}k) \in \mathrm{int}(\gamma) \text{ for all } \eta \in (0, \eta_0). \tag{3.11}$$

By assumption, for sufficiently small $\eta_0$ the curves $\{\lambda(-\eta + \mathrm{i}k) \,|\, k \in [0, 2\pi]\}$ do not intersect the essential spectrum. Hence, we can define $j$ to be the constant Morse-index in the connected component of the essential spectrum in the exterior of $\gamma$ whose boundary contains $\gamma$. Since $\mathrm{int}(\gamma)$ does not contains essential spectrum $i(\overline{\mathrm{int}(\gamma)}) = j + 1$, because the Morse index counts center-unstable dimensions. (In case of exterior normals: $i(\gamma) = j$, $i(\mathrm{int}(\gamma)) = j - 1$.)

The strategy of the remaining proof is to find certain iso-real spectrum and then conclude $j$-iso-real spectrum in $\overline{\mathrm{int}(\gamma)}$, see also figure 14.

Firstly, we construct a curve $z_\lambda(\eta)$ in the $\lambda$–plane, whose endpoints lie on $\gamma$ and which consists of solutions to $d_{\mathrm{per}}(z_\lambda(\eta), \eta) = 0$, where $\eta \in [0, \eta_1]$ is real, i.e. there exists $k_1 \in \mathbb{R}$ such that $d_{\mathrm{per}}(z_\lambda(\eta_1), \mathrm{i}k_1) = 0$. So there are two distinct spatial Floquet exponents at $\lambda = z_\lambda(\eta_1)$, namely $\eta_1$ and $\mathrm{i}k_1$. The only obstruction to finding this curve are double spatial Floquet exponents, involving $\eta$, i.e. iso-real spectrum involving $\eta$, which will imply $j$-iso-real spectrum.

Secondly, in case no double root occurred, we construct a curve $z_\nu(\eta)$, $\eta \in [0, \eta_1]$, where $z_\nu(\nu_1) = \mathrm{i}k_1$ by pathfollowing in $\mathrm{i}k_1$ in the $\nu$–plane along the curve $z_\lambda(\eta)$. Again, the only obstruction to this construction are double spatial Floquet exponents involving $z_\nu(\eta)$, i.e. iso-real spectrum involving $z_\nu(\eta)$, which will imply $j$-iso-real spectrum. In case there are no double roots there are two curves of distinct spatial Floquet exponents along a single curve in the $\lambda$–plane. We then show that the difference in real parts changes sign along the curve, which implies iso-real spectrum and presence of $j$-iso-real spectrum will follow.

As to the first step, constructing $z_\lambda(\eta)$ with $z_\lambda(0) = \lambda(0)$, which solves $d_{\mathrm{per}}(z_\lambda(\eta), \eta) = 0$ is possible for $0 < \eta < \eta_0$ by the implicit function theorem. From (3.11) we have $z_\lambda(\eta) \in \mathrm{int}(\gamma)$ for all sufficiently small $\eta > 0$, and for all $\lambda \in \overline{\mathrm{int}(\gamma)}$ we have $\partial_\lambda d_{\mathrm{per}}(\lambda, \nu) \neq 0$ by assumption. Thus, if $\lim_{\eta \to \eta_0} \partial_\nu d_{\mathrm{per}}(z_\lambda(\eta), \nu) \neq 0$ then the implicit function theorem allows to extend $z_\lambda(\eta)$ to $0 < \eta < \tilde{\eta}_0$ for some $\tilde{\eta}_0 > \eta_0$. Since spatial Floquet exponents are bounded for bounded $\lambda$ we have that $\nu \to \infty$ and $d_{\mathrm{per}}(\lambda, \nu) = 0$ implies $\lambda \to \infty$. Thus

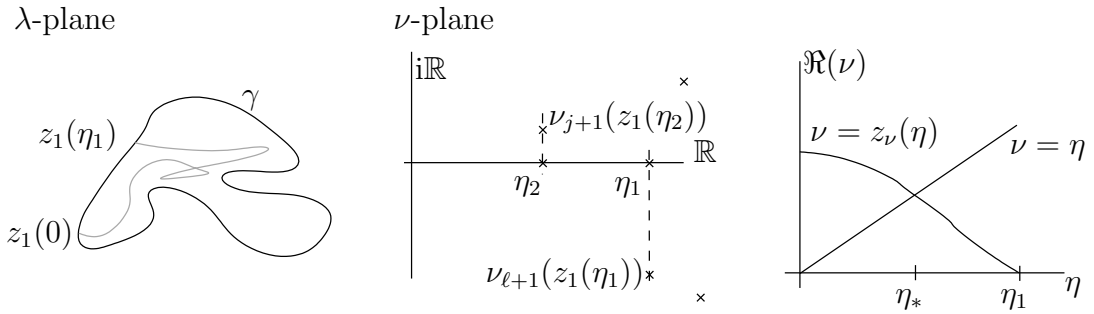


Figure 14: Configuration of $\gamma$ and spatial Floquet exponents in the iso-real spectrum involving $\eta$.

we can extend until $z_\lambda(\eta_1) \in \gamma$ or $d_{\mathrm{per}}(z_\lambda(\eta_1), \nu)$ has a double root in $\nu$.

The following argument shows that if there is iso-real spectrum in $\{z_\lambda(\eta) \,|\, \eta \in [0, \eta_1]\}$ involving $\eta$, then there is also $j$-iso-real spectrum. In particular, this holds for double spatial Floquet exponents. Assume $z_\lambda(\eta)$ lies in the $\ell$-iso-real spectrum. The Morse index $i(\mathrm{int}(\gamma)) = i(z_\lambda(\eta)) = j+1$ is constant for $\eta \in (0, \eta_1)$ and so the real parts of two unstable spatial Floquet exponents coincide. Since no Floquet exponent crosses the imaginary axis for $\eta \in (0, \eta_1)$ we have $\eta = \nu_{j+1}$ in the ordering of real parts, and so $\ell \in \{1, \dots, j+1\}$. Any sufficiently small $\eta$ is to the left of all Floquet exponents, which are continuous along $z_\lambda(\eta)$. Hence, if $\ell \neq j$, there is $0 < \eta_2 < \eta_1$ such that $z_\lambda(\eta_2)$ lies in the $j$-iso-real spectrum, see figure 14. We will refer to this observation again later. It follows that in order to prove that $\overline{\mathrm{int}(\gamma)}$ contains $j$-iso-real spectrum we may assume $z_\lambda(\eta_1) \in \gamma$. Hence $z_\lambda(\eta_1) = \lambda(\mathrm{i}k_1)$ for some $k_1 \in [0, 2\pi)$ and $z_\lambda(\eta) \in \mathrm{int}(\gamma)$ for $\eta \in (0, \eta_1)$. (In case of exterior normals: two stable Floquet exponents coincide, and $\eta = \nu_j$ in the ordering, so $\ell \in \{j, \dots, N+M\}$.)

As to the second step, we use the implicit function theorem to construct $z_\nu(\eta)$ for $\eta \in [\tilde{\eta}_1, \eta_1]$ with $z_\nu(\eta_1) = \mathrm{i}k_1$ and $d_{\mathrm{per}}(z_\lambda(\eta), z_\nu(\eta)) = 0$. In the same way as for $z_\lambda$, we can choose $\tilde{\eta}_1$ so that either $d_{\mathrm{per}}(z_\lambda(\tilde{\eta}_1), \nu)$ has a double root in $\nu$, or $\tilde{\eta}_1 = 0$. In case of a double root, we have iso-real spectrum involving $z_\nu(\eta)$. Now $z_\nu(\eta) \in \mathrm{int}(\gamma)$ for any $\eta < \eta_1$ close to $\eta_1$ and (3.11) implies $\Re(z_\nu(\eta)) > 0$ for these $\eta$, and we have $\Re(z_\nu(\eta_1)) = 0$. In the same way as in the previous paragraph, iso-real spectrum involving $z_\nu(\eta)$ implies $j$-iso-real spectrum. In particular, this applies to double spatial Floquet exponents involving $z_\nu(\eta)$. Hence, to prove that $\overline{\mathrm{int}(\gamma)}$ contains $j$-iso-real spectrum, it suffices to establish iso-real spectrum involving $z_\nu(\eta)$ in $\overline{\mathrm{int}(\gamma)}$, and we may assume $\tilde{\eta}_1 = 0$.

Since $\lambda(z_\nu(\eta)) \in \mathrm{int}(\gamma)$ and by assumption there is no essential spectrum in $\mathrm{int}(\gamma)$, we

have $\Re(z_\nu(\eta)) > 0$ for all $\eta \in (0, \eta_1)$. Suppose $\Re(z_\nu(0)) = 0$, i.e. $z_\nu(0) = \mathrm{i}k_2$ for some $k_2 \in [0, 2\pi)$. Since we excluded double roots involving $z_\nu(\eta)$, and $z_\nu(\eta_1) = \mathrm{i}k_1 \neq \eta_1$, it follows $z_\nu(\eta) \neq \eta$ for $\eta \in [0, \eta_1]$. Therefore, $k_2 \neq 0$, and so there are two Floquet exponents $\nu = 0$ and $\nu = \mathrm{i}k_2$ at $\lambda(0)$, i.e. iso-real spectrum involving $\eta$, which implies $j$-iso-real spectrum as shown previously. The remaining case is $\Re(z_\nu(0)) > 0$, which implies $\Re(z_\nu(\eta))$ is positive at $\eta = 0$, zero at $\eta_1$. By continuity there is $\eta_* \in (0, \eta_1)$ such that $\Re(z_\nu(\eta_*)) = \eta_*$, and so $z_\lambda(\eta_*)$ lies in the iso-real spectrum involving $\eta$, cf. figure 14, hence $\overline{\mathrm{int}(\gamma)}$ contains $j$-iso-real spectrum. □

**Remark 9** *We emphasize that for $j = N$ if $c > 0$, or $j = M$ if $c < 0$, isola as in theorem 3.3 contain absolute spectrum, and circles of essential spectrum associated to point spectrum of a sufficiently close pulse satisfy the assumption of the theorem except possibly $\partial_\lambda d_{\mathrm{per}} \neq 0$ in $\mathrm{int}(\gamma)$, cf. [55]. Notice that double roots of $d_{\mathrm{per}}(\lambda, \nu)$ in $\lambda$ typically mean that two curves of 'essential spectrum' in a weighted space meet. If such collisions can be excluded, we expect that the premise of the theorem excluding these double roots can be ignored.*

In analogy to asymptotically constant travelling waves, unstable absolute spectrum causes instability in any exponentially weighted space.

For codimensions of heteroclinic connections, the Morse indices $i(0)$ of the asymptotic states are relevant. As noted in lemma 10 iii), this is tightly linked to the local orientation of unstable dispersion curves induced by $o(\lambda, k) := -\mathrm{sgn}(\frac{\mathrm{d}\Im(\lambda(\mathrm{i}\beta))}{\mathrm{d}\beta}|_{\beta=k})$. If $\lambda = 0$ is a simple eigenvalue then $o(0, 0)$ is the sign of the group velocity $c_g := -\frac{\mathrm{d}\Im(\lambda(\mathrm{i}k))}{\mathrm{d}k}|_{k=0}$. These signs determine whether $i(\lambda)$ increases or decreases when crossing a dispersion curve. The following observation is implicit in [57], but for completeness we give a proof.

**Lemma 15** *Assume zero is a simple eigenvalue of $L_*$ for an asymptotically constant or periodic travelling wave $U^*$. Let $I := (0, R)$ with $R$ from lemma 14, and set $o_g := 0$ if $c_g \leq 0$ and $o_g := 1$ if $c_g > 0$. If $I$ intersects $\mathrm{spec}_{\mathrm{ess}}(U^*)$ at finitely many points where $o(\lambda, k) \neq 0$, then for $c > 0$ (if $c < 0$ replaced $N$ by $M$) we have*

$$i^{\pm}(0) \quad = \quad N + o_g + \sum_{\{\lambda(\mathrm{i}k) \in I\}} o(\lambda, k).$$

**Proof.** The assumption implies, that at $\lambda = 0$ the trivial Floquet exponent is simple, cf. e.g. [51]. By assumption, $\frac{\mathrm{d}}{\mathrm{d}k}\Im(\lambda(\mathrm{i}k)) \neq 0$ at all crossing points $\lambda(\mathrm{i}k) \in (0, R)$ with $\mathrm{spec}_{\mathrm{ess}}(U^*)$, and so there exists a local inverse function $\nu(\lambda)$. By the Cauchy-Riemann equations:

$$\mathrm{sgn}\left(\frac{\mathrm{d}\Re(\nu(\lambda))}{\mathrm{d}\Re(\lambda)}\right) = \mathrm{sgn}\left(\frac{\mathrm{d}\Re(\lambda(\nu))}{\mathrm{d}\Re(\nu)}\right)^{-1} = \mathrm{sgn}\left(\frac{\mathrm{d}\Im(\lambda(\nu))}{\mathrm{d}\Im(\nu)}\right)^{-1} = -o(\lambda(\mathrm{i}k), k).$$

Hence, upon crossing a curve from right to left, the Morse index changes by $o(\lambda(\mathrm{i}k), k)$. Since the Morse index $i(R) = N$ for $c > 0$, lemma 14 implies $i(\epsilon) = N + \sum_{\{\lambda(\mathrm{i}k)\in I\}} o(\lambda, k)$ for $\epsilon > 0$ sufficiently small, and the sum is finite by assumption.
Since the center direction counts towards the Morse index, $c_g > 0$ implies $i(0) = i(\epsilon) + 1$, and $c_g \leq 0$ implies $i(0) = i(\epsilon)$. For $c < 0$ replace $N$ by $M$, cf. lemma 14. □

By lemma 14 the spatial Morse-index $i(0)$ for a *stable* constant travelling wave is necessarily $N$ for $c > 0$ and $M$ for $c < 0$. Now lemma 15 implies for stable $U_*$ and $c > 0$ that for $c_g > 0$ we have $i(0) = N + 1$, and if $c_g < 0$ then $i(0) = N$. For $c < 0$ the same holds with $N$ replaced by $M$. Hence, we can conclude the Morse index of a stable wave through the group-velocity, which can be numerically computed more reliably than Floquet exponents in some cases.

**Lemma 16** *A heteroclinic cycle in spatial dynamics between a stable steady state and a stable wave train of (3.2) is codimension–1 in the sense of definition 1 in chapter 2.*

**Proof.** We first consider $c > 0$. Lemmas 10 and 14 imply for $c_g > 0$ that the Morse indices are $N$ and $N + 1$ in $N + M$ ambient dimensions, so both have $M$ stable dimensions. Hence, the codimension of one connection is $N + 1 + M - (N + M) - 1 = 0$, while the other is $N + M - (N + M) - 1 = -1$. For $c_g < 0$ the codimensions are interchanged. If $c < 0$, the same holds, with $M$ and $N$ interchanged. □

By remark 8, a heteroclinic connection (a 'front') between stable steady states is codimension–1, which can be interpreted as a selected speed. Lemma 16 shows that for a heteroclinic connection to a periodic orbit, the group velocity is relevant. The group velocity determines the direction of transport, which can be made rigorous in an amplitude description

in some cases, cf. [57] and the references therein. If the group velocity points away from the steady state, then lemma 16 implies that the front is codimension–1, i.e. has a selected speed, otherwise it comes in a family.

### 3.1.3 Point spectrum near heteroclinic cycles

If the kinetics $F$ of the reaction diffusion system (3.1) depends on a parameter $\phi$, the travelling wave ODE (3.7) has two parameters $\mu = (\phi, c)$. Since homoclinic orbits to an equilibrium $u_1$ are generically codimension–1, i.e. one parameter is needed for transversality, cf. e.g. [39], we expect a given homoclinic orbit yields a curve of homoclinic orbits $h(L) = h(\mu(L))$ with a curve $\mu(L)$ in the parameter plane $\{\mu = (\phi, c)\}$. As discussed in the introduction and proven in chapter 2, possible obstacles to continue this curve are collisions with another equilibrium or a periodic orbit $u_1$ in a codimension–2 heteroclinic cycle at some $L_0 \in \mathbb{R} \cup \{\infty\}$. This involves a heteroclinic orbit $h_b$ connecting $u_0$ to $u_1$, and $h_f$ connecting $u_1$ to $u_0$.

Lemma 16 shows that for a spatial codimension–2 heteroclinic cycle in the sense of definition 1, the wave train or steady state is necessarily unstable. Indeed, one might expect that a connection involving an unstable state does not yield a travelling wave by specifying the speed alone. The bifurcation from a heteroclinic cycle is not a small perturbation of the associated eigenvalue problem(s), and concerning stability the question is how the spectra of the travelling waves associated to $h(L)$ behave as $L \to L_0$. It was proved in [52] that the main influence of $u_1$ on the spectrum of $h(L)$ stems from its point and iso-real spectrum.

**Definition 9 ([53])** *The $j$-iso-real spectrum is called reducible, if hypothesis 8 of [53] is satisfied with $i_\infty$ replaced by $j$. This means that the set of points is dense where precisely two spatial eigenvalues (or Floquet exponents) have the same real part and the derivative with respect to $\lambda$ of their difference is nonzero.*

**Theorem 3.4 ([52])** *Assume that the essential spectrum of $u_0$ is contained in the open left half plane and a T-point occurs. Let $\Omega$ be a bounded, open subset of a connected component of $\mathbb{C} \setminus \mathrm{spec}_{\mathrm{ess}}(u_0)$, and let $i_\Omega$ be the Morse index of $A(\xi; \lambda)$ in $\Omega$. The point*

*spectrum of* $h(L)$ *in* $\Omega \setminus \mathrm{spec}_{\mathrm{iso}}^{i_\Omega}(u_1)$ *converges to the union of the point spectra of* $h_b$ *and* $h_f$ *in* $\Omega$*. Assume* $\Omega$ *is not entirely filled with point spectrum*[4]*. If* $\mathrm{spec}_{\mathrm{iso}}^{i_\Omega}(u_1)$ *is reducible, then it is the set in* $\Omega$ *where eigenvalues accumulate as* $L \to L_0$*.*

This theorem has been proved in [52] for a 'T-point', but applies to codimension–2 heteroclinic cycles with a periodic orbit. It can be proved in the same way as in [52] by replacing eigenvalues with Floquet exponents and using the estimates obtained in theorem 2.3.

**Corollary 1** *For generic* $F$*, let* $U_L$ *be pulses which correspond to homoclinic orbits in travelling wave ODEs with speed* $c_L \neq 0$ *or invertible* $D$*. Assume these homoclinics converge to a codimension–2 heteroclinic cycle with an absolutely unstable periodic orbit* $U^*$ *as* $L \to \infty$*. If* $\mathrm{spec}_{\mathrm{abs}}(U^*)$ *is reducible, then infinitely many eigenvalues accumulate at* $\mathrm{spec}_{\mathrm{abs}}(U^*)$ *as* $L \to \infty$*.*

**Proof.** Theorem 2.5 proves that such a scenario is possible and provides the exponential estimates for parameters and solutions needed in theorem 3.4, if $F$ satisfies the hypotheses. Recall $\mathrm{spec}_{\mathrm{iso}}^{N}(U^*) = \mathrm{spec}_{\mathrm{abs}}(U^*)$ and $i_{\Omega_\infty} = N$ for $c > 0$, and for $c < 0$ replace $N$ by $M$. For a stable pulse $\Omega_\infty \supset \{\Re(\lambda) \geq 0\}$ and by assumption on $U^*$ we have $\mathrm{spec}_{\mathrm{abs}}(U^*) \cap \{\Re(\lambda) \geq 0\} \neq \emptyset$. As mentioned above, we can apply theorem 3.4 in its formulation for a collision with a periodic orbit assuming the genericity conditions therein. This implies that eigenvalues accumulate at $\Omega_\infty$ when approaching the heteroclinic cycle, i.e. increasing $L$. □

## 3.2 Weak diffusion limit

As mentioned in the introduction to this chapter, many reaction-diffusion models have components which do not diffuse, so the diffusion matrix $D$ has a kernel. In section 3.1, this gave rise to the difference of $M$ and $N$ and the case distinctions $c > 0$ and $c < 0$. In this section, we show that one the hand, for vanishing diffusion, one can typically rely on the more convenient PDE framework for an invertible diffusion matrix. On the other hand,

[4] This is e.g. the case if $\Omega = \Omega_\infty$ is the component containing an unbounded set of $\mathbb{R}^+$.

weak diffusion can be typically accurately modeled by zero diffusion. The dependence of spectral properties on the sign of the speed $c$ can also be derived from this approach.
On bounded domains for the asymptotically constant case, zero diffusion may have a stabilizing effect for the boundary spectrum of formally reduced boundary conditions. In this reduction, conditions on weakly diffusing components are ignored, and we denote the arising spectrum by $\mathrm{spec}^0_{\mathrm{bc}}$.
Let $D_\delta = \mathrm{diag}(D_1, \delta, \dots, \delta)$, where $D_1 = \mathrm{diag}(d_1, \dots, d_M) > 0$ is invertible. Let $(3.2)_\delta$ and $(3.3)_\delta$ denote the comoving reaction diffusion system with $D$ replaced by $D_\delta$.

**Hypothesis 8** *The travelling wave vector field unfolds the heteroclinic connection transversely in its parameters, i.e. has linearly independent Melnikov-integrals and the point spectrum of the travelling wave does not contain open sets.*

**Theorem 3.5** *Assume $(3.3)_0$ satisfies hypothesis 8 and $\dim(\mathrm{Rg}(D_0)) \geq 1$ for an asymptotically constant or periodic travelling wave $U_0^*$ with speed $c \neq 0$. Then for any sufficiently small $\delta$, there exists an asymptotically constant or periodic travelling wave $U_\delta^*$ with speed $c_\delta = c + O(\delta)$ solving (3.3) and $\sup_{\xi \in J} |U_0^* - U_\delta^*| = O(\delta)$ for any bounded interval $J \subset \mathbb{R}$. Let $B \subset \mathbb{C}$ be bounded. In symmetric Hausdorff-distance $\mathrm{dist}_H$ we have*

$$\mathrm{dist}_H(\mathrm{spec}(U_\delta^*) \cap B, \mathrm{spec}(U_0^*) \cap B) = O(\delta).$$

*On a bounded domain for asymptotically constant $U^*$ there is $C > 0$ such that*

$$\mathrm{spec}^0_{\mathrm{bc}}(U^*) \cap B \subset \{\lambda \in \mathbb{C} \,|\, \mathrm{dist}(\lambda, \mathrm{spec}_{\mathrm{bc}}(U_\delta^*) \cap B) \leq C\delta\}.$$

**Proof.** The following proof is essentially a consequence of the treatments in [33, 44, 45], where more details regarding singular perturbation theory and the correspondence of spectra and exponential dichotomies can be found.
We consider the travelling wave ODE $(3.3)_\delta$ as a first order system analogous to (3.7). To simplify notation, let $v \in \mathbb{R}^M$ denote the diffusing species, $w \in \mathbb{R}^{N-M}$ the weakly diffusing, and $g(v, w) = P_M F(v, w)$ as well as $h(v, w) = (\mathrm{Id} - P_M)F(v, w)$. Note that

$M \geq 1$ by assumption. We obtain the so-called slow system

$$\begin{aligned} \dot{v} &= \tilde{v} \\ \dot{\tilde{v}} &= -D_1^{-1}(c\tilde{v} + g(v,w)) \\ \dot{w} &= \tilde{w} \\ \delta\dot{\tilde{w}} &= -(c\tilde{w} + h(v,w)) \end{aligned} \tag{3.12}$$

and bounded solutions for $\delta \geq 0$ are in one-to-one correspondence with (bounded) travelling wave solutions of $(3.2)_\delta$. In the scaling $\zeta = \delta\xi$, $' = \frac{\mathrm{d}}{\mathrm{d}\zeta}$ we obtain the so-called fast system, which is equivalent to the slow system for $\delta > 0$:

$$\begin{aligned} v' &= \delta\tilde{v} \\ \tilde{v}' &= -\delta D_1^{-1}(c\tilde{v} + g(v,w)) \\ w' &= \delta\tilde{w} \\ \tilde{w}' &= -(c\tilde{w} + h(v,w)) \end{aligned}$$

At $\delta = 0$ the fast system has a normally hyperbolic manifold of equilibria

$$M_0(\lambda) = \{\tilde{w} = -c^{-1}h(v,w)\},$$

because its linearization is lower left triangular with diagonal $-c(0,0,0,1)$ and by assumption $c \neq 0$. In fact, for $c > 0$ the manifold $M_0(\lambda)$ is exponentially stable as $\zeta \to \infty$, and for $c < 0$ as $\zeta \to -\infty$ independent of $f$ with rate of convergence $c$.

From Fenichel's results, cf. the review [33] and the references therein, it follows that $M_0$ persists for any sufficiently small $\delta > 0$ as a $\delta$-close locally invariant smooth manifold $M_\delta$. Moreover, for $\delta > 0$, the manifold inherits a strong stable (unstable) continuous fibration for $c > 0$ ($c < 0$) and the flow on $M_\delta$ is given by the slow system for $\delta = 0$ with a correction of order $\delta$, cf. [33, 58]:

$$\begin{pmatrix} \dot{v} \\ \dot{\tilde{v}} \\ \dot{w} \end{pmatrix} = \begin{pmatrix} \tilde{v} \\ -D_1^{-1}(c\tilde{v} + g(v,w)) \\ -c^{-1}h(v,w) \end{pmatrix} + O(\delta).$$

Note that the exponential rates for the flow transverse to $M_\delta$, i.e. in the Fenichel fibers, are $-c/\delta$ in this scaling. The system in $M_\delta$ is now regularly perturbed.

Let $u_0$ be the heteroclinic or homoclinic orbit associated to $U^*$, and consider a compact neighborhood of $u_0$ in $M_0$. The hyperbolic asymptotic states correspond to hyperbolic equilibria or periodic orbits $u_0^{\pm}(\xi)$ in the slow system, where sub-indices $\pm$ denote $\xi \to \pm\infty$. By hyperbolicity these states persist as $\delta$-close equilibria or as $\delta$-close (locally in $\xi$) periodic orbits. Hypothesis 8 guarantees that $u_0$ is transversely unfolded using the parameters of $f$. Hence, there is $\delta_0 > 0$ such that $u_0$ persists with order $\delta$ adjustments of these parameters as a (locally in $\xi$) $\delta$-close hetero- or homoclinic orbit $u_\delta$ in $M_\delta$ for any $\delta_0 \geq \delta > 0$. Hence, we obtain a family of travelling waves $U_\delta^*(\xi)$ for $(3.2)_\delta$ for $\delta \geq 0$.

We next address spectra of these waves. The eigenvalue problem (3.5) becomes $\lambda U = L_*^\delta U$ where $L_*^\delta = D_\delta \partial_{\xi\xi} + c\partial_\xi + \partial_U F(U_\delta^*)$ and can be cast as the non-autonomous linear ODE

$$\begin{pmatrix} \dot{V} \\ \dot{\tilde{V}} \\ \dot{W} \\ \delta\dot{\tilde{W}} \end{pmatrix} = \begin{pmatrix} \tilde{V} \\ -D_1^{-1}(c\tilde{V} + \partial_U g(U_\delta^*(\xi)) \cdot (V,W) - \lambda V) \\ \tilde{W} \\ -(c\tilde{W} + \partial_U h(U_\delta^*(\xi)) \cdot (V,W) - \lambda W) \end{pmatrix} \tag{3.13}$$

Replacing $U_\delta^*(\xi)$ with $(v,w)$, we can write (3.13) together with (3.12) as a skew product system. As above, the associated fast system has a normally hyperbolic manifold of equilibria at $\delta = 0$ with rate of convergence $-c$. This persists for all $\delta \leq \delta_0$, with possibly decreased $\delta_0 > 0$. Due to the skew product structure and linearity of (3.13), the invariant manifold is the product of $M_\delta$ and a vector bundle $N_\delta(\lambda) = \cup_{\xi\in\mathbb{R}} N_\delta(\xi;\lambda)$. Again, the sign of $c$ determines the stability and we can write the projection of (3.13) to $N_\delta(\lambda)$ as a non-autonomous linear ODE of the form

$$\begin{pmatrix} \dot{V} \\ \dot{\tilde{V}} \\ \dot{W} \end{pmatrix} = \begin{pmatrix} \tilde{V} \\ -D_1^{-1}(c\tilde{V} + \partial_U g(U_\delta^*(\xi)) \cdot (V,W) - \lambda V) \\ -c^{-1}(\partial_U h(U_\delta^*(\xi)) \cdot (V,W) - \lambda W) \end{pmatrix} + O(\delta). \tag{3.14}$$

Let $A_\delta(\xi;\lambda)$ denote this matrix and $A_\delta^{\pm}(\xi;\lambda)$ the asymptotic matrix functions as $\xi \to \pm\infty$, i.e. $|A_\delta^{\pm}(\xi;\lambda) - A_\delta(\xi;\lambda)| \to 0$.

The following theorem is a reformulation of results in [44, 45]. It shows that relating exponential dichotomies of (3.13) and (3.14) for $\delta > 0$ implies a relation of spectra of the operators $L_*^\delta$. Note that at $\delta = 0$ (3.14) casts the eigenvalue problem of $L_*^0$ as an ODE.

**Theorem 3.6 ([44, 45])** *Let $\delta$ be so that $\delta_0 > \delta > 0$. A complex number $\lambda$ is in the resolvent set of $L_*^\delta$, if and only if (3.13) has an exponential dichotomy on $\mathbb{R}$. It lies in the point spectrum, if and only if (3.13) has exponential dichotomies on $\mathbb{R}^-$ with unstable space $E_-^{\mathrm{u}}(\xi;\lambda)$ and $\mathbb{R}^+$ with stable space $E_+^{\mathrm{s}}(\xi;\lambda)$ such that $\dim(E_-^{\mathrm{u}}(0;\lambda) \cap E_+^{\mathrm{s}}(0;\lambda)) > 0$. Finally, $\lambda$ lies in the essential spectrum, if and only if (3.13) does not have an exponential dichotomy on $\mathbb{R}^+$ or $\mathbb{R}^-$, or $i_+(\lambda) \neq i_-(\lambda)$.*
*For $\delta = 0$ the same holds for the spectrum of $L_*^0$ and exponential dichotomies of (3.14).*

Concerning the claim about point, boundary, absolute and essential spectra, we first show that for $\delta > 0$ the spectrally relevant dichotomy properties of (3.13) and (3.14) are equivalent, i.e. we can reduce to the smaller system (3.14) which is defined for $\delta \geq 0$. In a second step we show that these properties behave well as $\delta \to 0$.
Fix $\delta > 0$ and let $E_\delta(\xi;\lambda)$ be the linear Fenichel fiber at $\xi$ of (3.14), so $E_\delta(\xi;\lambda)$ is transverse to $N_\delta(\xi;\lambda)$ and (a suitable unit basis) is at least continuous with respect to $\xi \in \mathbb{R}$. Therefore, we can find a continuous family of 'Fenichel projections' $P^{\mathrm{f}}(\xi;\lambda)$ for $\xi \in \mathbb{R}$ with kernel $E_\delta(\xi;\lambda)$ and range $N_\delta(\xi;\lambda)$.
Let $\Phi(\xi,\tau;\lambda)$ be the evolution of (3.13). Since this maps Fenichel fibers into Fenichel fibers, it holds for $v(\tau) \in E_\delta(\tau;\lambda)$ and $\xi,\tau \in \mathbb{R}$ that $|\Phi(\xi,\tau;\lambda)v(\tau)| \leq C\mathrm{e}^{-c(\xi-\tau)/\delta}$ . Hence, for any bounded $B \subset \mathbb{C}$ there is $\delta_1$ such that $\delta_1 \leq \delta_0$ and for $0 < \delta \leq \delta_1$ the eigenvalues or Floquet multipliers $\nu = \nu(\lambda)$ of the asymptotic states satisfy $|\Re(\nu)| < c/\delta$.
Let $B \subset \mathbb{C}$ be bounded and assume that for $\lambda \in \mathbb{C}$ and $0 < \delta \leq \delta_1$ system (3.13) has exponential dichotomies $P_\pm^{\mathrm{s/u}}(\xi;\lambda) : \mathbb{R}^\pm \to E_\pm^{\mathrm{s/u}}(\xi;\lambda)$. For $c > 0$ the Fenichel fibers are stable directions, so $E_\pm^{\mathrm{u}}(\xi;\lambda) \subset N_\delta(\xi)$ and $P^{\mathrm{f}}(\xi;\lambda)P_\pm^{\mathrm{u}}(\xi;\lambda) = P_\pm^{\mathrm{u}}(\xi;\lambda)$. By choice of $\delta_1$ there is a spectral gap which allows for a decomposition of $P_+^{\mathrm{s}}(\xi;\lambda) = P_+^1(\xi;\lambda) + P_+^2(\xi;\lambda)$ into projections, such that $P^{\mathrm{f}}(\xi;\lambda)P_+^{\mathrm{s}}(\xi;\lambda) = P_+^2(\xi;\lambda)$. These projections are continuous in $\xi \geq 0$, and analytic in $\lambda$ for each $\xi$ by virtue of the following. Exponential weights can be chosen so that (3.13) has exponential dichotomies with stable projection $P_+^2(\xi;\lambda)$. Since (3.13) is analytic in $\lambda$, the projection $P_+^2(\xi;\lambda)$ is unique and analytic in $\lambda$ for each $\xi$, because it can be derived from a uniform contraction principle, cf. e.g. [50]. Similarly $P_+^{\mathrm{s}}(\xi;\lambda) = (P_+^1 + P_+^2)(\xi;\lambda)$ is analytic, hence $P_+^1(\xi;\lambda)$ is.
Analogously, it follows that the projections $P^{\mathrm{f}}(\xi;\lambda)$ are analytic in $\lambda$ for each $\xi \in \mathbb{R}^+$,

and for $c < 0$ the same holds with 's', 'u' and '+', '-' interchanged. Hence, the projections $p^{\mathrm{s/u}}_{\pm}(\xi;\lambda) := P^{\mathrm{f}}(\xi;\lambda)P^{\mathrm{s/u}}_{\pm}(\xi;\lambda)$ in particular define exponential dichotomies of (3.13) with stable and unstable spaces $e^{\mathrm{s/u}}_{\pm}(\xi;\lambda) \subset N_\delta(\xi;\lambda)$.

As to point spectrum, for $c > 0$ we have $E_\delta(\xi;\lambda) \subset E^{\mathrm{s}}_{\pm}(\xi;\lambda)$ and $E_\delta(\xi;\lambda) \cap E^{\mathrm{u}}_{\pm}(\xi;\lambda) = \{0\}$, and for $c < 0$ the same holds with 's' and 'u' interchanged. Hence, by theorem 3.6 point spectrum cannot be generated by intersections involving $E_\delta(\xi;\lambda)$. Therefore, point spectrum solely depends on the projected spaces $e^{\mathrm{s/u}}_{\pm}(\xi;\lambda)$, i.e. exponential dichotomies of (3.14). As to the behavior with respect to $\delta$, analyticity of the vector field in (3.13) with respect to $\lambda$ implies analytic Evans functions, cf. [1], whose roots are eigenvalues counted with multiplicities. By analyticity of the above projections, we obtain analytic Evans functions $e_\delta(\lambda)$ for the dichotomies of (3.14) for $\lambda$ in any bounded set and $0 < \delta < \delta_1$. At $\delta = 0$ system (3.14) is analytic in $\lambda$, thus there is an analytic Evans function $e_0(\lambda)$, and $\lim_{\delta\to 0} e_\delta(\lambda) = e_0(\lambda)$, because the vector fields converge. By hypothesis 8 the set of eigenvalues does not contain open sets and we can apply Rouché's theorem, cf. e.g. [15], which implies that eigenvalues of $L^\delta_*$ converge to those of $L^0_*$ as $\delta \to 0$.

As to boundary spectrum, note that the above construction of dichotomies applies to the analogues of (3.13) and (3.14) with the asymptotic matrices $A^{\pm}_\delta(\xi;\lambda)$. In the same way as for the point spectrum, there are analytic Evans-type functions constructed from the dichotomies of (3.13) at the asymptotic states, whose roots count (with multiplicity) non-trivial intersections of spaces of boundary conditions and subspaces of eigenspaces as in definition 7. The Evans-type functions can be projected to (3.14) as above, which corresponds to the formally reduced boundary spectrum $\mathrm{spec}^0_{\mathrm{bc}}$. If the spaces of boundary conditions only trivially intersect $E_\delta(0;\lambda)$ then no information on intersections is lost by this reduction. Therefore, we conclude that the reduced boundary spectrum of (3.14) restricted to any bounded set is contained in an order $\delta$ neighborhood of that of (3.13).

Finally, essential and absolute spectra only depend on Floquet exponent (or eigenvalue) configurations of the asymptotic states, and we do not need Evans functions. The analogues of (3.13) and (3.14) with the asymptotic matrices are analytic in $\lambda$, which implies eigenvalues (or Floquet exponents) are analytic, cf. e.g. [14]. Due to the spectral gap

for $\lambda$ in any bounded set $B$ and $0 < \delta \leq \delta_1$, no absolute spectrum (restricted to $B$) is generated by the interaction with the spatial eigenvalue (or Floquet exponent) $-c/\delta$ in the Fenichel fibers. Since $c/\delta \neq 0$, the existence of exponential dichotomies for these asymptotic systems, and thus essential spectrum, only depends on the reduced system. By Rouché's theorem, dispersion curves and boundaries of absolute spectra are in $O(\delta)$ symmetric Hausdorff-distance restricted to any bounded set. Therefore, essential and absolute spectra of $L_*^\delta$ and $L_*^0$ are close as claimed. □

# 4 Tracefiring in the Oregonator

Building upon chapter 3, we now apply the bifurcation results from chapter 2 to the self-organized pattern formation process tracefiring in reaction diffusion equations. In particular, this occurs in the three-component Oregonator model for the light-sensitive Belousov-Zhabotinskij reaction, which is the following reaction-diffusion system.

$$\begin{aligned} U_t &= U_{xx} + (U(1-U) + V(U-q))/\epsilon \\ V_t &= D_V V_{xx} + (fW + \phi + V(U+q))/\epsilon' \\ W_t &= U - W \end{aligned} \tag{4.1}$$

We keep the parameters $D_V = 1.12$, $q = 0.001$, $f = 1.5$, $\epsilon = 0.09$ and $\epsilon' = 0.01125$ fixed, as in [59]. We vary the parameter $\phi$, which corresponds to the intensity at which the medium is globally uniformly illuminated.

The main goals are to establish organizing centers to partially explain tracefiring and the instability in the Oregonator which leads to tracefiring. This will involve numerical investigations guided by chapters 2 and 3. First, we report on related experimental and numerical results and describe the phenomenology.

## 4.1 Backfiring and tracefiring

Paradigmatic examples of self-organization and pattern formation are pulses in excitable media. In the simplest case, these media are spatially homogeneous and support a spatially uniform rest state, which is stable with respect to sub-threshold perturbations. Localized perturbations beyond a threshold size cause the components of the system (the 'species'), to undergo a large excursion before relaxing back to the rest state. The return to the rest state constitutes a refractory phase in which the excitation threshold is significantly higher. Typically, there are two types of species involved: an activator, which is fast, and an inhibitor, which is slower and lags behind the activator, creating the refractory phase after an excitation. These pointwise reaction kinetics are spatially mainly coupled by diffusion. A spatially localized super-threshold perturbation then often causes an invasion of the excitation loop into the medium at rest, which in one space dimension creates travelling pulses with a selected constant speed. Our focus is on parameter values which

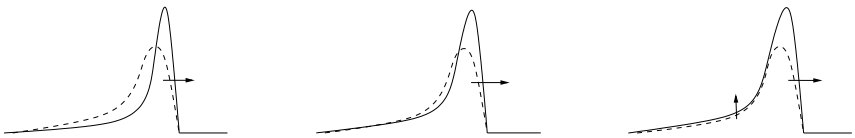

Figure 15: Schematic picture of an excitation pulse instability due to vanishing refractory phase from left to right. Solid lines denote the activator, dashed lines the inhibitor. Arrows indicate propagation direction, and onset of instability.

shorten the refractory phase, so that the pulse's wake causes a self-sustained re-excitation of the medium, cf. figure 15. The simplest scenario is that a secondary pulse forms in the primary pulse's wake, which then travels in the same or the opposite direction, and this process repeats periodically, see figures 2 and 16. In [71] such effects, triggered at inhomogeneities, reportedly evoke dramatic motor dysfunction of mutated mice. The case where secondary pulses created in this fashion travel in the opposite direction has been called backfiring in [6]. Similar phenomena have been observed in experiments, cf. [3, 43, 61, 71], and numerically in [38]. The backfired pulses may then backfire themselves and create intricate patterns reminiscent of Sierpinski gaskets, cf. [30]. A related effect is pulse splitting, where pulses split in or near their centers which creates pairs of initially counter-propagating pulses, cf. e.g. [21]. An interpretation of the case where secondary pulses do not backfire is for instance a self-organized control signal which informs the sender, using the medium itself, that it reached a certain distance measured by the number of backfired pulses.

In the second simple scenario after loss of an effective refractory phase, secondary pulses travel in the trace of the primary pulse, see figures 2 and 16, and we call this phenomenon tracefiring. It was first observed in [67], where it was referred to as 'secondary trailing waves' and has also been found in numerical simulations in [66] as well as by the author in the Oregonator model (4.1). An interpretation of this phenomenon is a self-organized replication process, or informing a receiver through the medium itself how far a signal travelled from its source, measured by the number of pulses. If tracefiring can be turned on and off, as is the case in the Oregonator, it is possible to create arbitrarily long chains of pulses, which can be used as a chemical memory storage. This has been suggested for a related process in [17].

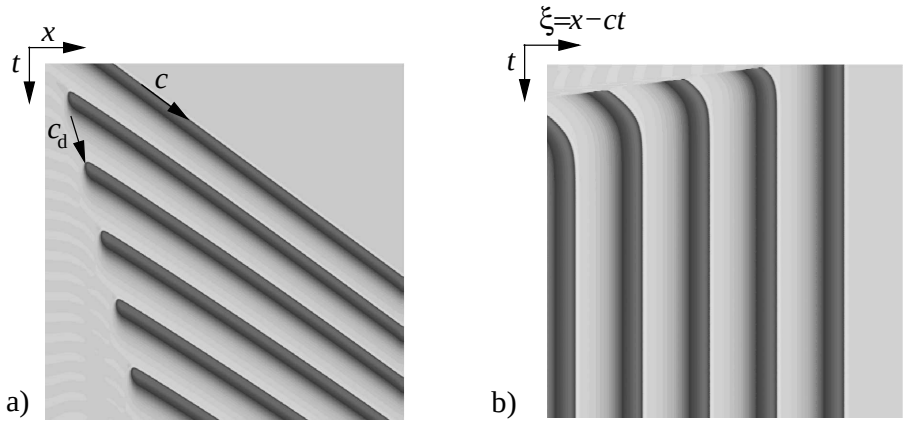


Figure 16: Space-time plots of Oregonator's tracefiring, $\phi \sim 0.000155$. a) standing frame, b) comoving with the primary pulses speed $c \sim 3.414$. The defect speed is $c_\mathrm{d} \sim 0.55$. Domain length 400, uniform 0.1 length grid. Left b.c.: Neumann, right: a) Neumann, b) Dirichlet.

Concerning the spatio-temporal geometry of tracefiring, we find two characteristic speeds: the pulse's speed $c$ and the smaller speed $c_\mathrm{d}$ of the periodic creation of secondary pulses, which we refer to as the defect speed, see figures 2 and 16. Comoving with speed $c_\mathrm{d}$, the omega limit set can be viewed as a defect, i.e. an interface between the background state and a spatio-temporally periodic state, cf. figure 2. This is not an object in the travelling wave ODE, cf. (3.3), but may be cast as a heteroclinic connection in a function space, e.g. in the space of periodic functions with the temporal period of tracefiring. Defects in this sense have recently been classified analytically [57]. However, we will not further pursue this perspective here.

The difference between the two characteristic speeds creates a wedge of non-constant dynamics in space-time. Except for the model in [17], where $c = 0$, this plateau travels in the primary pulse's direction while broadening, i.e. $\mathrm{sgn}(c_\mathrm{d}) = \mathrm{sgn}(c) \neq 0$. Hence it is transient on a bounded domain. However, comoving with speed $c$, the omega limit set is a connection between a periodic pulse-train and the homogeneous background state, which we call invading pulse chain, cf. figure 2. From a spatial dynamics perspective, as introduced in chapter 3, we expect to find a heteroclinic orbit from a periodic orbit to an equilibrium in the travelling wave ODE (3.3) with speed $c$. In addition, the reverse of an invading pulse-chain can be expected, i.e. a spatial connection from the background state to the pulse-train, which we call evading pulse-chain. In contrast, the limit of backfiring

is not stationary in any comoving frame.

For tracefiring, arbitrarily many copies of pulses, which occur in the tracefiring process appear to co-exist with the stable pulse in the reported cases. These $n$-pulses are reminiscent of $n$–homoclinic orbits with small inter-pulse distance, but we interpret them as homoclinic orbits near a heteroclinic cycle with a periodic orbit. Therefore, we expect a heteroclinic cycle with a periodic orbit, namely the pulse-train with small interpulse distances, which occurs in the in- and evading pulse chains, cf. figures 2 and 3. From this perspective, we view the $n$-pulses as a result of the interaction with the pulse-train, i.e. the spatially homoclinic orbit shadows the pulse-train which resembles concatenated copies of pulses with small distances. Assuming the pulse-train is stable for the PDE, lemma 16 shows that the heteroclinic cycle would be codimension–1. Theorem 2.3 then implies that a family of curves of 1–homoclinic orbits accumulates at such a heteroclinic cycle, if parameters unfold transversely. We may choose a sequence $(h_n)_{n\geq n_0}$ of these, for some $n_0 \geq 0$, such that $h_n$ has $n$ 'spikes' shadowing the pulse-train, see figure 3, and thus resembles an $n$-pulse with small interpulse distances.

**Remark 10** *From this perspective, tracefiring is the subcritical loss of stability of the primary pulse and convergence to the invading pulse chain via n-pulses with n increasing in steps of* 1 *after time steps of constant length. Basic building blocks of tracefiring are n-pulses for any* $n \geq 1$ *as well as the invading and evading pulse chains.*
*An organizing center for the constituents of tracefiring is a codimension–1 heteroclinic cycle between a stable pulse-train and steady state.*

In terms of the model equations, we expect to find 1–homoclinic orbits in the travelling wave ODE with a parameter dependent speed $c$. Numerical analyses of tracefiring in [67] and backfiring in [38] show that the primary pulse's loss of stability occurs near a collision of the homoclinic orbit with another *equilibrium*[5]. These collisions occur along parameter changes in the kinetics (with adapted change in the speed) and correspond to heteroclinic cycles of codimension–2 with one transverse heteroclinic orbit and one codimension–2 heteroclinic orbit. As mentioned in chapter 1, points in parameter space

[5]Such a point has been found numerically also in the Gray-Scott model, which exhibits pulse-splitting (M. Bär, private communication).

where this happens are called 'T-points', cf. [28]. The equilibria in all cited cases have complex conjugate leading eigenvalues, hence a homoclinic orbit is of Shil'nikov-type and the existence of the constituents of tracefiring typically follows, cf. [63, 39]. However, the $n$-pulses that accompany the homoclinic orbit a priori have large interpulse distances.
For the system in [38], the second equilibrium is absolutely unstable with absolute spectrum passing through zero, cf. [52][6]. The results in [52], see theorem 3.4 in section 3.1.3, explain the loss of stability: the unstable absolute spectrum will be inherited by nearby homoclinic orbits in terms of clustering unstable point spectrum. Moreover, the leading eigenvalues of the second equilibrium are complex conjugate, and the path in parameter space will spiral to leading order, cf. [28].

**Remark 11** *The codimension–2 heteroclinic cycle between two equilibria, and leading stable complex conjugate eigenvalues can be interpreted as an organizing center for the constituents and onset of tracefiring.*

This organizing center does not distinguish backfiring or tracefiring and does not explain the periodic nature of tracefiring, nor the small interpulse distances in tracefiring. Nevertheless, we follow the idea of establishing a similar organizing center for the onset of tracefiring in the Oregonator, where no second equilibrium is relevant.
The remainder of this chapter is to devoted to an analysis of pulses, their spectra and tracefiring in the Oregonator model. This involves numerical computations, which rely on and are guided by the theoretical framework laid out in chapters 2 and 3.

## 4.2 Simulations of the Oregonator

In this section, we describe results regarding tracefiring from numerical simulations of the Oregonator model. Several threshold values for the parameter $\phi$ are found, which will be recovered and better understood in bifurcation analyses of the kinetics and travelling wave ODEs in the next section.

The Oregonator kinetics, cf. (4.1), allow for the aforementioned excitation loops which create pulses in a certain parameter range. In this investigation, we fix all parameters

[6] And for other parameter values, the two equilibria and homoclinic interact in a saddle-node homoclinic.

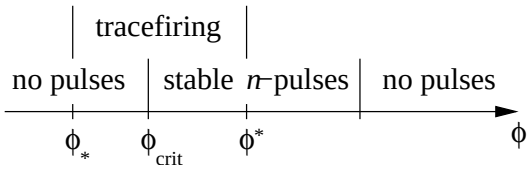


Figure 17: Schematic bifurcation diagram of pulses and tracefiring for the Oregonator.

as above and vary only $\phi$ in the range $[0.00015, 0.0035]$. Smallness of the parameters $\epsilon$ and $\epsilon'$ creates three time scales: $u$ is the fast activator, $v$ slower and $w$ the slowest inhibitor. The tracefiring instability occurs near the illumination-intensity parameter value $\phi_{\text{crit}} \sim 0.000154$. More details on the instability and bifurcations will be given in the following sections. For each parameter value larger than $\phi_{\text{crit}}$ in this range, the medium supports a stable excitation pulse with speed $c \in [2.3, 3.415]$ depending on $\phi$, see figure 17. For PDE simulations, the Oregonator model as given in (4.1) is discretized by an explicit Euler-method in time and space, implemented in the program 'EZPULSE' (based on 'EZ-SPIRAL' [7]). To implement the comoving frame, we use the boundary conditions described in chapter 3, i.e. Neumann on the left and Dirichlet on the right for a pulse with speed $c > 0$ moving right. In the program, the comoving frame is modeled by comoving boundary conditions rather than discretized convection. The pulse is identified in a search for a peak, and the medium is moved so that the pulse remains at a fixed position, i.e. Neumann data is fed in one of the boundaries and cut away at the other end. This yields numerically equivalent results to discretized convection, but is less costly and more convenient for exploration of parameter space. The program allows to change parameters interactively and provides estimates for the speed $c$ from following the pulse rather than prescribing it.

The bifurcation parameter is the illumination-intensity parameter $\phi$; the speed $c$ is then adjusted 'by the PDE'. We start away from the instability, at $\phi \sim 0.003$, with a single sufficiently wide and large step in the activator component $u$ from the stable uniform background state as an initial condition. This causes an excitation loop of the three species and creates a pair of pulses travelling in opposite directions as described in the previous sections. In these simulations, the comoving frame picks the rightward travelling pulse and the leftwards travelling pulse will disappear through the boundary.

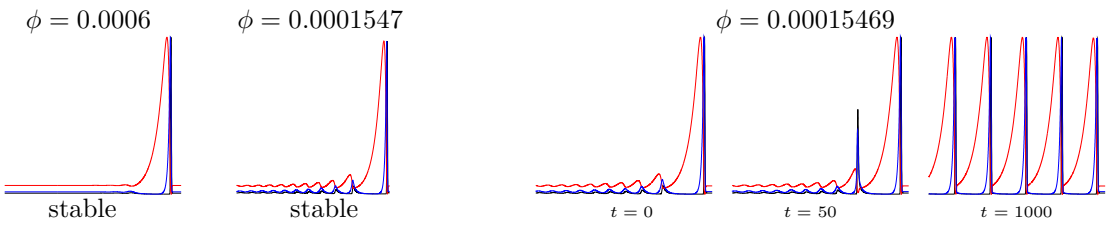


Figure 18: Oregonator's stable pulses and snapshots after the onset of tracefiring from PDE simulations. Domain size 400, with uniform grid of 4000 points, Dirichlet b.c. ahead and Neumann b.c. behind the pulse; for finer grid the instability threshold approaches $\phi_{\text{crit}}$ and the phenomenology persists. Components are scaled by constant factors for readability.

We next investigate the phenomenology as the parameter $\phi$ is decreased, which corresponds to lowering the excitation threshold. In real experiments, the medium switches from being excitable to oscillatory when decreasing the illumination intensity on the Petri dish where the reaction takes place.

In the simulations, the tails of the pulses decay along damped spatial oscillations for $\phi$ below $\phi \sim 0.0023$, where leading relevant eigenvalues of the background state as an equilibrium in spatial dynamics become complex conjugate. These oscillations increase when decreasing $\phi$, and pronounced humps form in the immediate wake of the pulse, see figure 18. Below $\phi_{\text{crit}}$, the pulse loses stability and the first of these humps grows to become a pulse of its own. Tracefiring continues periodically until the medium is filled with pulses behind the primary pulse, which is reminiscent of an invading pulse-chain, see figure 18. In the standing frame, the onset of tracefiring creates the aforementioned defect, i.e. a connection between the background state and the spatio-temporal periodic behavior. Tracefiring destabilizes below another threshold parameter value $\phi_*$, while increasing $\phi$ beyond a value $\phi^* > \phi_{\text{crit}}$, will 'turn off' tracefiring and stable $n$-pulses emerge, see figure 17. Note that changing $\phi$ changes $c$ as expected from the homoclinic orbit being codimension–1. Here $c$ increases monotonically for decreasing $\phi$.

Under Neumann-type boundary conditions behind *and* ahead of the pulse, i.e. kinetic b.c. for the non-diffusing species, spatially uniform, temporally periodic oscillations occur below $\phi_{\text{tH}} \sim 0.00017$. At $\phi_{\text{tH}}$ the kinetics undergoes a supercritical Hopf bifurcation, see figure 19. These only slightly perturb the pulse, as predicted by the bifurcation to trans-

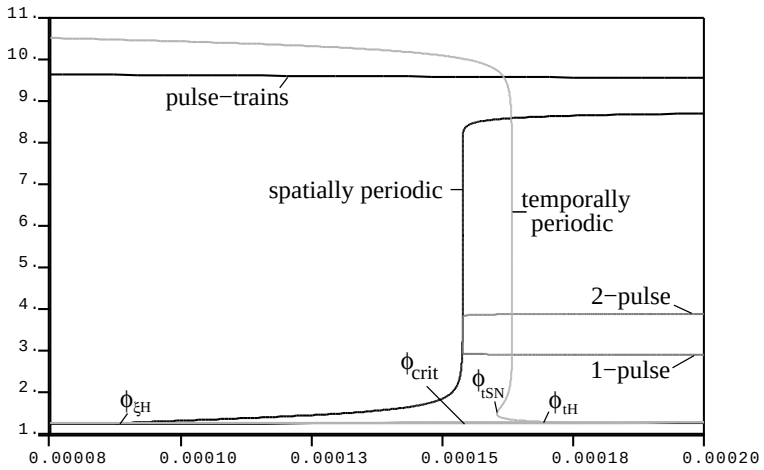


Figure 19: Kinetics (light gray) and travelling wave ODE (black) bifurcations for $c \sim 3.4142$ along $\phi$, and path of homoclinic orbit (dark grey) in $(\phi, c)$ projected to $c \sim 3.4142$.

mission defects described in [54]. Below yet another threshold value $\phi = \phi_{\mathrm{tSN}} \sim 0.00016$, the spatially homogeneous oscillations become too large, and the pulse is eventually destroyed. Nevertheless, tracefiring occurs transiently when decreasing $\phi$ fast enough, or using appropriate initial conditions. Dirichlet boundary conditions stabilize this as predicted by lemma 12 for weakly diffusing $w$, and thus determine tracefiring as the nature of transient dynamics in the transition from the excitable to oscillatory medium.

For $0 < \epsilon, \epsilon' \ll 1$ the singular-perturbation structure becomes predominant, and we expect its exploitation would shed light on the phenomenology from a different perspective. We do not pursue this further and refer to [21, 34] for investigations in this spirit.

### 4.3 Bifurcations in kinetics and travelling wave ODEs

The framework for the threshold values given in the previous section are bifurcations in the kinetics and travelling wave ODE, which we will describe in more detail next. While some bifurcation values can be computed analytically, we rely on the aforementioned path-following software AUTO [20] for their detection.

As observed in section 3.1, bifurcations in the kinetics give rise to spatially uniform patterns, i.e. wavenumber $k = 0$. Here, a Hopf bifurcation occurs at $\phi_{\mathrm{tH}}$, which produces the aforementioned spatially uniform, temporally periodic solutions, and we refer it as the temporal Hopf-bifurcation. From lemma 12, and since $c > 0$, we expect that these

oscillations are suppressed by Dirichlet boundary conditions ahead of the pulse and supported by Neumann-type boundary conditions. The lemma applies if all species diffuse, but theorem 3.5 shows that we can expect the stabilization from weak diffusion to persist. Figure 19 depicts the supercritical bifurcation from the Oregonator's background state and the associated path of temporally periodic solutions. It has been observed previously, cf. [10], that this path undergoes a so-called 'canard' explosion due to the singularly perturbed structure: the periodic orbit's amplitude rapidly grows in an exponentially small parameter region, cf. [22] for the analysis of canards. For the Oregonator, this is accompanied by saddle-node bifurcations, one of which occurs at $\phi_{\mathrm{tSN}}$, where the medium switches in completion from excitable to large scale oscillatory. Under Neumann-type boundary conditions, the aforementioned transmission defects cease to exist at this point, and in simulations large amplitude spatially homogeneous, temporal oscillations are approached. However, Dirichlet boundary conditions still suppress this bifurcation and the pulse persists for $\phi < \phi_{\mathrm{tSN}}$.

We next consider the Oregonator's travelling wave ODE, cf. (3.7), for $c \sim 3.4142$, which is close to the speed of the pulse at $\phi_{\mathrm{crit}}$. This ODE is five dimensional, and is therefore large enough to permit a codimension–2 heteroclinic cycle, cf. remark 1. As discussed in section 3.1, bifurcations in this ODE create stationary spatial patterns. A Hopf bifurcation occurs at $\phi_{\xi\mathrm{H}} \sim 0.00009$, and a branch of time-independent, spatially periodic orbits bifurcates for increasing $\phi$, see figure 19, and we refer to this as a spatial Hopf-bifurcation. This branch appears to undergo a similar canard-explosion, folds several times and connects to a branch of large amplitude periodic orbits, see 'wave-trains' in figure 19 (part of this branch is not shown). This branch reaches from $\phi = 0.0008$ beyond $\phi = 0.0002$ and the large amplitude periodic orbits are reminiscent of wave trains created by tracefiring behind the primary pulse. Associated to each $\phi$ there is a (typically locally unique) speed $c = c(\phi)$, but the geometry of the branches changes only slightly for all $\phi$ for which we find tracefiring.

To find the branch of 1–homoclinic orbits that corresponds to the primary pulse, we can use initial conditions generated by EZPULSE, or path-follow periodic orbits from the upmost branch, cf. 'pulse trains' in figure 19, in $c$ and the period $L$. In the latter case so-

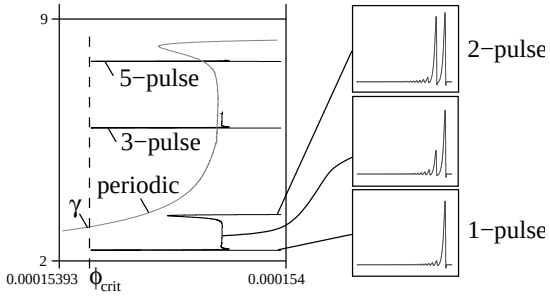


Figure 20: The curve of spatially periodic orbits for $c \sim 3.4142$ at the saddle-node of the homoclinic branches, and branches of $n$–pulses bifurcating to $(n+1)$–pulses for $n = 1, 3, 5$ by growth in the wake reminiscent of tracefiring; insets show the $v$-component profile. The branches for $n = 3, 5$ are shown only in part, they continue qualitatively like the one for $n = 1$.

called anomalous dispersion occurs, which is oscillatory as predicted in [55] for Shil'nikov pulses with long wave length. Moreover, the slope of the dispersion is related to the group velocity introduced in section 3.1 via $L\frac{\mathrm{d}c}{\mathrm{d}L} = c - c_g$. The group velocity influences the interaction of the pulses in the pulse train and its stability for large inter-pulse distance. Indeed PDE simulations allow to trigger secondary pulses further behind the primary pulse and show locking phenomena in the humps of the primary pulse's wake. This is similar to the correction of the peak positions in tracefiring shown in figure 16 b). From path-following these periodic orbits first until large $L$, we can then path-follow the branch of 1–homoclinic orbits that corresponds to pulses we see in PDE simulations. This branch is also included in figure 19. For large $\phi$ outside the figure, the branch of 1–pulses folds and connects stable large pulses with unstable smaller ones. This is far away from the relevant parameter values for tracefiring, which are near $\phi_{\mathrm{crit}}$ and $c \sim 3.4142$.

At the parameter value $\phi_{\mathrm{crit}}$ the branch of homoclinic orbits folds and connects to a branch of 2–pulses with small interpulse distance, cf. figures 19 and 20. We used the speed associated to $\phi_{\mathrm{crit}}$ for the travelling wave ODE bifurcation diagram in figure 19. The connection of the 1–pulse to the 2–pulse branch appears to undergo an amplitude explosion reminiscent of a canard explosion, see figure 20. The same scenario connects branches of 3–homoclinic with 4–homoclinic and 5–homoclinic with 6–homoclinic orbits, where saddle nodes occur very close to $\phi_{\mathrm{crit}}$. We conjecture that for any $n \geq 1$ branches of $n$– and $(n+1)$–homoclinics are connected this way, i.e. there is a cascade of saddle nodes

near $\phi_{\text{crit}}$. This is similar to cascades found numerically for pulse splitting in the Gray-Scott and FitzHugh-Nagumo models, cf. [23, 34], where these serve as organizing centers to explain e.g. transient dynamics in transitions from slow pulses to large amplitude Turing patterns.

At the saddle-node parameter value $\phi_{\text{crit}}$ for the travelling wave ODE, there exists a small amplitude periodic orbit $\gamma$ on the branch of spatially periodic orbits, i.e. stationary wave trains, cf. figure 20. This wave train is reminiscent of the pronounced oscillations in the pulse's wake, and we conjecture there is a heteroclinic cycle from the steady state to that periodic orbit for nearby values of the many other parameters in the Oregonator model. In the 2–component version of the Oregonator model[7] with one diffusing species, an analogous heteroclinic orbit from a relevant periodic orbit to the background state via a pulse excursion has been found numerically in [8]. There is no heteroclinic cycle in that case, because the equilibrium is stable in the associated travelling wave ODE. Note that a heteroclinic cycle in the travelling wave ODEs of the 2–component Oregonator could not be codimension–2, because the ambient space is only three-dimensional, cf. remark 1.
To determine the codimension of the conjectured heteroclinic cycle, the Floquet exponents associated to $\gamma$ are needed. However, these could not be computed reliably by AUTO, apparently due to large differences in scales. From spectral analyses in the next section, we will conclude the Morse index of $\gamma$ and that the heteroclinic cycle would be codimension–2 in the sense of chapter 2. Theorem 2.3 then shows that we can expect a family of curves of 1–homoclinic orbits accumulating at this heteroclinic cycle. Since $\gamma$ stems from a nearby Hopf bifurcation, we expect that hypothesis 5 holds with winding number 1. Then theorem 2.5 proves bifurcation of a unique connected curve of 1–homoclinic orbits from the heteroclinic cycle with $\gamma$.
However, the winding number way be zero, which would explain why the heteroclinic cycle with $\gamma$ could not be found numerically. The branch of 1–homoclinics might connect only to one of the disjoint curve segments of the family of curves of 1–homoclinic orbits in theorem 2.3.

[7] This is derived from (4.1) by multiplying the $v$ equation by $\epsilon'$ and setting $\epsilon' = 0$.

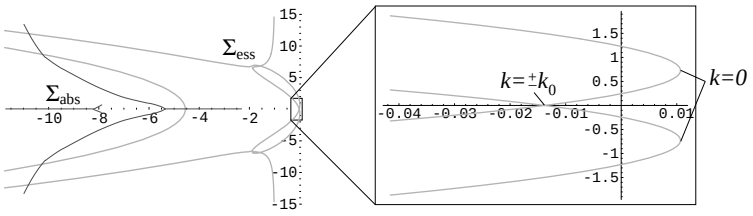


Figure 21: Absolute and essential spectrum of the background state for $\phi = \phi_{\text{crit}}$, inset enlarges the critical part. Decreasing $\phi$ mainly moves the critical spectrum rightwards. At the temporal Hopf-bifurcation $\phi_{\text{tH}}$, $\lambda(0)$ crosses the imaginary axis. At the spatial Hopf-bifurcation $\phi_{\xi\text{H}}$, $\pm k_0$ cross $\mathrm{i}\mathbb{R}$ in the travelling wave ODE.

## 4.4 Spectra of the background state and periodic orbits

As discussed in chapter 3, the essential spectrum of the pulse is the spectrum of the background state, and is typically the union of the algebraic dispersion curves in (3.6). Since this is third order in the eigenvalues $\lambda$ for the Oregonator, parametrizations $\lambda(\mathrm{i}k)$ in the wavenumber $k$ can be computed by computer algebra packages, e.g. MATHEMATICA. Part of these curves are shown in figure 21. The folds of these curves correspond to wavenumber $k = 0$, where the spatial eigenvalues are the eigenvalues of the linearization of the kinetics, cf. section 3.1.1. Hence the aforementioned temporal Hopf bifurcation occurs when the rightmost folds cross the imaginary axis at $\phi = \phi_{\text{tH}}$. On the other hand, at $\lambda = 0$ the linearization of the travelling wave ODE is recovered, and for $\phi = \phi_{\xi\text{H}}$ the crossing point of the two symmetric critical dispersion curves passes the origin with wavenumbers $\pm k_0 \sim \pm 0.27$. Thus, a pair of complex conjugate spatial eigenvalues crosses the imaginary axis at the aforementioned spatial Hopf bifurcation.

The tracefiring instability occurs near $\phi_{\text{crit}}$ which lies between these two values, and we focus on $\phi = \phi_{\text{crit}}$ in the following. To determine the critical parts of the dispersion curves from diffusing species, lemma 10 shows that it suffices to consider $k \leq R_k$, where $R_k^2 = \max_{j=1,\ldots,N} \frac{1}{d_j} \left( a_{ii} + \sum_{j=1, i\neq j}^{N} |a_{ij}| \right)$. It is readily seen from the linearization of (4.1), that the real parts along the dispersion curve for $w$ converge to $-1$. For an approach to computing the essential spectrum by path-following we refer to [47].

The background states' absolute spectrum has been computed with AUTO by path-following in the following manner. By lemma 11 the dispersion relation $d(\lambda, \nu) = 0$ for the Oregona-

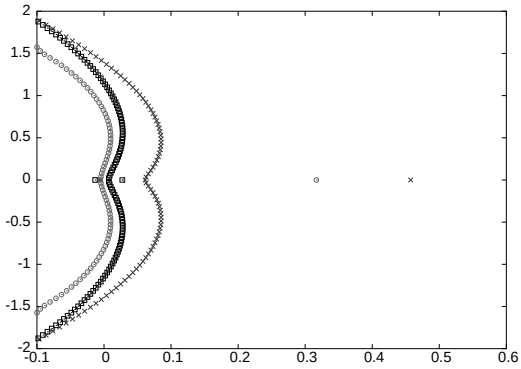


Figure 22: Critical spectra of 1–pulses on domain length 200, uniform grid length 0.1 with periodic b.c. and symmetric finite differences. Black ('□'): at $\phi_{\text{crit}}$, dark gray ('x', most unstable): unstable branch $\phi > \phi_{\text{crit}}$, light gray ('∘'): unstable branch, closer to the 2-pulse branch, cf. figure 20.

tor has at most $3(2 \cdot 3 - 1) - (3 - 2)^2 = 14$ double spatial eigenvalues $\nu$; in this case this number is attained. When path-following spatial eigenvalues with equal real parts at each of these double roots, we can find all curves of the iso-real spectrum, cf. [46]. Accounting for changes in the order of the real parts, we can identify the absolute spectrum. Its critical parts are shown in figure 21 and it is stable with real parts less than 1. The essential spectrum destabilized at the temporal Hopf-bifurcation and the background state is (only) convectively unstable on the unbounded domain in this parameter regime. As mentioned above, Dirichlet boundary conditions stabilize the unstable spatially uniform eigenmode as predicted by lemma 12. On bounded domains with increasing domain length eigenvalues of the pulse cluster precisely at the stable absolute spectrum, cf. theorem 3.2 from [53]. In conclusion, for stable isolated point spectrum and resonance poles, the tracefiring instability is not caused by the background state, and thus should be explained by the pulse's *point* spectrum from the unbounded domain.

Approximating the 1-pulse's point spectrum numerically by finite differences is expensive and was reliable only near the imaginary axis and for symmetric finite differences with periodic boundary conditions, cf. figure 22. These computations show a saddle-node bifurcation occurs near $\phi_{\text{crit}}$ as expected from the bifurcations in figure 20. The clusters of eigenvalues occur near the essential spectrum, see figure 21, as predicted by theorem 3.2. Other than the eigenvalue crossing zero, isolated point spectrum of the pulses appears to be stable in this parameter regime. The spectrum becomes more stable for pulses further

along the branch shown in figure 20, see figure 22.

In the spirit of corollary 1 and remark 11, we conjecture the instability is caused by the interaction of the pulse with the (unstable) wave-train corresponding to $\gamma$ in figure 20. As a periodic orbit, $\gamma$ has no point spectrum and the essential spectrum is given by means of the boundary value problem (3.10). We solve it using the initial condition $\gamma'$ at $\lambda = 0$, $\nu = 0$ and path-following in $k$, i.e. $\nu = \mathrm{i}k$, yields a small unstable circle attached to zero, see figure 23. More precisely, we solve the nonlinear problem for the periodic orbit and the complex valued boundary value problem simultaneously, i.e. 15 equations and pose periodic boundary conditions for the nonlinear part. To fix the periodic orbit and the eigenfunction, we impose two integral conditions, as well as one phase condition. The full system is solved using the period of the nonlinear solution as well as the real and imaginary parts of $\lambda$ for each $k$, see also [47]. Figure 23 shows two further curves and an unstable small circle of essential spectrum. These were found by path-following in the real part of the spatial eigenvalue $\nu$ by imposing the boundary condition $v(L) = \mathrm{e}^{\eta} v(0)$, $\eta \in \mathbb{R}$. When $\eta = 0$ occurred along this path, another curve of essential spectrum was intersected and we switched to path-following in the imaginary part again.

The curves of essential spectrum are oriented by $o(\lambda, k)$ from section 3.1.2 as shown in figure 23, in particular $c_g > 0$ in this case. Since the group velocity indicates direction of transport, a positive sign explains the correction of the secondary pulses' positions seen in the Oregonator's tracefiring, cf. figure 16. Using lemma 15 and that $c > 0$ we can now conclude $i(\gamma) = 2$. For the Oregonator $N = 3$, so the Morse index of $\gamma$ is 2, i.e. the Morse-index difference $i_{p_0} - i_\gamma = 1$, and the heteroclinic cycle would be codimension–2 by remark 1.

For illustration we count the Morse indices explicitly in this case: To the right of the rightmost curve the spatial Morse-index $i(\lambda) = N$, cf. section 3.1.1, and from the orientation of the rightmost curve it increases when crossing from left to right, i.e. it is $N - 1$ outside the circle attached to zero. Since the orientation on the circle is counter-clockwise, i.e. $c_g > 0$, the Morse index drops to $N - 2$ when going inside the circle, whence it is $N - 1$ on the circle, in particular at $\lambda = 0$.

To apply corollary 1 from section 3.1.3, we now aim at finding unstable absolute spectrum

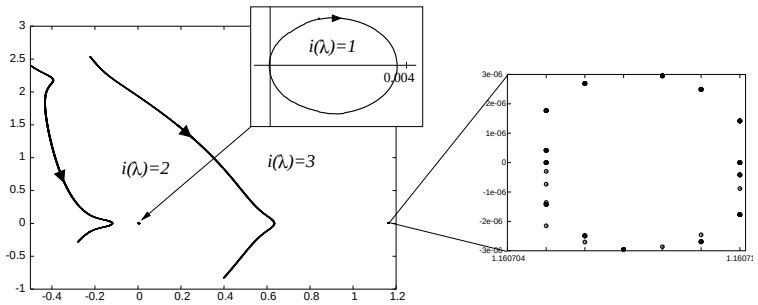


Figure 23: Parts of essential spectrum of $\gamma$ from path-following and spatial Morse-indices. Insets show isolated circles: one attached to zero, one in $\Omega_\infty$. Orientation by $o(\lambda, k)$ from section 3.1.2.

of $\gamma$, which would explain the loss of stability of the primary pulse close to the heteroclinic cycle. Knowing the spatial Floquet exponents $\nu_j$ would easily allow to identify absolute spectrum. However, reliable values for Floquet multipliers and exponents could not be computed numerically in this case. The problem appears to be the large period at the Hopf bifurcation, which causes extremely large and small quantities. Nevertheless, Theorem 3.3 allows to infer unstable absolute spectrum from the small unstable circle of essential spectrum, see figure 23, cf. remark 9: The circle lies in $\Omega_\infty$, the region with Morse-index $N$, and path-following the curve $\lambda(\eta)$, in $\eta \in \mathbb{R}$, starting at $\lambda(0)$, suggests the theorem applies, i.e. the circle does not contain a double root of $d_{\text{per}}(\lambda, \nu)$ in $\lambda$. Note that this does not imply a real-type absolute instability or a spiraling path in parameter space near the heteroclinic cycle as predicted in theorem 2.6.

The spectra in figure 23, show a stabilization of the 1–pulse's spectrum further towards 2–pulse along the branch, i.e. with growing secondary pulse in its wake, cf. figure 20. In fact, finite difference computations and the PDE simulations corroborate that the 2–pulse is stable. This is expected from the spectral influence of $\gamma$ on the pulses' stability in theorem 3.4: The further away from $\gamma$ the homoclinic orbit is, the weaker is the destabilizing effect of $\gamma$'s absolute spectrum.

Finally, to partially explain tracefiring from the perspective of remark 10, we aim at finding a codimension–1 heteroclinic cycle with a stable pulse-train, which is composed of copies of the pulse with small distances. Indeed, the upmost branch of periodic orbits in figure 19 labelled 'pulse-trains' is such a pulse-train and PDE simulations suggest it is

in a heteroclinic cycle with the background state. Simulations allow for the creation of arbitrary $n$-pulses, as well as arbitrarily long invading and evading pulse chains, see figure 3. From these $n$–pulses, $n$–homoclinic orbits were successfully path-followed with AUTO for $n = 1, \ldots, 6$, as described above, see figure 20. The Morse index in the travelling wave ODE of the pulse-train is $N + 1 = 4$ with $c_g > 0$ and $c > 0$. Moreover, $c_g > c$, which again is in accordance with the direction of transport towards the primary pulse, see figure 16. From lemma 16 the invading pulse chain can be expected to have one-dimensional transverse intersection, while the evading pulse chain is codimension–1 and has a selected speed, cf. figure 3. This corroborates the persistence of tracefiring under changes in the parameter $\phi$ with an adjusted $c$.

We close this discussion with remarks on the defect with speed $c_{\mathrm{d}}$ that occurs generally in tracefiring, cf. figure 2. While an equilibrium does not produce transport by a group velocity, in terms of Morse indices the invading pulse chain corresponds to a sink-type defect in the sense of Sandstede and Scheel in [57]. The tracefiring defect with speed $0 < c_d < c$ corresponds to a source-type defect in this sense, because from the numerical computations $c_g - c_d > c$. We refer to this paper for details of the classification. In this spirit, we may view the process of tracefiring as a source-sink defect interaction, and leave its further investigation to the future.

## References


[1] J. Alexander, R. Gardner, C.K.R.T. Jones. *A topological invariant arising in the stability analysis of travelling waves.* J. Reine Angew. Math. **410**, 167-212 (1990).

[2] A.A. Andronov, E.A. Leontonvich. *Generation of limit cycles from a separatrix forming a loop and from the separatrix of an equilibrium state of saddle-node type.* Mat. Sb., N. Ser. **48**(90), 335–376 (1959).

[3] J. Annamalai, M. Liauw, D. Luss. *Temperature patterns on a hollow cylindrical catalytic pellet*, CHAOS **9**, 36–42 (1999)

[4] A. Back, J. Guckenheimer, M.R. Myers, F.J. Wicklin, P.A. Worfolk. *DsTool: Computer assisted exploration of dynamical systems.* Notices Amer. Math. Soc. **39**, 303–309 (1992)

[5] W.J. Beyn. *Global bifurcations and their numerical computation.* Continuation and bifurcations: Numerical techniques and applications, Proc. NATO Adv. Res. Workshop, Leuven/Belg. 1989, NATO ASI Ser., Ser. C 313, 169-181 (1990)

[6] M. Bär, M. Hildebrand, M. Eiswirth, M. Falke, H. Engel, M. Neufeld, *Chemical turbulence and standing waves in a surface reaction model: The influence of global coupling and wave instabilities.* Chaos **4**, 499–507 (1994)

[7] D. Barkley. *A model for fast computer simulation of waves in excitable media.* Physica D **49**, 61–70 (1991)

[8] G. Bordiuogov, H. Engel. In preparation.

[9] P.L. Buono, M. Golubitsky, A. Palacios. *Heteroclinic cycles in rings of coupled cells.* Physica D **143**, 74–108 (2000)

[10] M. Brons, K. Bar-Eli. *Canard explosion and excitation in a model of the Belousov-Zhabotinskii reaction.* J. Phys. Chem. **95** 8706–8713 (1991)

[11] V.V. Bykov. *The bifurcations of separatrix contours and chaos.* Physica D **62**, 290–299 (1993)

[12] A.R. Champneys, A.J. Rodriguez-Luis. *The non-transverse Shil'nikov-Hopf bifurcation: uncoupling of homoclinic orbits and homoclinic tangencies.* Physica D **128**, 130–158 (1999)

[13] Shui-Nee Chow, J.K. Hale. *Methods of bifurcation theory.* Grundl. math. Wiss. 251, Springer, New York (1982)

[14] E.A. Coddington, N. Levinson. *Theory of ordinary differential equations.* New York, Toronto, London: McGill-Hill Book Company, Inc. XII (1955)

[15] J.B. Conway. *Functions of one complex variable.* 2nd ed., Springer (1978)

[16] W.A. Coppel. *Dichotomies in stability theory*. Lecture Notes in Mathematics **629**. Springer, Berlin-Heidelberg-New York (1978)

[17] P. Coullet, C. Riera, and C. Tresser. *Stable Static Localized Structures in One Dimension*. Phys. Rev. Lett. **84**, 3069–3072 (2000)

[18] Bo Deng, K. Sakamoto. *Sil'nikov-Hopf bifurcations*. J. Differ. Equations **119**, 1–23 (1995)

[19] L.J. Diaz, J. Rocha. *Heterodimensional cycles, partial hyperbolicity and limit dynamics*. Fundam. Math. **174**, 127–186 (2002)

[20] E. Doedel, A.R. Champneys, T.F. Fairgrieve, Yu.A. Kuznetsov, B. Sandstede and X. Wang. *AUTO97: Continuation and bifurcation software for ordinary differential equations (with HOMCONT)*. Technical Report, Concordia University (1997)

[21] A. Doelman, T.J Kaper. *Semi-strong pulse interactions in a class of coupled reaction-diffusion equations*. SIAM J. Appl. Dyn. Syst. **2**, 53–96 (2003)

[22] F. Dumortier, R. Roussarie. *Canard cycles and center manifolds.* Mem. Am. Math. Soc. **577**, (1996)

[23] Y. Nishiura, D. Ueyama. *A skeleton structure of self-replicating dynamics*. Physica D **130** 73–104 (1999)

[24] B. Fiedler. *Global pathfollowing of homoclinic orbits in twoparameter flows*. In: Dynamics of nonlinear waves in dissipative systems: reduction, bifurcation and stability. Dangelmayr, Gerhard et al. (Eds.). Harlow: Longman. Pitman Res. Notes Math. Ser. **352**, 79–145, 263–277 (1996)

[25] B. Fiedler, A. Scheel. *Spatio-Temporal Dynamics of Reaction-Diffusion Patterns*. In: Trends in Nonlinear Analysis. M. Kirkilionis, S. Krömker, R. Rannacher, F. Tomi (Eds.), Springer-Verlag, Berlin (2003).

[26] J.R. Field, R.M. Noyes. *Oscillations in chemical systems. IV. Limit cycle behavior in a model of a real chemical reaction*. J. Chem. Phys **60**, 1877–1884 (1974)

[27] Gardner, R.A. *On the structure of the spectra of periodic travelling waves.* J. Math. Pures Appl., IX. **72**, 415–439 (1993)

[28] P. Glendinning, C. Sparrow. *T-points: a codimension two heteroclinic bifurcation*. J. Stat. Phys. **43**, 479–488 (1986)

[29] G. Haller, S. Wiggins. *Geometry and chaos near resonant equilibria of 3-DOF Hamiltonian systems.* Physica D **90**, 319–365 (1996)

[30] Yumino Hayase, Takao Ohta. *Self-replicating pulses and Sierpinski gaskets in excitable media*. Phys. Rev. E **62**, 5998–6003 (2000)

[31] D. Henry. *Geometric Theory of Semilinear Parabolic Equations*. Lecture Notes in Mathematics, **840**, Springer Berlin Heidelberg (1981)

[32] P. Hirschberg, E. Knobloch. *Shilnikov-Hopf bifurcation.* Physica D **62**, 202–216 (1993)

[33] C.K.R.T. Jones. *Geometric singular perturbation theory.* In: Dynamical systems. Johnson, Russell (ed.). Berlin, Springer-Verlag. Lect. Notes Math. **1609**, 44–118 (1995)

[34] T. Kolokolnikov, M.J. Ward and J. Wei. *The Existence and Stability of Spike Equilibria in the One-Dimensional Gray-Scott Model: The Pulse-Splitting Regime.* Physica D (submitted)

[35] Wang Sang Koon, M.W. Lo, J.E. Marsden, S.D. Ross. *Heteroclinic connections between periodic orbits and resonance transitions in celestial mechanics.* Chaos **10**, 427–469 (2000)

[36] H. Kokubu. *Heteroclinic bifurcations associated with different saddle indices.* In: Dynamical Systems and Related Topics, Adv. Ser. Dyn. Syst. **9**. River Edge, NJ: World Scientific. (1991)

[37] H. Kokubu. *A construction of three-dimensional vector fields which have a codimension two heteroclinic loop at Glendinning-Sparrow T-point.* Z. Angew. Math. Phys. **44**, 510–536 (1993)

[38] J. Krishnan, I.G. Kevrekidis, M. Or-Guil, M.G. Zimmermann, M. Bär. *Numerical bifurcation and stability analysis of solitary pulses in an excitable reaction-diffusion medium.* Comp. Methods Appl. Mech. Engrg. **170**, 253–275 (1999)

[39] Xiao-Biao Lin. *Using Melnikov's method to solve Silnikov's problems.* Proc. R. Soc. Edinb., Sect. A **116**, 295–325 (1990)

[40] Mielke, A. *The Ginzburg-Landau equation in its role as a modulation equation.* In: Handbook of dynamical systems II. B. Fiedler (ed.). North-Holland, Amsterdam, Vol. 2, 759–834 (2002)

[41] J. Moehlis, E. Knobloch. *Bursts in oscillatory systems with broken $D_4$ symmetry.* Physica D **135**, 263–304 (2000)

[42] Nii, Shunsaku. *The accumulation of eigenvalues in a stability problem.* Physica D **142**, 70-86 (2000)

[43] R.D. Otterstedt, P.J. Plath, N.I. Jaeger, J. L. Hudson. *Modulated electrochemical waves*, Phys. Rev. E **54**, 3744–3751 (1996)

[44] K.J. Palmer. *Exponential dichotomies and transversal homoclinic points.* J. Differ. Equations **55**, 225–256 (1984)

[45] K.J. Palmer.*Exponential dichotomies and Fredholm operators.* Proc. Am. Math. Soc. **104**, 149-156 (1988)

[46] J.D.M. Rademacher, A. Scheel. *Absolute spectra and the topology of the iso-real spectrum.* In preparation.

[47] J.D.M. Rademacher, B. Sandstede, A. Scheel. *A path-following approach to the computation of absolute and essential spectra.* In preparation.

[48] T. Rieß. *Using Lin's method for an almost Shilnikov problem.* Diploma thesis, Technical University of Illmenau, Faculty of Mathematics and the Sciences (2003)

[49] M. Romeo, C.K.R.T. Jones. *The stability of traveling calcium pulses in a pancreatic acinar cell.* Physica D **177**, 242–258 (2003)

[50] B. Sandstede. *Verzweigungstheorie homokliner Verdopplungen.* Dissertation, University of Stuttgart (1993)

[51] B. Sandstede. *Stability of travelling waves.* In: Handbook of Dynamical Systems II. B. Fiedler (ed.). Elsevier, 983–1055 (2002)

[52] B. Sandstede, A. Scheel, *Gluing unstable fronts and backs together can produce stable pulses*, Nonlinearity **13**, 1465–1482 (2000)

[53] B. Sandstede, A. Scheel. *Absolute and convective instabilities of waves on unbounded and large bounded domains.* Physica D **145**, 233–277 (2000)

[54] B. Sandstede, A. Scheel. *Essential instabilities of fronts: bifurcation, and bifurcation failure.* Dynamical Systems **16** 1–28 (2001)

[55] B. Sandstede, A. Scheel. *On the stability of periodic travelling waves with large spatial period.* J. Diff. Eqns. **172**, 134–188 (2001)

[56] B. Sandstede, A. Scheel. *Basin boundaries and bifurcations near convective instabilities: A case study.* Journal of Differential Equations (to appear)

[57] B. Sandstede, A. Scheel. *Defects in oscillatory media - towards a classification.* SIAM J. Appl. Dyn. Syst. **3**, 1–68 (2004)

[58] K. Sakamoto. *Invariant manifolds in singular perturbation problems for ordinary differential equations.* Proc. R. Soc. Edinb., Sect. A **116**, 45–78 (1990)

[59] I. Schebesch, H. Engel. *Interacting spiral waves in the Oregonator model of the light-sensitive Belousov-Zhabotinskii reaction.* Phys. Rev. E **60**, 6429–6434 (1999)

[60] G.R. Sell, Youngchen You. *Dynamics of Evolutionary Equations.* Appl. Math. Sc. **143**. Springer, New York (2002)

[61] H. Sevcikova, M. Marek, S. Müller, *The reversal and splitting of waves in an excitable medium caused by an electrical field.* Science **257**, 951–954 (1992)

[62] A.L. Shilnikov, L.P. Shilnikov, D.V. Turaev. *Blue sky catastrophe in singularly perturbed systems.* Accepted in Moscow Mathematical Journal (2003)

[63] L.P. Shil'nikov *On the generation of a periodic motion from a trajectory which leaves and re-enters a saddle-saddle state of equilibrium.* Sov. Math., Dokl. **7**, 1155–1158 (1966)

[64] J. Sieber. *Numerical Bifurcation Analysis for Multisection Semiconductor Lasers.* SIAM J. Appl. Dyn. Sys. **1**, 248–270 (2002)

[65] D. Simpson, V. Kirk, J. Sneyd. *Complex oscillations and waves of calcium in pancreatic acinar cells.* Submitted to Physica D (2004)

[66] D. Snita, P. Hasal, J.H. Merkin. *Electric field induced propagating structures in a model of spatio-temporal signalling.* Physica D **141**, 155–169 (2000)

[67] J. Sneyd, A. LeBeau, D. Yule, *Traveling waves of calcium in pancreatic acinar cells: model construction and bifurcation analysis.* Physica D **145**, 158–179 (2000)

[68] L.N. Trefethen, D. Bau, III. *Numerical Linear Algebra.* SIAM (1997)

[69] A. Vanderbauwhede, B. Fiedler. *Homoclinic period blow-up in reversible and conservative systems.* Z. Angew. Math. Phys. **43**, 292–318 (1992)

[70] T. Valent. *Boundary value problems of finite elasticity. Local theorems on existence, uniqueness, and analytic dependence on data.* Springer Tracts in Natural Philosophy, Vol. 31, Springer, New York (1988)

[71] L. Zhou, A. Messing, S. Chiu, *Determinants of excitability at transition zones in Kv1.1-deficient myelinated nerves*, J. Neurosc. **19**, 5768–5781 (1999)

[72] Deming Zhu, Zhihong Xia. *Bifurcations of heteroclinic loops.* Sci. China, Ser. A **41**, 837–848 (1998)